CHAPTER 4

Polar Ozone: Past and Present

Lead Authors:
P.A. Newman
M. Rex

Coauthors:
P.O. Canziani
K.S. Carslaw
K. Drdla
S. Godin-Beekmann
D.M. Golden
C.H. Jackman
K. Kreher
U. Langematz
R. Müller
H. Nakane
Y.J. Orsolini
R.J. Salawitch
M.L. Santee
M. von Hobe
S. Yoden

Contributors:
G.E. Bodeker
K. Frieler
F. Goutail
M. López-Puertas
G.L. Manney
E.R. Nash
C.E. Randall
H.J. Singer
C.S. Singleton
R.M. Stimpfle
S. Tilmes
M. Weber

Final Release: February 2007
From *Scientific Assessment of Ozone Depletion: 2006*

CHAPTER 4

POLAR OZONE: PAST AND PRESENT

Contents

SCIENTIFIC SUMMARY

Arctic

- **Arctic spring total ozone values over the last decade were lower than values observed in the 1980s. In addition, spring Arctic ozone is highly variable depending on dynamical conditions.** For current halogen levels, anthropogenic chemical loss and variability in ozone transport are about equally important for year-to-year Arctic ozone variability. Colder-than-average vortex conditions result in larger halogen-driven chemical ozone losses. Variability of temperatures and ozone transport are correlated because they are both driven by dynamic variability.

- **For the coldest Arctic winters, the volume of air with temperatures low enough to support polar stratospheric clouds (V_{PSC}) increased significantly since the late 1960s.** This change of climate conditions is much larger than expected from the direct radiative effect of increasing greenhouse gas concentrations. The reason for the change is not clear and it could be due to long-term natural variability or an unknown dynamical mechanism.

- **Column ozone loss in the 2004/2005 Arctic winter was among the largest ever observed.** The 2004/2005 Arctic stratosphere was exceptionally cold, particularly below 18 kilometers (km), leading to a value of V_{PSC} 25% larger than the previous record value. Various independent studies and methods suggest that the chemical column ozone loss in 2004/2005 was among the largest ever observed. However, dynamical processes resulted in March-average Arctic total ozone amounts being comparable to those in other recent winters, while the large losses contributed to low total column ozone over parts of Europe during March 2005.

Antarctic

- **Over the last decade (1995-2005), Antarctic ozone depletion has stabilized.** Most ozone hole diagnostics show a leveling off after the mid-1990s. Saturation of ozone loss inside the ozone hole due to complete ozone destruction over a broad vertical layer plays a role in this leveling off. Ozone hole area, ozone mass deficit, and higher minimum column amounts were observed to be below average in some recent winter years. These improvements in the ozone hole resulted from higher levels of dynamical forcing, and not decreases in equivalent effective stratospheric chlorine levels.

- **In September 2002, the first ever observed Antarctic major stratospheric warming occurred. This early-spring warming caused a drastic reduction of the ozone hole area and resulted in a less severe ozone hole.** This warming resulted from anomalously strong dynamical wave activity in the Southern Hemisphere. The triggers of these very unusual waves are unknown, and it is not clear whether the 2002 warming is a random event due to internal atmospheric variability or whether it can be related to long-term changes in climate. The Antarctic winter 2004 was also dynamically very active and had less ozone mass deficit than previous years. The higher levels of ozone in these two years were dynamically driven and not related to halogen chemical reductions.

General

- **Large interannual variability in polar stratospheric temperatures complicates the interpretation of trends.** Previously reported estimates of temperature trends in polar regions have differed from assessment to assessment. It now is evident that trends determined over a time scale of one to two decades, though they may appear statistically significant, are not robust because of large interannual and decadal variability in observed temperatures. Therefore, changes in reported trends do not necessarily indicate systematic changes in physical or chemical processes.

- **There are indications that the chlorine monoxide (ClO) dimer cycle may be a more efficient process for polar ozone loss than previously thought.** Uncertainties in the laboratory absorption cross section of the chlorine

monoxide dimer (ClOOCl) are large. Good overall consistency between in situ observations of ClO and the ClOOCl and model calculations can be achieved if it is assumed that ClOOCl photolyzes faster than assumed in the previous Assessment. Faster photolysis of ClOOCl, combined with recent laboratory studies indicating more rapid formation of ClOOCl by the ClO self-reaction, leads to more efficient ozone loss by this catalytic cycle.

- **Recent measurements suggest that bromine may play a more important role in polar ozone depletion than previously thought.** Profiles of bromine monoxide (BrO) measured in the Arctic vortex suggest that inorganic bromine levels may be 3 to 8 parts per trillion by volume larger than the amount of bromine carried to the stratosphere by methyl bromide (CH_3Br) and halons. This observation indicates the BrO + ClO cycle is likely to be a more efficient ozone loss process than considered in the previous Assessment. The BrO + ClO cycle is now estimated to contribute up to half of total chemical loss of polar ozone, even considering the more efficient ozone loss by the ClO dimer cycle. However, the polar stratospheric bromine budget is a significant source of uncertainty.

- **Calculated chemical loss rates of polar ozone substantially increased in models that assume: (1) more efficient ozone destruction by the ClO dimer cycle and (2) higher levels of bromine.** These changes improve the comparison between measured and modeled Arctic ozone loss rates for cold Januaries that was noted in the past Assessment. These two changes also improve the comparison between theory and observation of Antarctic ozone loss rates.

- **The chemical loss of column ozone for Arctic winters exhibits a near linear relation with V_{PSC} during each winter.** A similar relation between ozone loss and V_{PSC} is now seen for two independent analyses of chemical ozone loss, increasing our confidence in the robustness of this relation. Observations of the large Arctic ozone loss in 2004/2005 are in line with the relationship established for prior winters. The slope of this relation provides an empirical measure of the sensitivity of chemical loss of Arctic ozone to changes in stratospheric temperature (for contemporary levels of chlorine and bromine) and provides an important metric for chemical transport models (CTMs) and coupled Chemistry-Climate Models (CCMs) that are used in both diagnostic and prognostic studies of polar ozone loss.

- **For the first time, measurements show unambiguously that nitric acid trihydrate (NAT) polar stratospheric cloud particles can nucleate above the ice frost point, and there is additional evidence of their widespread occurrence.** Widespread low number density NAT clouds can lead to denitrification and enhanced ozone loss. Incorporating NAT nucleation above the ice frost point into chemical transport models has improved denitrification simulations, but discrepancies in interannual variability remain, probably because the NAT nucleation mechanisms are not fully understood.

- **The most recent solar cycle was associated with frequent and exceptionally strong episodes of charged particle precipitation. This caused only small decreases in total column ozone in the polar region (<3%, <10 Dobson units).** However, the measured ozone reduction in the mid-to-upper stratosphere (30-50 km) exceeded 30% for weeks following certain episodes of intense particle precipitation.

4.0 INTRODUCTION

Since the discovery of the Antarctic ozone hole by Farman et al. (1985), considerable effort has been focused on observing these ozone losses, understanding the chemical, dynamical, and radiative processes, and predicting the future of polar ozone. This chapter builds upon a sequence of polar ozone chapters in the World Meteorological Organization (WMO) Assessment series.

The first publication of large Antarctic ozone losses by Farman et al. (1985) sparked scattered discussion of polar ozone in the 1985 Ozone Assessment (WMO, 1986). Chapter 14 of that Assessment (Ozone and Temperature Trends) showed the Farman et al. (1985) results and included Total Ozone Mapping Spectrometer (TOMS) total ozone images (subsequently published in Stolarski et al., 1986). These early satellite data confirmed the findings of Farman et al. and moreover displayed the horizontal dimensions of the ozone hole. The Ozone Trends Panel's 1988 report (WMO, 1990a) followed with an entire chapter on Antarctic ozone (Chapter 11) including an extensive discussion of both Antarctic observations and of the three competing theories of the ozone hole that were proposed originally in the mid-1980s. In particular, this WMO (1990a) chapter focused on (1) the drastic reduction in nitrogen dioxide (NO_2) abundance resulting from the formation of polar stratospheric clouds (PSC) consisting of nitric acid trihydrate (NAT) (Crutzen and Arnold, 1986; Toon et al., 1986), (2) the conversion of hydrogen chloride (HCl) and chlorine nitrate ($ClONO_2$) to active chlorine on PSC surfaces as a mechanism for freeing chlorine from reservoir species into radical species (McElroy et al., 1986; Solomon et al., 1986), (3) the two catalytic cycles involving chlorine monoxide (ClO) and bromine monoxide (BrO) that destroy Antarctic ozone (McElroy et al., 1986; Molina and Molina, 1987), and (4) observations from field campaigns that supported the theory that the ozone hole is caused by elevated ClO and BrO levels in the lower stratosphere from human-produced chlorofluorocarbons and halons (de Zafra et al., 1987; P. Solomon et al., 1987; S. Solomon et al., 1987; Farmer et al., 1987). This WMO (1990a) polar ozone chapter also discussed in situ observations of ClO and BrO (subsequently published in Brune et al., 1989a; Brune et al., 1989b; Anderson et al., 1989). The 1989 Ozone Assessment (WMO, 1990b) included a chapter on polar ozone (Chapter 1) that presented extensive observations from field campaigns that overwhelmingly established human-produced chlorine and bromine chemicals as responsible for the ozone hole. The 1991 Ozone Assessment (WMO, 1992) did not include a specific chapter on polar ozone, but it updated polar ozone science in various sections of the report. WMO (1995) included a Polar Processes chapter (Chapter 3) that confirmed chlorine- and bromine-catalyzed ozone loss in the Antarctic and the Arctic from both in situ (Anderson et al., 1991; Toohey et al., 1993) and satellite observations (Waters et al., 1993). WMO (1999) included a chapter on lower stratospheric processes (Chapter 7), noting a number of very low Arctic ozone years and stating that the Antarctic ozone losses were continuing.

This chapter provides an update to Chapter 3 of the WMO (2003) Assessment on Polar Ozone: Past, Present, and Future. This chapter is derived from research over the last 4 years, other reports, and recent and updated observations from various field campaigns and new satellite instrumentation. Discussion of the recovery of polar ozone can be found in Chapter 6 (The Ozone Layer in the 21st Century), and polar chemistry-climate interactions can be found in Chapter 5 (Climate-Ozone Connections).

The WMO (2003) polar ozone chapter reported that in the Antarctic, springtime ozone depletion has been large throughout the 1990s, and that the area of the ozone hole varies from one year to another, but that it was not yet possible to say whether the area of the ozone hole had maximized. It was also reported that the polar vortex and ozone hole were persisting into early summer, increasing the impact on ultraviolet radiation.

In the Arctic, the WMO (2003) polar ozone chapter reported that there were a number of cold Arctic winters in the 1990s in which maximum total column ozone losses due to halogens had been quite large. In particular, Arctic chemical ozone loss for the 1999/2000 winter/spring season was extensively discussed, and an ozone loss was observed that reached 70% near 20 kilometers (km) by early spring, and total column ozone losses greater than 80 Dobson units (DU) (~20 to 25%) by early spring. The large 1999/2000 ozone losses were a result of the colder than average stratospheric vortex, consistent with our understanding. It was also reported that the magnitude of chemical loss of ozone for all Arctic winters during the 1990s showed generally good agreement between different analyses for quantifying losses. For the 1999/2000 winter, agreement was better than 20% in the Arctic stratosphere around 20 km.

This chapter is divided into 4 basic sections. Section 1 provides an update of observations of polar stratospheric conditions. Section 2 provides an update of theoretical progress on understanding polar ozone processes. Section 2 is divided into subsections on chemical processes and polar stratospheric clouds and aerosols. Section 3 provides a discussion of our current observations and also a description of an unprecedented splitting of the ozone hole that was observed in September 2002 just prior to the publishing of WMO (2003). A number of large solar particle events have occurred in the last few years and they are described, together with their impacts, in Section 4.

4.1 POLAR STRATOSPHERIC OBSERVATIONS UPDATE

4.1.1 Polar Stratospheric Dynamics and Transport

Variability in the dynamical conditions in the troposphere/stratosphere system results in variability of ozone transport and temperatures in the stratosphere. Previous Assessments and Section 4.2.1 of this document show that on short time scales, interannual variability in polar ozone chemistry is mainly driven by temperature variability, which in turn is the result of variable dynamical conditions. The combined effect of dynamically induced variability in both chemistry and transport is the main driver of interannual variability of the abundance of ozone in the polar stratosphere. This section gives an update of the dynamical conditions, temperatures, and transport of the polar winter stratosphere since the previous Assessment.

4.1.1.1 Temperatures and PSC Formation Potential

WMO (1999) and WMO (2003) have dealt at length with the observed temperature changes detected over the polar regions using observations (radiosondes and satellite sensors) as well as objective analysis products (e.g., Ramaswamy et al., 2001). During the period 1979-1998, satellite measurements showed a cooling of 3 K/decade in the Arctic and Antarctic middle stratosphere and significant coolings of 1.8 K/decade at 70°N and 1.1 K/decade at 70°S in the lower stratosphere during spring.

Following the mostly cold stratospheric winter and spring seasons of the early to mid-1990s, polar regions in both hemispheres were characterized by an alternation of cold and warm winter seasons since the late 1990s. As seen in Figure 4-1, Arctic lower stratospheric temperatures show considerable interannual variability. The variability is strongest during winter and spring due to the occurrence of midwinter and final sudden stratospheric warmings. Although several recent northern winters were cold (e.g., 1999/2000, 2002/2003, and in particular 2004/2005; see Figure 4-1), the northern winters 1998/1999, 2000/2001, 2001/2002, 2003/2004, and 2005/2006 were disturbed by stratospheric warmings and thus exhibited periods with high temperatures. In the Antarctic, interannual variability is much weaker than in the Arctic and is strongest during spring due to the timing of the Antarctic vortex breakup. In the Antarctic, an anomalously warm spring season was observed in 2002 (see Section 4.3.1), and relatively high temperatures also occurred in the years 2000 and 2004 in the lower stratosphere (100 hPa) (see Figure 4-2).

Given the interannual variability of stratospheric temperatures in winter and spring, determining statistically significant trends requires both sufficient temporal and spatial coverage and a careful choice of the applied trend model. As discussed in Section 5.2.6 of Chapter 5, different temperature datasets are available to derive trends. All of them have their own advantages and limitations. Long-term stratospheric temperature trends (since the late 1950s) are usually derived from radiosonde measurements or radiosonde-based gridded datasets such as the United Kingdom Meteorological Office (UKMO) adjusted dataset (RAOB) or the Freie Universität Berlin (FUB) stratospheric analyses. Radiosonde limitations due to instrumental and other operational discontinuities could be eliminated by applying new adjustment methods, e.g., as in the radiosonde atmospheric temperature products for assessing climate (RATPAC) (Lanzante et al., 2003; Free et al., 2005) and Hadley Centre Radiosonde Temperature 2 (HadAT2) (Thorne et al., 2005) datasets. However, radiosonde data are biased toward Northern Hemisphere (NH) continental locations due to data scarcity in the Southern Hemisphere (SH) and over extended oceanic regions. Satellite data provide better spatial and altitude coverage than radiosondes, but are only available since 1979. Their vertical resolution is limited, and they have to be composed from different instruments to build continuous time series (see Section 5.2.6 of Chapter 5). Recent assessments of the uncertainties of radiosonde- and satellite-derived temperature trends revealed disagreement in the lower stratosphere, with an overestimation of the stratospheric cooling in the radiosonde data (Seidel et al., 2004). The bias was confined to the tropics, and thus polar temperature trends should not be affected (Randel and Wu, 2006).

Reanalysis products that result from the assimilation of radiosonde and satellite data provide an alternative source for long-term trend estimates. They are, however, affected by changes in the input data and the assimilation systems and therefore are not generally suited for trend estimates (Bengtsson et al., 2004; Santer et al., 2004). Labitzke and Kunze (2005) compared North Pole temperature trends for the lower and middle stratosphere derived from the National Centers for Environmental Protection/National Center for Atmospheric Research (NCEP/NCAR) and European Centre for Medium-Range Weather Forecasts (ECMWF) Re-Analysis 40 (ERA40) reanalyses with those derived from subjective FUB stratospheric analyses that are closely matched to direct radiosonde measurements. They confirmed that largest discrepancies between ERA40 and FUB data exist during the winter months in

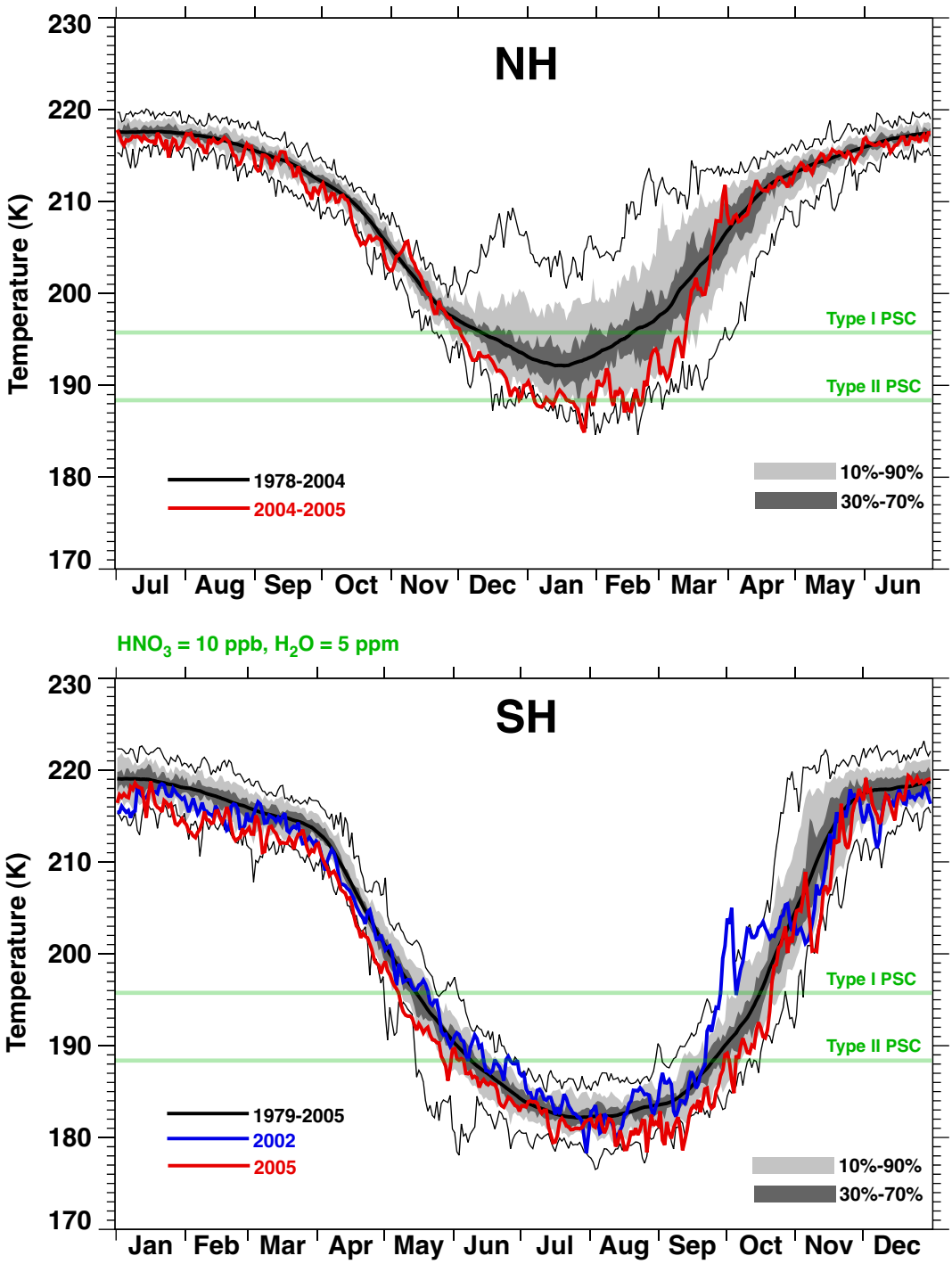

Figure 4-1. Annual temperature cycle and variability at 50 hPa for minimum temperature between 50°N and 90°N (top), and between 50°S and 90°S (bottom) from the National Centers for Environmental Prediction/National Center for Atmospheric Research (NCEP/NCAR) reanalysis data. The black line shows the mean annual cycle for the periods 1978-2004 (Northern Hemisphere, NH) and 1979-2005 (Southern Hemisphere, SH). The red line shows the evolution during 2004/2005 (NH) and 2005 (SH). In the case of the SH, the blue line shows the evolution during 2002, i.e., the year with the anomalous Antarctic vortex behavior. Dark gray shading shows the 30 to 70% probability of observations, light gray shading shows the 10 to 90% probabilities, and the lower and upper thin black lines show the record values for the 27 years of observations. Green lines indicate the thresholds for PSC formation (nitric acid (HNO_3) = 10 ppb and H_2O = 5 ppm). Updated from Figure 3-13 in WMO (2003).

the middle stratosphere, when the enhanced cold polar bias of the pre-satellite era in ERA40 affects the long-term trends (1958-2001) (Bengtsson et al., 2004). The use of reanalyses for polar spring temperature trends is justified because the discrepancies between the ERA40, NCEP/NCAR, and FUB datasets are negligible.

Figure 4-2 shows spring stratospheric temperature trends derived from NCEP/NCAR reanalyses for the period 1958-2005 at the altitudes of maximum cooling for the Arctic polar cap (60°N-90°N) at 30 hPa in March (Figure 4-2a) and for the Antarctic polar cap (60°S-90°S) at 100 hPa in October (Figure 4-2b) (updated from Labitzke and Kunze, 2005). Post-volcanic periods (24 months) following the three eruptions of Mt. Agung in 1963, El Chichón in 1982, and Mt. Pinatubo in 1991 were excluded to avoid a contamination of the trend.

During the past 25 years, Arctic temperatures showed a clear downward trend of −1.70 ± 0.20 K/decade in March. Compared with the trend estimates for the period 1979-1998 (WMO, 2003) however, the magnitude of the stratospheric temperature trend in Arctic spring has decreased by about 50%. For the full period 1958-2005, only a very small, non-significant trend of −0.25 ± 0.20 K/decade can be detected due to a warming of the Arctic stratosphere during the 1960s and early 1970s (Figure 4-2a), which nearly compensates the cooling of the later decades. The dependence of the trends on the underlying time period demonstrates the strong impact of low-frequency dynamical variability on polar temperatures. Multidecadal time series are thus required to minimize the effect of low-frequency dynamical variability in trend calculations, in particular in the Arctic. This observational result is further supported by idealized model experiments (Nishizawa and Yoden, 2005).

In the Antarctic lower stratosphere (100 hPa), the cooling trend since the late 1970s is substantially smaller than that reported in WMO (2003) due to increased dynamical variability of the Antarctic polar vortex that led to unusually high spring temperatures of the polar cap in the years 2000, 2002, and 2004. Consistently, the temperature change in October between 1979 and 2005 is very small at 100 hPa (−0.23 ± 0.20 K/decade) (Figure 4-2b) and becomes even positive at higher altitudes (+1.01 ± 0.25 K/decade at 50 hPa and +2.02 ± 0.24 K/decade at 30 hPa). On the long-term scale, a small warming of 0.36 ± 0.18 K/decade occurred at 100 hPa.

As in Figure 4-2, long-term atmospheric changes are usually described in terms of linear trends per decade using multiyear time series, or the derivation of differences between averaged sub-periods, e.g., the temperature difference between 1990s and the 1970s. The magnitude and the statistical significance of the calculated changes in both methods strongly depend on the

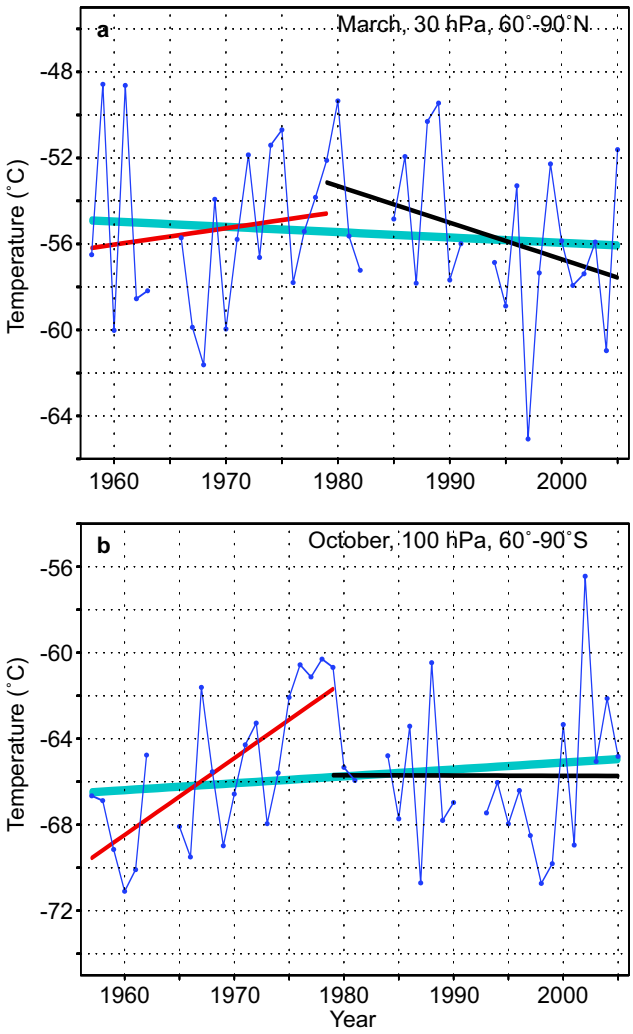

Figure 4-2. Arctic 30-hPa March (a) and Antarctic 100-hPa October (b) temperatures (°C) derived from the NCEP/NCAR reanalysis data. Trend lines were added for the periods 1958-1979 (red), 1979-2005 (black), and 1958-2005 (turquoise). Updated from Labitzke and Kunze (2005).

data period, as seen in Figure 4-2. For the purpose of understanding the nature of the observed changes, new statistical approaches were suggested in which trends may occur in flat or sloped steps including breakpoints with abrupt changes (Seidel and Lanzante, 2004) or the use of polynomials (Malanca et al., 2005). A comparison of the methods showed that a description of stratospheric cooling by a gradual linear change since the late 1950s (without considering the singular volcanic eruptions) is as equally valid as a description by a more step-like downward trend concentrated in the two-year periods after the three major volcanic eruptions (Seidel and Lanzante, 2004), which was also suggested by Pawson

et al. (1998). Climate model simulations suggest that the stratospheric cooling since 1979 was driven by anthropogenic factors (i.e., ozone depletion and increases in well-mixed greenhouse gases) but modulated by natural factors (i.e., solar variability and volcanic aerosols) (Ramaswamy et al., 2006).

In summary, the Arctic stratosphere has cooled over the past 27 years, however due to stronger dynamical variability in a number of recent winters and springs, the negative temperature trend is only about half the magnitude of the estimate in WMO (2003). In the Antarctic lower stratosphere, the cooling trend since the late 1970s has become less negative than that reported in WMO (2003) due to increased dynamical variability.

Estimating the overall trend of the polar stratospheric temperatures is not sufficient to assess the impact of long-term temperature changes on ozone chemistry. The large Arctic ozone losses are driven by the evolution of conditions during cold winters. Warm winters are much less relevant for ozone chemistry, because chemical loss of ozone is very limited and the chemistry is not very sensitive to small changes in temperature. Section 4.2.1 shows that the interannual variability in Arctic chemical ozone loss mainly follows the volume of temperatures cold enough to activate chlorine on particle surfaces (i.e., V_{PSC}). Figure 4-3 shows the long-term evolution of V_{PSC} derived from stratospheric temperature analyses for the Arctic (updated from Rex et al., 2004). Over the past 40 years, the cold Arctic winters became colder, resulting in larger values for V_{PSC} and chemical ozone loss. The long-term data shown in Figure 4-3 relies on the FU-Berlin subjective radiosonde analysis. Hence, the dataset is relatively independent of the introduction of satellite observations or assimilation system changes (e.g., Manney et al., 2003b). A linear fit through the solid points in Figure 4-3, which represents maximum values of V_{PSC} for 5-year intervals, has a slope of $9.9 \pm 1.1 \times 10^6$ km^3 per decade, with very similar results if 4- to 10-year intervals are chosen to select the maximum values (update of Rex et al., 2004). Rex et al. (2006) also have shown that it is unlikely (well below 1% probability) that this estimated tendency toward colder Arctic winters is a purely random event or is caused by inconsistencies in the meteorological datasets.

The tendency of decreasing temperatures during cold winters is in contrast to the clustering of a series of warmer than average winters during recent years. Hence, the temperature trend during the cold winters is different from the overall temperature trend. The change in temperature during the cold winters is much larger than expected from the direct radiative effect of increasing greenhouse gas concentrations. The reason for the change is not clear and it could be due to long-term natural climate variability or an unknown dynamical feedback mechanism.

4.1.1.2 Vortex Parameters

The mean structure and seasonal evolution of the polar vortices and their hemispheric differences were discussed in detail in WMO (2003). The Arctic polar vortex is much more perturbed by planetary wave activity propagating upward from the troposphere than the Antarctic vortex. It is important to assess such dynamical variations and their changes as they determine, together with

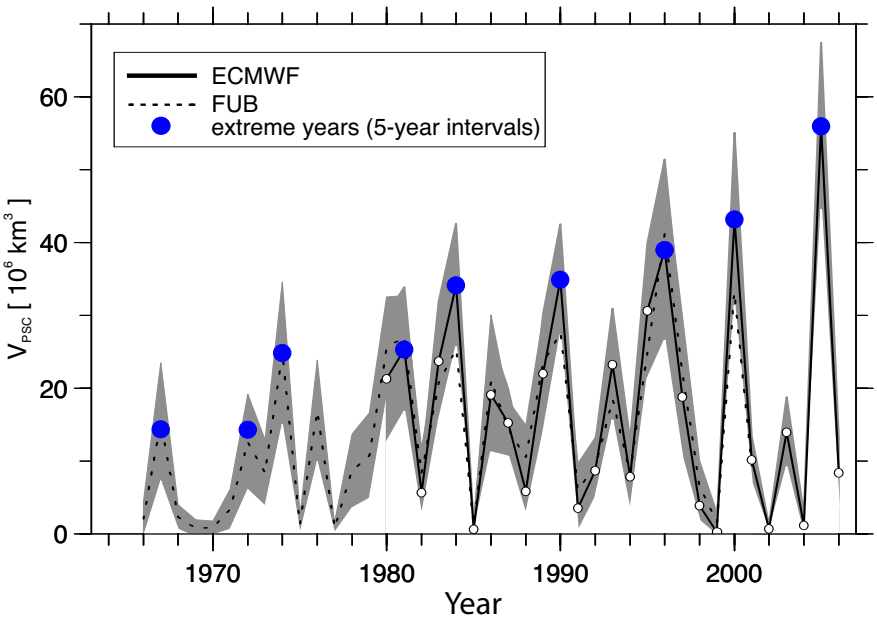

Figure 4-3. Evolution of V_{PSC} for the Arctic over the past four decades, composed from ECMWF and FUB data. The blue dots represent the maximum values of V_{PSC} during five-year intervals. The dotted line is based on radiosonde analyses of the FUB, and the solid line is ECMWF ERA-15 data extended by operational analyses. The gray shading represents the uncertainty of V_{PSC} based on a 1-K uncertainty of the long-term stability of radiosonde temperatures. Updated from Rex et al. (2004).

chemical processes, the ozone column at polar latitudes during spring (Randel et al., 2002; Huck et al., 2005).

The breakup dates of the Arctic and Antarctic vortices (Figure 4-4) as determined by the wind average along the vortex edge vary from year to year in both hemispheres (WMO, 2003). For the Arctic vortex, no discernible long-term trend in the breakup date appears since the 1960s (Langematz and Kunze, 2006). The period between the mid-1980s to the mid-1990s however showed a tendency toward later breakdown dates. These years were characterized by a reduced dynamical variability, with nine consecutive winters without major stratospheric warmings from 1989/1990 to 1997/1998 (Labitzke et al., 2002; Manney et al., 2005c). In contrast, since 1998/1999, the Arctic exhibited a clustering of warmer than average and dynamically disturbed winters. Major warmings took place in the winters 1998/1999, 2000/2001, 2001/2002, 2002/2003, 2003/2004 and 2005/2006, leading to weak or split vortices. Consistent with these changes in dynamical variability, the vortex breakup date varied between mid-February 2001 and early May 1997, with three late breakups since 2002. However, this recent delay in the breakup date is not statistically significant and does not indicate a trend (Langematz and Kunze, 2006). The described alternation of cold (1989/1990-1997/1998) and warm (1998/1999-2005/2006) clusters may be interpreted as shifts between warmer/weaker and colder/stronger vortex regimes (Perlwitz and Graf, 2001; Perlwitz and Harnik, 2003). These shifts may be caused by anthropogenic processes (i.e., ozone depletion and greenhouse gases) that nonlinearly force natural modes of variability (Corti et al., 1999; Pawson et al., 1998; Christiansen, 2003). Such a clustering also could be a random occurrence, as shown in model simulations by Taguchi and Yoden (2002).

The Antarctic vortex exhibited a delay of the breakup date from late November into mid-December which is consistent with an intensification of the vortex (Huth and Canziani, 2003; Renwick, 2004) caused by additional radiative cooling following strong Antarctic ozone loss in spring (Shine, 1986; Jones and Shanklin, 1995). However, since the late 1990s, there is larger variability in the breakup date over Antarctica with the process taking place sometime between the second half of November (1997, 2000, and 2002) and late December (1999, 2001). The tendency toward a later vortex breakup date has stopped and perhaps reversed (Langematz and Kunze, 2006). This means that, compared with the 1960s and 1970s, the Antarctic vortex is still more persistent; however, compared with the 1980s/early 1990s, the Antarctic vortex broke down earlier in recent years. This is probably the result of the large interannual variability in recent Antarctic winters and springs (see Section 4.1.2).

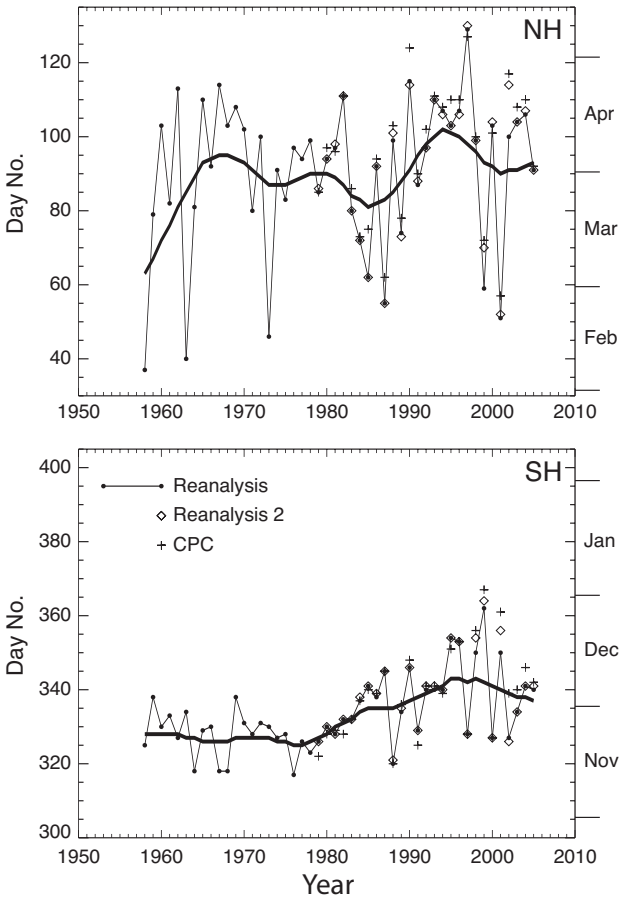

Figure 4-4. Vortex breakup dates from 1958 to 2005 on the 500-K isentropic surface over the NH (top) and the SH (bottom) using the method described in Nash et al. (1996). The filled lines with dots are the dates calculated from the NCEP/NCAR reanalysis data. The thick lines are the same data, time-filtered to remove interannual fluctuations. The crosses are the breakup dates calculated from NCEP/Climate Prediction Center analyses for the period 1979-2005. Updated from Figure 3-10, WMO (2003).

Summing up, since the previous Assessment (WMO, 2003) changes in the interannual behavior of both polar vortices have been observed. The Artic vortex continues to show large variability with a shift from a period of dynamically undisturbed winters between 1989/1990 and 1997/1998 to a period of more dynamically disturbed winters from 1998/1999 to 2005/2006. The Antarctic vortex has shown an enhanced variability since the late 1990s compared with previous decades, which culminated in the anomalous vortex split in 2002. The reasons for the observed changes in the interannual variability in both hemispheres are not yet understood.

4.1.1.3 TRANSPORT

Besides chemistry, transport is the main driver for ozone variability at high latitudes. Chemical and transport-related causes for polar ozone variability are closely coupled, particularly in the Arctic. Transport contributions to polar ozone variability are closely controlled by the strength of the middle atmospheric residual circulation that, in turn, is driven by tropospheric (planetary and gravity) wave forcing; strong winter planetary wave forcing leads to larger transport of ozone to high latitudes due to a stronger residual circulation and a higher-than-average Arctic lower stratosphere temperature and a weaker vortex in early spring, whereas weak winter forcing leads to less transport and lower Arctic temperatures in spring and to a stronger vortex (Fusco and Salby 1999; Newman et al., 2001). For the Arctic, Rex et al. (2004) find that for the current halogen loading, about one-half of the year-to-year variability in total ozone is caused by variability in anthropogenic chemical ozone loss and one-half by variability in transport with the variable residual circulation. Because temperatures influence chemistry, both terms are correlated.

Although the variability is larger in the Arctic compared with the Antarctic, wave activity,has been shown to correlate well with the observed change of polar column ozone over the course of winter for both hemispheres (Randel et al., 2002; Weber et al., 2003; see also Figure 4-5). It has been shown that in the Antarctic, this is due to the same co-action of transport and chemistry as in the Arctic. Newman et al. (2004) and Huck et al. (2005) showed that the year-to-year variability of Antarctic ozone depletion is driven by the year-to-year variability of the polar vortex temperatures. Huck et al. (2005) also showed that interannual variability in Antarctic stratospheric temperatures and ozone loss are affected by midlatitude wave activity, while the decadal increase in Antarctic ozone loss is driven by the increase in halogens.

In climate models, planetary wave activity has been shown to partially depend on sea surface temperatures, among other forcings (Schnadt et al., 2002). It is therefore susceptible to climate change. The external factors determining stratospheric wave forcing and its interannual variability (i.e., stochastic tropospheric dynamics, quasi-biennial oscillation (QBO), sea surface temperatures (SSTs), solar variability, and volcanic eruptions) are difficult to quantify; Chapter 6 discusses the impact of these uncertainties for the predictability of future changes of polar ozone.

Besides the systematic transport of ozone to high latitudes with the residual circulation, another important aspect of transport is mixing. Although mixing across the vortex edge is relatively weak, it has an effect on the distribution of ozone within the polar vortices. The Antarctic vortex is divided into two distinct regions of approximately

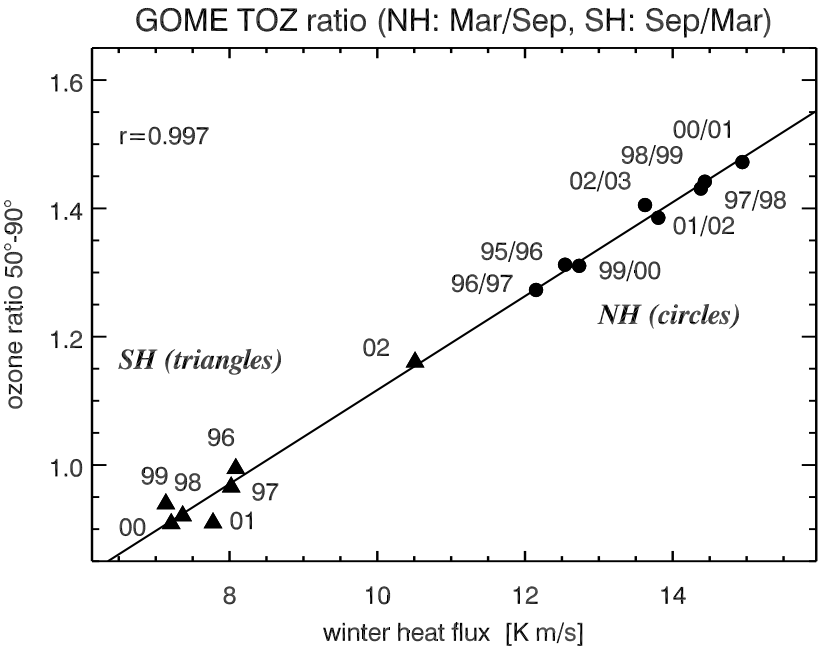

Figure 4-5. Increase of ozone over the winter as a function of planetary wave activity. Planetary wave activity is measured as winter eddy heat flux in the respective hemisphere. The ozone ratio of the zonal mean between 50° and 90° latitudes from March over that from September is shown for the NH, and September over March for the SH. Circles are NH values, and triangles represent SH values. Total ozone is from weighting function differential optical absorption spectroscopy (WFDOAS) V1 (Weber et al., 2005). The monthly mean eddy heat flux at 100 hPa averaged from 40 to 75 degrees latitude is derived from ECMWF ERA40/operational analysis, and has been averaged from fall to spring in each hemisphere. SH winter eddy heat flux is negative, but is shown here as absolute values. Updated from Weber et al. (2003).

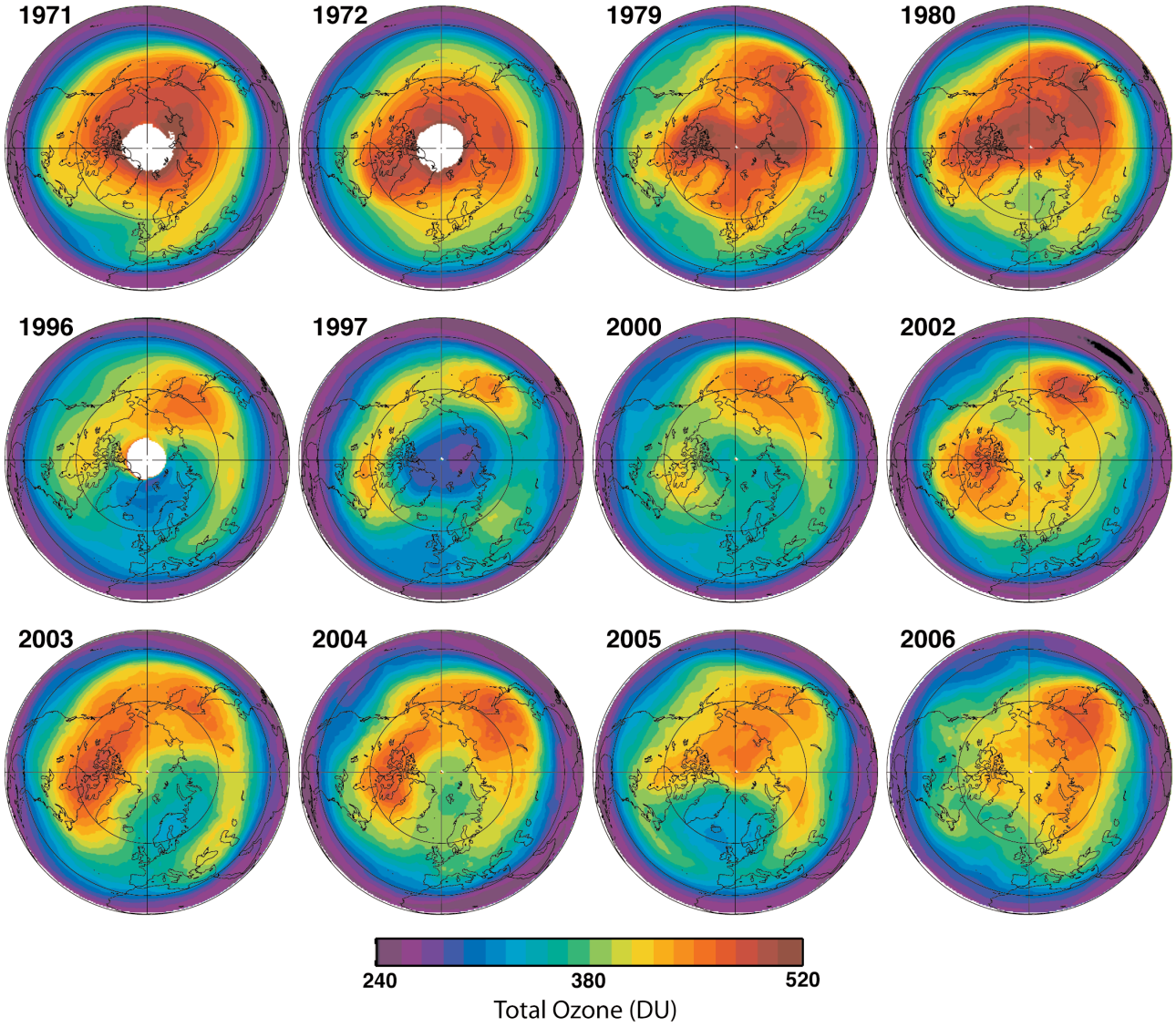

Figure 4-6. March monthly averaged total ozone for the Arctic. The 1971 and 1972 images are from the Nimbus-4 Backscatter Ultraviolet (BUV) instrument; the 1979 and 1980 images are from the Nimbus-7 TOMS instrument; the 1996 image is from the NOAA-9 SBUV/2 instrument; the 1997, 2000, 2002, 2003, and 2004 images are from the Earth Probe TOMS instrument; and the 2005 and 2006 images are from the Aura Ozone Monitoring Instrument (OMI). This figure is updated from Figure 7-21 of WMO (1999).

equal area: a strongly mixed vortex core and, separated from the core, a broad ring of weakly mixed air extending to the vortex boundary (Lee et al., 2001). This division was deduced from an analysis of a mixing diagnostic (the so-called "equivalent length") based on transport calculations of an artificial tracer field on an isentropic surface (480 K) for the period from July to November. A transport barrier within the Antarctic vortex between July and November, is likewise apparent for the altitude range between 475 and 650 K in the potential vorticity field (Tilmes et al., 2006b) and, moreover, extends to the setup phase of the Antarctic vortex in March and April (Tilmes et al., 2006a). During March and April, ozone-tracer relations in the two vortex regions are clearly distinct (Tilmes et al., 2006a). Further, measurements of ozone and volcanic aerosol show rather different vertical profiles within the vortex core and in the edge region (Godin et al., 2001). A better understanding of the dynamical mechanisms responsible for the occurrence of transport barriers within the vortex is important, because temperature variations in the weakly mixed air mass between the vortex boundary and the vortex core drive the year-to-year variability of

about 10-20% in the area of the ozone hole (measured as the area enclosed in the 220-DU contour) (Newman et al., 2004).

4.1.2 Polar Ozone

This section presents observations of ozone and diagnoses of ozone destruction in both polar regions. Section 4.1.2.1 gives an update of observations of ozone and the primary chlorine species involved in stratospheric ozone destruction, along with a discussion of various indicators that capture different aspects of ozone hole area and severity. A discussion of other trace gas species such as BrO and chlorine dioxide (OClO) can be found in Section 4.2.1 and Chapter 2 (Section 2.5.1), and nitrogen dioxide (NO_2) is discussed in Chapter 3 (Section 3.3.2). In Section 4.1.2.2, refinements since the previous Assessment (WMO, 2003) of various methods for quantifying chemical ozone loss in the Arctic polar vortex are presented. Near-record ozone losses during the Arctic 2004/2005 winter are discussed. Finally, recent progress in quantifying ozone loss rates in the Antarctic is discussed.

4.1.2.1 Ozone and Other Constituents

The ozone content in the Arctic stratosphere is dependent on chemical and dynamical conditions and shows great interannual variability. This section discusses resulting interannual variability of ozone and other constituents, which is due to the combined effect of transport and chemistry. Section 4.1.2.2 isolates the impact of anthropogenic chemical loss on polar ozone variability from the variability in transport.

As noted in the previous section, the formation, evolution, and breakup of the polar vortex and the occurrence of stratospheric warmings are subject to large year-to-year variations. Figure 4-3 shows that the variability in amplitude of V_{PSC} (PSC formation potential derived from stratospheric temperature analyses) in the Arctic has clearly increased over the last 40 years, with 1995/1996, 1999/2000 and 2004/2005 standing out as cold winters with high PSC formation potential, whereas 1998/1999, 2001/2002, and 2003/2004 were warm winters with very low PSC formation potential. As discussed in the previous section, this variability in dynamical conditions has a correlated impact on ozone transport and chemistry and is therefore reflected in the total ozone column over the polar regions.

Total Ozone Average

Arctic total ozone has remained low over the last few years in comparison with pre-1982 observations. Figure 4-6 displays a series of March averages for selected years from 1971 to 2006 (updated from Figure 7-21 in WMO, 1999). The 60°N latitude circle generally encloses the region of low ozone, but in some years (e.g., 2005) the vortex and low-ozone region are displaced from the pole, extending southward of 60°N. Nevertheless, Arctic ozone levels during March of recent years are low in comparison with the observations prior to 1980, as shown in the top row of Figure 4-6.

The springtime average total ozone values in the Arctic and Antarctic poleward of 63° latitude are shown in Figure 4-7 in comparison with the average total ozone for the years 1970-1982 (gray lines). The difference between the observed values and the 1970-1982 average indicates the combined changes in ozone due to chemistry and dynamics. In the last 9 years, Arctic column ozone exceeded the low values of the mid-1990s, except in the cold and chemically active winter of 1999/2000, when a large decrease of 63°-90° NH total ozone was observed. The record-cold winter of 2004/2005, however, showed a less pronounced impact on the March polar average total ozone. Although NH polar column ozone averages are in general a good indicator of Arctic ozone depletion (WMO, 2003), the March average in 2004/2005 reflects the strong influence of dynamics (e.g., vortex fragments moved outside the 63°-90° region during March, see Figure 4-6) and is consequently high relative to those of other recent cold winters even though the magnitude of chemical ozone

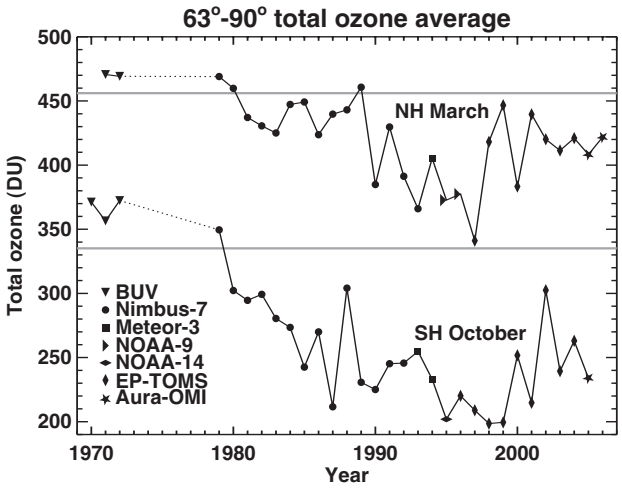

Figure 4-7. Total ozone average of 63°-90° latitude in March (NH) and October (SH). Symbols indicate the satellite data that have been used in different years. The horizontal gray lines represent the average total ozone in March for the years prior to 1983 for the NH and SH. Updated from Figure 3-2, WMO (2003).

loss in the lower stratospheric vortex was as high as or higher than in those years (cf. Section 4.1.2.2).

In the SH polar region, the lowest average October total ozone values were observed in the late 1990s (Figure 4-7, bottom panel). The last 6 years have shown an increase in polar column ozone averages, with a high degree of variability and notably higher ozone values in 2000, 2002, and 2004 resulting from greater dynamical activity.

To aid the detection of the recovery of the Antarctic ozone hole (discussed in detail in Chapter 6), various metrics that capture different aspects of the ozone hole are used to describe the severity of ozone depletion, such as ozone hole area, ozone minimum, ozone mass deficit, and date of ozone hole appearance and disappearance. Figure 4-8 displays ozone hole area (top panel), ozone hole minimum (middle), and ozone mass deficit (bottom). Following Newman et al. (2006), we have added a fit of these metrics (gray line) to a quadratic function of Antarctic equivalent effective stratospheric chlorine (EESC) (see Box 8.1 for a description of Antarctic EESC).

Ozone Hole Area

A primary estimate of the severity of the Antarctic ozone hole is its geographic area (WMO, 2003). Figure 4-8 (top panel) shows the ozone hole area calculated from the area contained by total column ozone values less than 220 DU during 21-30 September from Total Ozone Mapping Spectrometer (TOMS) and Ozone Monitoring Instrument (OMI) observations. The value 220 DU was chosen to define the ozone hole because it is almost always a middle value in a strong gradient of total ozone, and because it is lower than pre-1980 observed ozone values. The average ozone hole area currently reaches approximately 25 million km^2 each spring, while the single largest daily value reached nearly 30 million km^2 in September 2000 (Newman et al., 2004). Ozone depletion can be enhanced by volcanic perturbations (e.g., Hofmann and Oltmans, 1993) as could be seen in the very strong ozone depletion (or "deep ozone holes") observed in the 1990s after the Mt. Pinatubo eruption (e.g., 1994). The area growth of the ozone hole slowed during the mid-1990s, with a large dip in 2002.

Ozone Minimum

The daily total column ozone minimum value is a widely used measure of the state of the ozone hole. Average minimum ozone columns calculated over Antarctica for the period 21 September to 16 October show a clear decrease from 1979 to the mid-1990s, with the

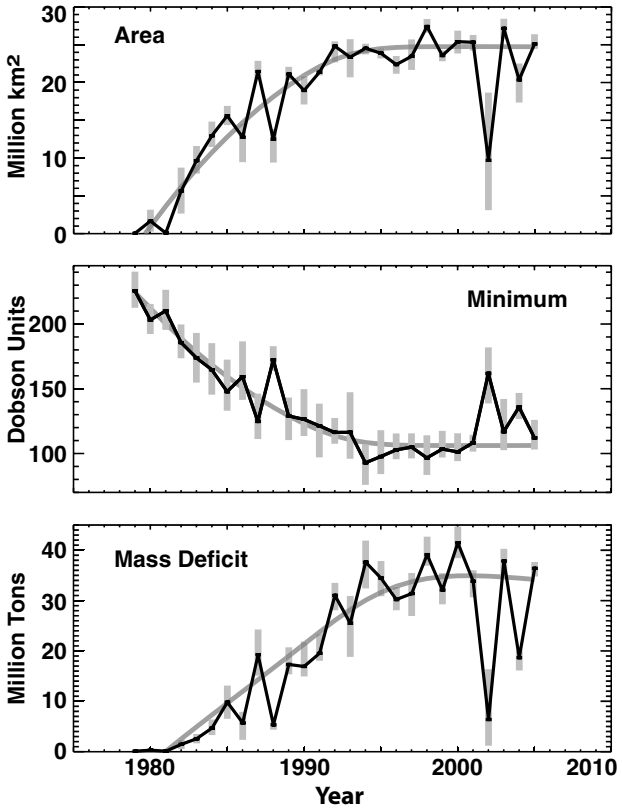

Figure 4-8. Top panel: Area of the Antarctic ozone hole for 1979-2005, averaged from daily total ozone area values contained by the 220-DU contour for 21-30 September. The gray bars indicate the range of values over the same time period. The gray line shows the fit to these area values as was shown in Newman et al. (2004), and now using EESC, as derived in Newman et al. (2006) (see also Box 8.1 in Chapter 8). The EESC has a mean age of 5.5 years, an age spectrum width of 2.75 years, and a bromine-scaling factor of 50. The fit is quadratic in EESC. Middle panel: An average of daily minimum ozone values over Antarctica during the period from 21 September to 16 October. The gray bars indicate the range of ozone values over the same time period. The gray line is the fit as described for the top panel. Bottom panel: Ozone mass deficit (OMD) average over the 21-30 September period. The gray bars indicate the range of values over the same time period. The gray line is the fit as described for the top panel. This figure was generated using the merged ozone data courtesy of Greg Bodeker (NIWA) and NCEP/NCAR reanalysis 2 data. Updated from Figures 3-5 and 3-7 from WMO (2003).

lowest minimum value observed in 1994 (Figure 4-8, middle panel).

Ozone Mass Deficit

The ozone mass deficit (OMD) combines the effects of changes in ozone hole area and depth, and provides a direct measure of the deficit relative to the mass present for a value of 220 DU (e.g., Uchino et al., 1999). Figure 4-8 (bottom panel) shows the OMD averaged over the period 21-30 September. While the long-term evolution of the OMD follows the halogen loading, there is higher frequency year-to-year variability; years with anomalously high wave activity (1988, 2002, and 2004) show weak Antarctic ozone depletion, and years with suppressed wave activity show severe depletion (Huck et al., 2005, and references therein).

Daily values of OMD over Antarctica for the years 2002-2005 are compared with the range of values over the period 1990-2001 in Figure 4-9. This plot shows that, apart from 2002, the year 2004 also stands out as having a weak ozone hole, while the OMD in the 2003 and 2005 Antarctic winters is more comparable to those observed during the 1990s. Although lower stratospheric (50 hPa) minimum temperatures were below average over much of the 2004 Antarctic winter, they increased and remained near average after mid-August (Santee et al., 2005). The lower stratosphere warmed rapidly in September, halting further heterogeneous processing of vortex air by the end of the month. This resulted in a slow increase in OMD and a leveling off in late September (see Figure 4-9). At the end of September, a large increase in mixing accompanied by a weakening vortex transport barrier signaled vortex erosion leading to the breakup (Manney et al., 2005b).

Hoppel et al. (2005b) used measurements from both the Polar Ozone and Aerosol Measurement (POAM) instrument and South Pole ozonesondes to investigate changes in the ozone mixing ratio near the top (20-22 km) of the ozone hole, comparing the years 2001-2004 with the previous six years of POAM observations (1994-1996; 1998-2000). They found that in this altitude range, the year 2004 was distinguished by the highest minimum vortex temperatures throughout August and September, the lowest observed PSC frequency, and the smallest photochemical ozone loss.

Chlorine Partitioning

The evolution of chlorine partitioning in the winter polar vortices of both hemispheres is shown in Figure 4-10. In this figure, contemporaneous measurements from two recent satellite missions are used to update the conceptual sketch of wintertime chlorine par-

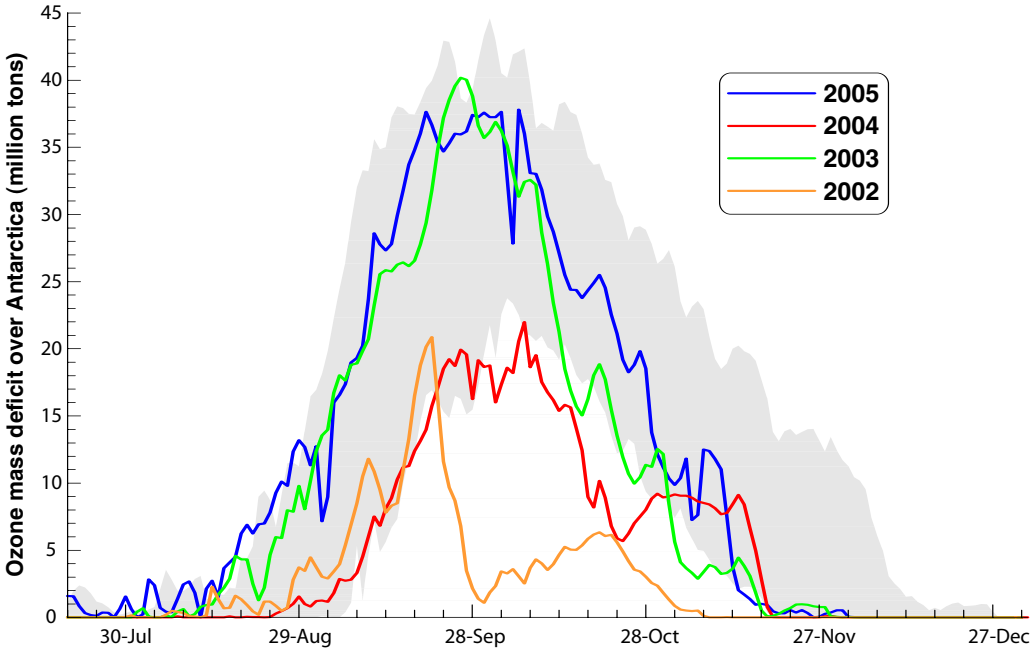

Figure 4-9. Daily OMD over Antarctica for the years 2002-2005 compared with the range of values over the period 1990-2001. The grayed area shows the daily range from 1990 to 2001. Adapted from Bodeker et al. (2005).

titioning presented in a previous WMO Assessment (WMO, 1995; Figure 3-1). Although several studies based on satellite, aircraft, balloon, and ground-based measurements over the last decade have provided insight into both the relative abundances of the main chlorine reservoirs prior to activation and the interhemispheric differences in their recovery at the end of winter, the new data from the Atmospheric Chemistry Experiment Fourier Transform Spectrometer (ACE-FTS) (e.g., Dufour et al., 2006) and the Aura Microwave Limb Sounder (MLS) (e.g., Santee et al., 2005) are of unprecedented scope for studying seasonal changes in chlorine partitioning. In particular, the dominant chlorine reservoir before the onset of PSC processing is confirmed to be HCl, not $ClONO_2$ as indicated in the schematic shown in WMO (1995).

In the Antarctic (Figure 4-10, left panel), chlorine is converted into the active form ClO by early June; elevated abundances of ClO then persist through mid-September. In the severely denitrified and ozone-depleted conditions characteristic of late Antarctic winter, HCl production is highly favored and $ClONO_2$ production is suppressed.

In the Arctic (Figure 4-10, right panel), the magnitude and duration of chlorine activation are much smaller than the Antarctic, even in a relatively cold winter. The ACE-FTS and Aura MLS measurements clearly support the canonical picture of initial chlorine deactivation in the Arctic, with the primary pathway the reformation of $ClONO_2$, followed by slow repartitioning between $ClONO_2$ and HCl.

4.1.2.2 Polar Ozone Loss Studies

Quantifying Arctic Ozone Loss

Diagnosing chlorine-catalyzed ozone destruction requires distinguishing the effects of chemical processes from those of transport and mixing, especially in the Arctic, where ozone abundances are strongly controlled by dynamics. WMO (2003) presented an overview of the methods commonly used to estimate chemical ozone loss and discussed the limitations and sources of uncertainty of each, as well as the degree of consistency between them. Most of these techniques have been significantly refined since the previous Assessment, with a particular emphasis

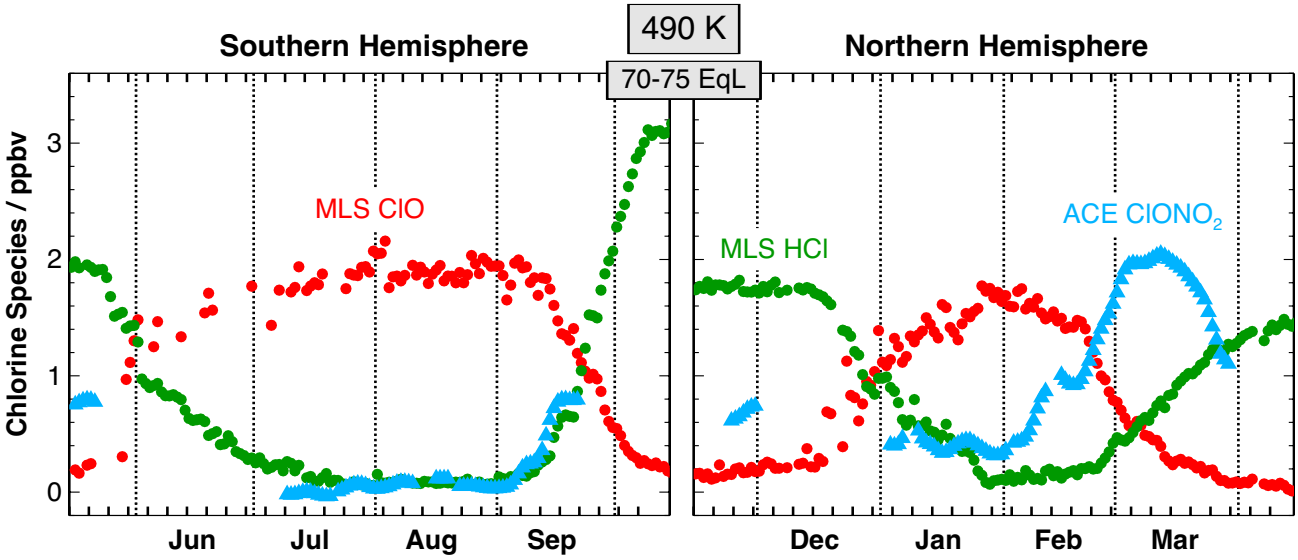

Figure 4-10. Left panel: Daily averages of ClO (red dots) and HCl (green dots) observed by Aura MLS, and $ClONO_2$ (cyan triangles) observed by ACE-FTS at 490 K (~20 km) during the 2005 Antarctic winter/spring period, calculated over the 70°-75° equivalent latitude band using the Global Modeling and Assimilation Office Goddard Earth Observing System (GEOS-4) temperatures and potential vorticity. Only daytime measurements are included in the averages for ClO; ClO data appear sparser because measurements in sunlight are not always available at high equivalent latitudes, especially in early winter. The sampling pattern of ACE-FTS, a solar occultation instrument, does not provide coverage of this equivalent latitude band at all times throughout the winter. Right panel: As in the left panel, for the 2004/2005 Arctic winter/spring period.

on quantifying the uncertainties in the loss estimates. This section presents an update of recent progress in separating chemical and dynamical effects and quantifying ozone destruction, mainly in the context of the 2002/2003 Arctic winter. In 2002/2003, an unusually cold early winter promoted an earlier inception of significant ozone destruction than in most other recent cold winters (e.g., Goutail et al., 2005; Streibel et al., 2006). The mid- to late winter was very dynamically active and warmer than average, but with a series of stratospheric warming events that limited cumulative ozone loss. Aircraft and ground field campaigns in the 2002/2003 winter provided an excellent opportunity to assess understanding of polar ozone loss processes, especially under the high solar zenith angle conditions of early winter. The different approaches to calculating chemical ozone loss generally agree well, lending confidence in the estimates.

Ozone/Tracer Correlation Method. In this technique, changes in the compact correlations between ozone and long-lived tracers over the winter are ascribed to chemical loss. This approach assumes that a reference ozone/tracer relation representative of the early-winter polar vortex can be established and that transport and mixing processes do not significantly alter it, assumptions that had been questioned at the time of the previous Assessment (e.g., Harris et al., 2002; WMO, 2003; Sankey and Shepherd, 2003). The technique was refined in recent applications (Müller et al., 2002; Tilmes et al., 2003), and a comprehensive re-evaluation of ozone loss in the Arctic winters 1991-2003 was performed (Tilmes et al., 2004). Ozone loss estimates generally agreed well with those based on other approaches, with the smallest estimated errors obtained in the coldest winters with greatest loss; the major contribution to the error in the calculated loss remained the uncertainty in the reference relation. Müller et al. (2005) confirmed the validity of ozone-tracer relations for quantifying chemical loss, provided that a reliable early vortex reference is obtained and vortex and midlatitude air masses are well separated by a strong transport barrier at the vortex edge.

Match Method. "Match" is a pseudo-Lagrangian technique involving identification (through trajectory calculations) of air parcels sampled two or more times in a prescribed interval; differences in the observed ozone mixing ratios are attributed to chemical loss. Match has received substantial attention since the previous Assessment. Morris et al. (2005) revisited the January-March periods in 1992 and 2000 using a different trajectory code and meteorological analyses than in the original Match studies (Rex et al., 1998, 2002). They confirmed the statistical error bars published previously, but concluded that actual uncertainties in the calculated ozone loss rates are larger because of additional systematic errors, consistent with earlier discussions of systematic Match uncertainties (e.g., Rex et al., 1998; Harris et al., 2002). Morris et al. (2005) recommended that future Match studies employ extended (14-day) trajectory calculations and suggested that some of the filter criteria built into the approach may be unnecessary. In contrast, Grooß and Müller (2003) carried out a virtual Match campaign in the Chemical Lagrangian Model of the Stratosphere (CLaMS) three-dimensional (3-D) chemical transport model and found that these filter criteria reduce the statistical uncertainty of the estimated ozone loss rates and remove a systematic bias induced by mixing across the vortex edge, particularly during periods of strong vortex disturbances.

Lehmann et al. (2005) developed a statistical approach to take into account the error correlation between matches that share a common ozone measurement and found that it depends nearly linearly on the "oversampling rate" (i.e., the average number of matches to which an ozone measurement contributes). For ozonesonde Match studies, the oversampling rate is low and the average increase in the error bars is 15%. For satellite Match studies, however, the oversampling rate is typically much higher and uncertainties increase by more than 50% compared with those estimated assuming uncorrelated errors. This updated approach to estimating uncertainties was used for the 2002/2003 Match study (Streibel et al., 2006), which also included the use of higher-resolution wind fields for the trajectory calculations, the imposition of a backward match radius in addition to the criterion along the forward trajectory, and the earliest start of a Match campaign, allowing investigation of ozone loss starting in December.

Vortex-Average Method. In this method, the difference between an initial profile altered using diabatic descent rates (estimated using a radiation code) and a final observed profile yields an estimate of chemical loss. Grooß and Müller (2003) used CLaMS simulations to quantify the influence of intrusions of midlatitude air into the vortex on ozone loss estimates derived with this method and showed that, although cross-vortex transport may often be insignificant, in some dynamically active periods neglecting it may introduce significant error in the estimated ozone loss rate. Christensen et al. (2005) applied the vortex-average method, corrected to account for transport into the vortex, to ozonesonde data from the 2002/2003 Arctic winter and compared the results with ozone loss estimates from other techniques, finding generally good agreement. A variant on the vortex-average method uses the evolution of a long-lived tracer, rather than trajectory calculations and a radiation code, to deduce diabatic descent. For example, Odin SubMillimeter

Radiometer (SMR) measurements of nitrous oxide (N_2O) were used to account for the effects of subsidence in estimating chemical loss during the 2002/2003 winter from both Odin/SMR (Urban et al., 2004) and ground-based millimeter-wave (Raffalski et al., 2005) ozone observations. This approach has been greatly facilitated by the availability of simultaneous global ozone and tracer measurements from recent satellite missions such as Odin, Envisat, and Aura (e.g., Manney et al., 2006).

Passive Subtraction Method. In this technique, differences between measured ozone and results from model runs in which ozone is treated as a passive dynamical tracer are assumed to arise from chemical changes. Recent refinements in 3-D chemical transport models (see Section 4.2.1.3) have improved estimates of chemical loss derived in this manner. Feng et al. (2005b) showed that seasonal runs of the updated Single-Layer Isentropic Model of Chemistry and Transport (SLIMCAT) model (Chipperfield, 2006) produced realistic representations of tracer transport and ozone loss for selected warm and cold Arctic winters, including 2002/2003. Goutail et al. (2005) compared ground-based total ozone columns from the 2002/2003 winter with modeled passive ozone columns from the Reactive Processes Ruling the Ozone Budget in the Stratosphere (REPROBUS) and updated SLIMCAT models; although both models indicated significant early-winter loss, full-chemistry simulations from REPROBUS did not reproduce all of the inferred loss. Singleton et al. (2005) compared the updated SLIMCAT with Polar Ozone and Aerosol Measurement (POAM) III ozone observations from 2002/2003, examining a "pure passive" ozone advected as an inert tracer with no chemical changes and a "pseudo passive" ozone for which only heterogeneous reactions on PSCs were switched off in order to explore the influence of gas-phase chemistry on inferred ozone loss. The timing, morphology, and magnitude of modeled (full chemistry) ozone loss agreed well with that deduced from POAM observations, with the largest differences (<1 parts per million by volume (ppmv)) in the two passive ozone fields, attributed to nitrogen oxides (NO_x) chemistry in the "pseudo passive" run, occurring above 450 K. Finally, Grooß et al. (2005b) showed that ozone loss inferred using CLaMS compared well with other estimates.

Lagrangian Transport Calculation Method. A method frequently applied to ozone measurements from the Upper Atmosphere Research Satellite (UARS) Microwave Limb Sounder (MLS) involves the use of a Lagrangian transport (LT) model advecting trace gases passively along parcel trajectories; departures from the observed ozone provide an estimate of chemical loss. Previous studies covered only the late-winter period for a subset of Arctic winters observed by UARS MLS and used different LT models and MLS data versions. Manney et al. (2003a) performed a comprehensive reanalysis that encompassed the entire Arctic winter for all years with sufficient data and used a consistent LT model and the definitive UARS MLS dataset, facilitating evaluation of interannual variability.

Chemical Loss in the 2004/2005 Arctic Winter

The potential for severe ozone depletion will exist so long as stratospheric chlorine loading remains well above natural levels. The degree of chlorine activation and consequent ozone destruction in the Arctic is primarily controlled by dynamical variability. Winters in which the polar vortex is cold and isolated are expected to experience large ozone losses, whereas ozone losses should be minimal in warmer than average, disturbed winters. The 2004/2005 Arctic winter was especially interesting in this context. The lower stratosphere was exceptionally cold, particularly below 400 K (~15 km), with temperatures below PSC existence thresholds on more days and over a broader region than previously observed (Manney et al., 2006; Rex et al., 2006). But the lower stratosphere was also dynamically active, with frequent intrusions of lower-latitude or vortex edge air into the vortex interior throughout the winter (Manney et al., 2006; Schoeberl et al., 2006). Moreover, the initial morphology of ozone in early winter, prior to the onset of chemical loss, exhibited a strong gradient in mixing ratio between low values in the vortex core and high values at the edge (Manney et al., 2006; Rex et al., 2006). Thus mixing processes may have masked or mimicked chemical loss, depending on the location in the vortex. A major final warming in early-March 2005 halted PSC processing, terminating ozone destruction earlier than in other recent cold winters. These effects made disentangling chemical and dynamical processes particularly difficult this year, possibly causing some analyses to be more sensitive to sampling biases and increasing uncertainties in the estimated losses. Nevertheless, a suite of studies using a variety of datasets and techniques provided fairly consistent ozone loss estimates for this winter.

Manney et al. (2006) deduced chemical ozone loss from Aura MLS measurements by using N_2O to account for the effects of diabatic descent in the vortex edge and core regions, and estimated loss of up to 2 ppmv in the outer vortex and ~1.5 ppmv averaged over the entire vortex, with maximum losses in both regions between 450 and 500 K. Manney et al. (2006) also applied the vortex-average method, using trajectory calculations and a radiation code, to both Aura MLS and POAM measurements (Figure 4-11) and found maximum vortex-averaged chemical loss near

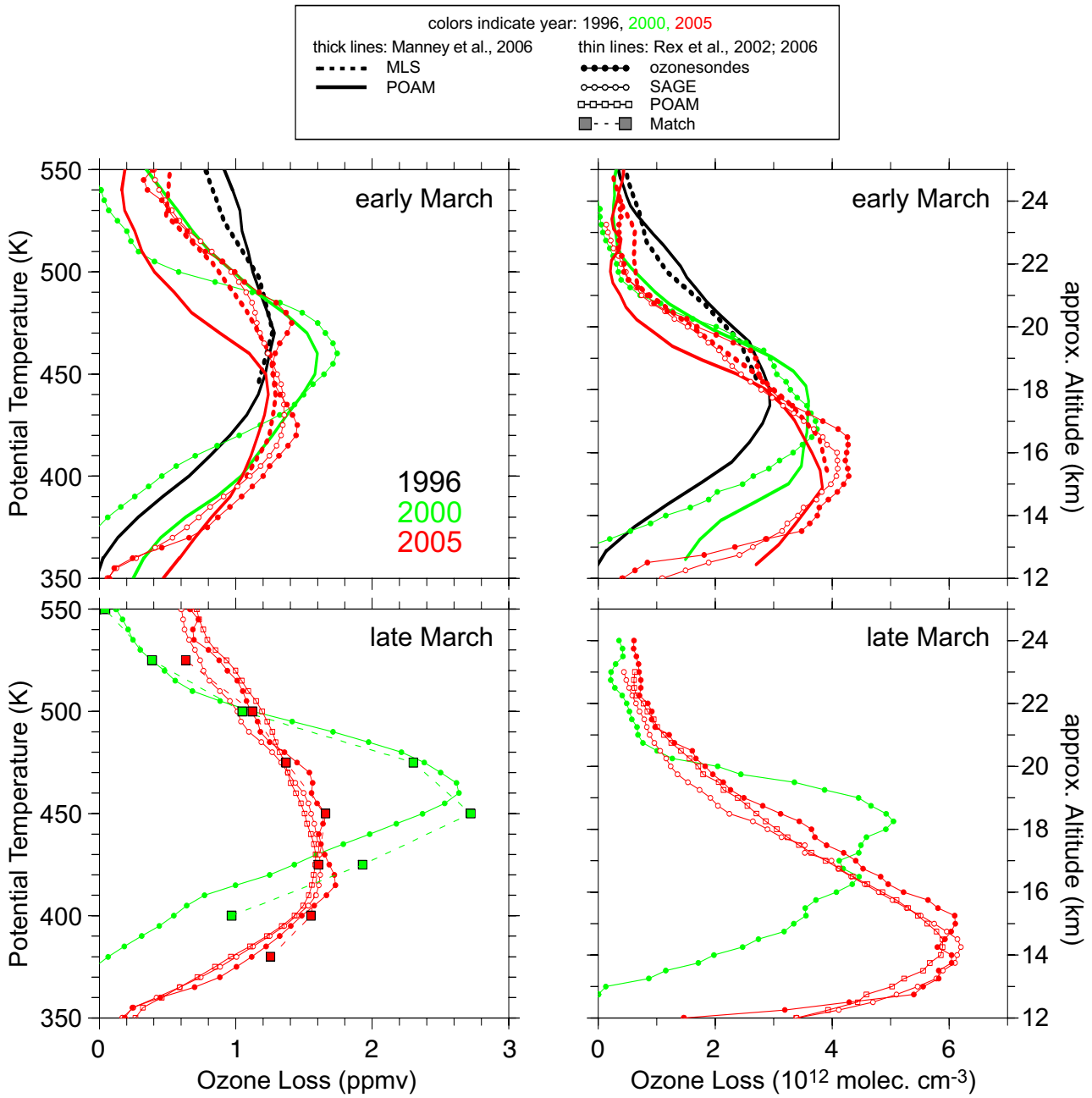

Figure 4-11. Profiles of chemical ozone loss in terms of mixing ratio versus potential temperature (left panels) and concentration versus altitude (right panels), over the intervals from 5 January to 10 March (top panels) and 5 January to 25 March (bottom panels) for three cold Arctic winters, estimated using various data sources and techniques. Although different line styles and symbols have been used to denote the different datasets and approaches, in most cases it is not necessary to clearly distinguish the curves, as the derived ozone loss values are generally in quite good agreement. All lines represent results from the vortex-average descent method. Thick lines without symbols are from Manney et al. (2006), with solid lines based on POAM II/III and dotted lines based on UARS MLS (1996) and Aura MLS (2005). Thin lines with small symbols are from Rex et al. (2002) and Rex et al. (2006), with lines marked by filled dots based on ozonesonde data, lines marked by open circles based on SAGE III data, and lines marked by open squares based on POAM II/III data. Large square symbols (connected by dashed lines) show results from Match (Rex et al., 2002, 2006). Ozone loss in 2005 terminated earlier and was smaller in terms of mixing ratios compared with 2000. But, because the 2005 loss extended to lower altitudes where ozone concentrations are high, it was larger in terms of concentration, which is the relevant quantity for total column loss.

450 K of 1.2-1.3 ppmv, slightly less than the estimates based on MLS N_2O. These results imply that, in terms of mixing ratios, chemical loss in 2004/2005 was slightly less than that in 1999/2000 and comparable to that in 1995/1996, but with maximum loss occurring at a lower altitude.

Singleton et al. (2006) used the updated SLIMCAT model to infer chemical ozone loss from POAM III, Aura MLS, ACE-FTS, Measurement of Aerosol Extinction in the Stratosphere and Troposphere Retrieved by Occultation (MAESTRO), and Stratospheric Aerosol and Gas Experiment (SAGE) III measurements; all instruments provided similar results, with a maximum inferred loss of 2-2.3 ppmv near 450 K (Figure 4-12). Jin et al. (2006) also examined ACE-FTS measurements, using correlations between ozone and methane (CH_4) (modified to account for mixing processes), correlations between ozone and an artificial tracer constructed to have a linear correlation with ozone in early winter, and the vortex-averaged descent method to diagnose an average maximum loss of ~2.1 ppmv near 500 K, with an average column loss of 119 DU over the region 375-800 K (14-30 km).

Results from Match (Rex et al., 2006; Figure 4-11) indicated chemical loss characterized by a broad peak of ~1.5 ppmv from ~400-450 K, smaller than the maximum mixing ratio loss in 1999/2000, but with more loss occurring at lower altitudes. However, Rex et al. (2006) showed that, in terms of concentration (rather than mixing ratio), ozone loss in 2004/2005 was considerably more severe than that in 1999/2000, particularly below about 16 km. For the total column and, hence, the ultraviolet (UV) reaching the surface, the large concentration losses at lower altitude have the biggest impact. Therefore, total column losses during 2004/2005 were at least on the order of the largest losses recorded previously (Rex et al., 2006).

The 2004/2005 winter stands out as having the largest V_{PSC} and partial column ozone loss (ΔO_3 = 121 ± 20 DU over 380-550 K) of the last 14 years, although the differences between column ozone losses in 1995/1996, 1999/2000, and 2004/2005 are within the uncertainties in the calculation. The compact and nearly linear relationship between the influence of chemical ozone loss on ΔO_3 and the winter average of V_{PSC} reported by Rex et al. (2004) and confirmed by Tilmes et al. (2004) was maintained in 2004/2005 (Figure 4-13; Rex et al., 2006). In contrast, comparisons of ground-based total ozone measurements with passive ozone from REPROBUS (e.g., Goutail et al., 2005) indicated that the total column loss in 2004/2005 rivaled that in 1999/2000 but was smaller than that in 1995/1996. The various partial and total column ozone loss estimates for the 2004/2005 Arctic winter discussed here are compared with those available from previous years in Figure 4-14.

The March 2005 averaged total ozone in Figure 4-6 clearly shows a distinct minimum (near 60°N) that is comparable to that in other years with strong depletions. As discussed in Section 4.1.2.1, total column ozone (data from the OMI on Aura; Figure 4-7) averaged over the Arctic region in March 2005 was below normal but comparable to that in other recent winters, even though the magnitude of chemical ozone destruction in the lower stratospheric vortex was substantially larger. The March 2005 average in Figure 4-6 clearly shows a distinct minimum (near 60°N) that is comparable to other years with strong depletions. Several factors account for these apparent discrepancies.

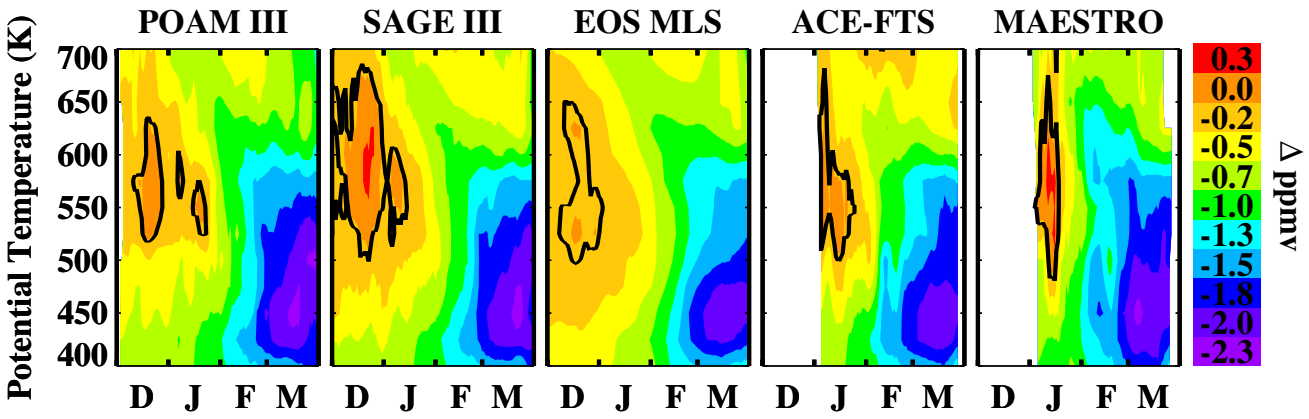

Figure 4-12. Daily average chemical ozone loss (ppmv) inside the vortex during the 2004/2005 Arctic winter inferred by differencing passive ozone calculated by the updated SLIMCAT chemical transport model, and ozone measured by the POAM III, SAGE III, Aura MLS, ACE-FTS, and MAESTRO instruments. Days on which data are missing or an instrument did not sample the vortex have been interpolated in time. Data have been smoothed with a seven-day running average. The solid black line denotes the zero contour.

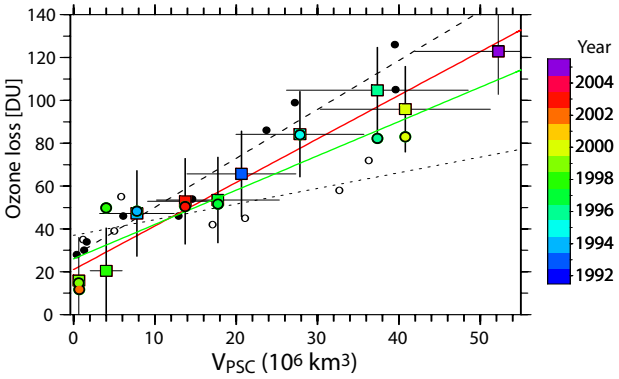

Figure 4-13. Scatter plot of vortex-average chemical loss of column ozone (ΔO_3, calculated over the range 380 to 550 K) versus V_{PSC} inferred from ozonesonde observations for the 1991/1992 to 2004/2005 Arctic winters (update from Rex et al., 2004). Colored squares and the red fit line show results based on ozonesonde analyses; colored circles and the green fit line show results from tracer correlation studies based on Halogen Occultation Experiment (HALOE) data (update from Tilmes et al., 2004). Also shown are results from SLIMCAT model simulations. Open black circles and the dotted fit line show results from an older version of the model, run at a resolution of 7.5° for the 1990/1991 to 1999/2000 winters (same model results as shown in Figure 2 of Rex et al., 2004). Closed black circles and the dashed fit line show results from a new version of the model, run at higher resolution (2.8°) for the 1994/1995 to 2003/2004 winters (same model results as shown in Figure 1 of Chipperfield et al., 2005). See Section 4.2.1 for descriptions of the old and newly updated versions of the SLIMCAT model. Adapted from Rex et al. (2006), Rex et al. (2004), Tilmes et al. (2004), and Chipperfield et al. (2005).

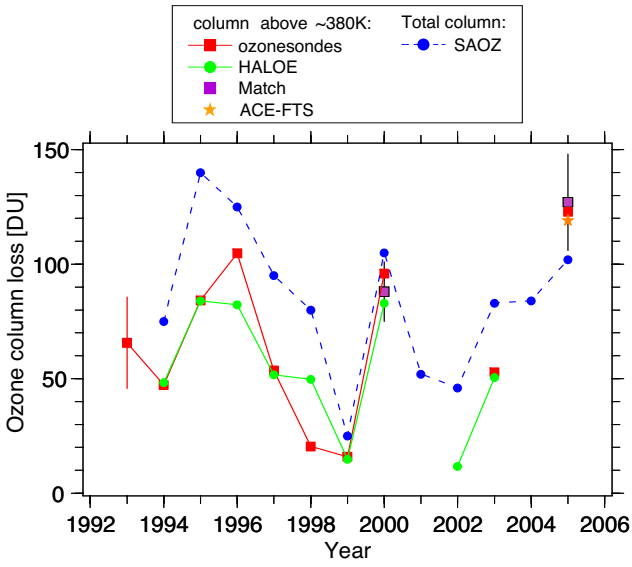

Figure 4-14. Interannual variation of the ozone column losses in the Arctic since the early 1990s based on Système d' Analyse par Observation Zénithale (SAOZ) satellite data (blue, update of Goutail et al., 2005); ozonesonde analyses (red, typical uncertainty illustrated by the single error bar, update from Rex et al., 2004); HALOE data (green, Tilmes et al., 2004); Match (purple, Rex et al., 2002, 2006); and ACE-FTS data (orange, Jin et al., 2006). The sonde, HALOE, and Match analyses represent partial column losses between 380 and 550 K potential temperature. The other studies represent estimates of the total column losses, which can result in slightly larger estimates in some winters. Therefore, the loss estimates from the SAOZ data have been plotted with a dashed line to signify that they should not be directly compared with the results from the other two long-term studies.

In previous years with later final warmings, the March average reflected primarily winter vortex values that, for dynamical reasons, were much lower than the spring values dominating the 2005 average. Even before the final warming, the 2005 vortex had become highly distorted and shifted off the pole (Manney et al., 2006). The monthly average over the entire Arctic region, therefore, encompassed air from both inside and outside the vortex; together with the vigorous mixing following the vortex breakup, this effect muted the signature of chemical depletion in the average ozone north of 63°N. As a consequence, the average total column ozone over the Arctic in March 2005 was strongly influenced by dynamics and was not representative of chemical loss inside the polar vortex remnants.

As a result of dynamical processes during the warming in combination with the large chemical depletion, total ozone over large parts of Europe was very low (reaching values below 250 DU) for several days during late March of 2005. This led to elevated levels of UV at the ground over Europe during those days.

Quantifying Antarctic Ozone Loss

Over the past two decades, numerous studies have compared modeled and measured ozone in the Antarctic ozone hole region. Although in most cases the models were shown to be successful in simulating the general features of ozone hole development, such as the timing of the onset and the cumulative amount of ozone loss, these

did not provide a stringent test of theoretical understanding. Until recently, few studies have undertaken the kind of detailed quantitative estimations of ozone loss that have become routine in the Arctic. The inability to accurately model ozone loss during cold Arctic winters (e.g., WMO, 2003; Rex et al., 2003), however, has renewed interest in the Antarctic, where ozone losses are larger, the vortex is more isolated, and, consequently, transport and mixing processes are less important in controlling ozone abundances. Several recent studies have applied methods described above to quantify ozone loss using measurements from satellites and the first coordinated Antarctic ozonesonde Match campaign, conducted in 2003.

Hoppel et al. (2005b) used the vortex-average descent method with 10 years of ozone measurements from the POAM II and III instruments to deduce chemical loss, with a particular emphasis on the 20-22 km region near the top of the ozone hole (see 4.1.2.1 for further details). Hoppel et al. (2005a) used the satellite Match technique to calculate ozone loss rates at four potential temperature levels over the range ~450-520 K from five years of POAM III data and compared them with rates from a photochemical box model. Measured loss rates at the high solar zenith angles characteristic of the POAM-Match trajectories were found to increase slowly from late June to early August, and then increase rapidly until mid-September. The Match loss rates were also found to be highly sensitive to the meteorological analyses used for the trajectory calculations. Frieler et al. (2006) compared modeled ozone loss rates with those estimated for the 2003 ozonesonde Match campaign, as well as several Arctic winters. Detailed discussion of the implications of both the Hoppel et al. (2005a) and Frieler et al. (2006) studies for various model parameters is given in Section 4.2.1.3.

Tilmes et al. (2006b) used the tracer/tracer correlation technique with Improved Limb Atmospheric Sounder (ILAS)-II measurements to examine the temporal evolution of ozone loss throughout the 2003 Antarctic winter. Chemical loss began in July for all altitudes considered (380-620 K), and the accumulated ozone loss and loss rates were shown to be highly dependent on altitude. Ozone loss rates increased strongly during September throughout the lower stratosphere; half of the entire column ozone loss of 157 DU occurred during September, with virtually all ozone between 380 and 470 K destroyed by the end of the month. Simulations by the CLaMS box model confirmed that increasing solar illumination and persistent low temperatures led to enhanced ozone loss rates in mid-September.

4.2 PROGRESS IN OUR UNDERSTANDING OF THE PHYSICAL AND CHEMICAL PROCESSES

4.2.1 Polar Ozone Chemistry

The chemical loss of polar ozone during winter and spring occurs primarily by two gas-phase catalytic cycles that involve chlorine oxide radicals (Molina and Molina, 1987) and bromine and chlorine oxides (McElroy et al., 1986):

Cycle 1

$$ClO + ClO + M \rightarrow ClOOCl + M \quad (1a)$$

$$ClOOCl + h\nu \rightarrow 2\,Cl + O_2 \quad (1b)$$

$$2\,[Cl + O_3 \rightarrow ClO + O_2] \quad (1c)$$

$$\text{Net: } 2\,O_3 \rightarrow 3\,O_2$$

Cycle 2

$$BrO + ClO + h\nu \rightarrow Br + Cl + O_2 \quad (2a)$$

$$Br + O_3 \rightarrow BrO + O_2 \quad (2b)$$

$$Cl + O_3 \rightarrow ClO + O_2 \quad (2c)$$

$$\text{Net: } 2\,O_3 \rightarrow 3\,O_2$$

If loss of ClOOCl occurs by thermal decomposition:

$$ClOOCl + M \rightarrow ClO + ClO + M \quad (1d)$$

rather than photolysis (1b), a null cycle results that recycles ClO but leads to no change in ozone. Small contributions to polar ozone loss also occur due to cycles limited by the reactions ClO + O and ClO + HO_2.

Abundances of ClO in the polar vortex are greatly elevated by reactions of inactive chlorine reservoir species on various types of PSCs that form when temperatures drop below about 195 K (see Section 4.2.2). Abundances of BrO determine the removal rate by cycle (2), which may contribute almost half of the total chemical loss rate of Antarctic and Arctic ozone (e.g., Frieler et al., 2006). The abundance of BrO, in contrast to ClO, is not strongly affected by reactions involving PSCs (Pundt et al., 2002). The emerging issue involving BrO, important also for our understanding of polar ozone loss, is quantification of total inorganic bromine (Br_y) supplied to the stratosphere by very short-lived (VSL) bromocarbons (see Chapter 2).

Since the previous Assessment, numerous field and laboratory studies have provided advances in our

quantitative understanding of ozone destruction by cycles (1) and (2). These advances include the first measurements of the abundance of the chlorine monoxide dimer (ClOOCl) (Stimpfle et al., 2004; von Hobe et al., 2005); observations of BrO in the polar vortices (Fitzenberger, 2000; Pfeilsticker et al., 2000; Pundt et al., 2002; Canty et al., 2005; Giovanelli et al., 2005; Dorf et al., 2006; Sinnhuber et al., 2005b; Frieler et al., 2006; Schofield et al., 2006; Sioris et al., 2006); better representation of denitrification in models (Grooß et al., 2005b; Chipperfield et al., 2005); recognition that formation of ClOOCl likely occurs faster than previously assumed (Boakes et al., 2005); and better constraints on the equilibrium constant between ClO and ClOOCl from both laboratory studies (Plenge et al., 2005) and field observations (von Hobe et al., 2005; Stimpfle et al., 2004). As detailed below, these findings lead to better model representation of two key processes: (1) the apparent discrepancies between measured and modeled chemical loss rates of Arctic ozone during cold Januaries of specific winters (e.g., Rex et al., 2003) that was noted in Section 3.3 of the previous Assessment (Frieler et al., 2006), and (2) the relation between chemical ozone loss and the volume of air exposed to PSCs, based on more than a decade of observations, that was introduced in the previous Assessment (Rex et al., 2004; Chipperfield et al., 2005). These advances suggest better predictive capability for future ozone loss due to anthropogenic halogens is achievable in general circulation models (GCMs) and coupled Chemistry-Climate Models (CCMs), provided certain fundamental characteristics of the atmosphere (e.g., chlorine and bromine loading; photolysis and thermal decomposition of ClOOCl; denitrification) are well represented. However, as discussed below, certain aspects of polar chemistry are still subject to considerable uncertainty, due to differences in various laboratory measurements of the absorption cross section of ClOOCl (σ_{ClOOCl}) (Section 4.2.1.1) and uncertainty in the atmospheric abundance of BrO (Chapter 2).

4.2.1.1 CHLORINE

Attention since the previous Assessment has continued to be focused on reducing uncertainties in the parameters that control ozone loss by Cycle 1, such as the rate constant for formation of ClOOCl (k_{1a}), the photolysis rate of ClOOCl (J_{1b}), and the equilibrium constant between the concentrations of ClO and ClOOCl (denoted [ClO] and [ClOOCl], respectively) established if loss of ClOOCl occurs via thermal decomposition:

$$K_{EQ} = k_{1a}/k_{1d} = [ClOOCl] / [ClO]^2 \qquad (3)$$

This section begins with a description of recent laboratory measurements of reactions that affect polar ozone loss by chlorine. Then, we describe analyses of field studies that focus on consistency between measured and modeled representation of ClO and ClOOCl photochemistry.

Laboratory Studies

Boakes et al. (2005) reported a laboratory measurement of k_{1a} that is ~20% larger, over the temperature range 206 to 298 K, than the measurements of Bloss et al. (2001) and the Jet Propulsion Laboratory (JPL) Publication 02-25 compendium (Sander et al., 2003; hereafter referred to as *JPL 02-25*) recommendation for this rate constant. This new study suggests that ozone loss by Cycle 1 is faster than previously thought, which has implications for the partitioning between ClO and ClOOCl (see below). Boakes et al. (2005) support the upward revision in the recommended value of k_{1a} by *JPL 02-25* that followed the study of Bloss et al. (2001). The Bloss et al. (2001) and Boakes et al. (2005) values for k_{1a} are fast enough to pose a challenge to the theoretical understanding of this reaction (Golden, 2003).

Plenge et al. (2004) is the only published laboratory study of ClOOCl photolysis since the previous Assessment. They found complete production of chlorine atoms and chloroperoxy radicals (ClOO) upon photolysis of ClOOCl at 250 and 308 nm, leading to $2Cl + O_2$ upon the rapid thermal decomposition of ClOO at polar temperatures, resulting in catalytic loss of ozone by Cycle 1. This contrasts with an earlier study, described in the previous Assessment, that indicated a ~10% yield of 2 ClO at 308 nm (Moore et al., 1999) (this branch leads to a null cycle for ozone). Most ozone depletion models assume production of only ClOO + Cl upon photolysis of ClOOCl. Thus, Plenge et al. (2004) increase our confidence in the accuracy of this assumption. However, the primary contribution to photolysis of ClOOCl occurs longward of 308 nm, and there remains a need to define the product yields of ClOOCl photolysis for the atmospherically relevant spectral region.

Many of the ozone loss simulations described below use a value for σ_{ClOOCl} based on measurements by Burkholder et al. (1990) out to 410 nm, with a log-linear extrapolation to 450 nm using a formula given by Stimpfle et al. (2004). This Burkholder et al. (1990) photolysis rate of ClOOCl is 40 to 50% faster than J_{1b} based on the *JPL 02-25* cross section and results in a good overall description of measured ClO and ClOOCl, if the *JPL 02-25* value of k_{1a} is also used (Stimpfle et al., 2004; see below). The JPL Publication 06-2 compendium (Sander et al., 2006;

hereafter referred to as *JPL 06-2*) recommendation for σ_{ClOOCl} is the same as in the previous recommendation.

The correctness of a log-linear extrapolation relies on the assumption of a single dissociative state in the wavelength region of interest. The primary photolytic pathway for ClOOCl is excitation to a singlet electronic excited state. Peterson and Francisco (2004) suggested the existence of a weakly absorbing, dissociative triplet state, predicted to have an absorption maximum at about 385 ± 25 nm, based on an ab initio calculation of the structure of the ClOOCl molecule. This study calls into question the appropriateness of log-linear extrapolations of ClOOCl cross-section data.

Present uncertainty in J_{1b} underscores the need for laboratory studies able to quantify σ_{ClOOCl} to wavelengths as high as ~450 nm. Existing laboratory studies are based on spectra measured in the presence of other molecules, such as molecular chlorine (Cl_2), ozone, and/or dichlorine monoxide (Cl_2O). The ClOOCl cross sections must be determined by analysis of a composite spectrum that includes absorptions from multiple species. Large uncertainties in laboratory determinations of σ_{ClOOCl} persist at atmospherically important wavelengths because the procedures to correct for interfering species can be qualitative in nature and prone to error (e.g., Huder and DeMore, 1995).

Plenge et al. (2005) recently reported values of K_{EQ} based on the bond strength of ClOOCl determined using photoionization mass spectrometry. Their values of K_{EQ} are smaller than the *JPL 02-25* recommendation and the earlier laboratory study of Nickolaisen et al. (1994), but agree well with the laboratory measurement of Cox and Hayman (1988). The range of uncertainty for the *JPL 02-25* value of K_{EQ} encompasses results from all of these laboratory studies. A lower value of K_{EQ} implies that loss of ClOOCl by thermal decomposition occurs faster than previously thought, leading to higher levels of ClO during nighttime. Bröske and Zabel (2006) report a value for K_{EQ}, determined from a laboratory kinetics study over the temperature range 243 to 261 K, that lies between the values of Cox and Hayman (1988) and Plenge et al. (2005) but also exhibits a possible pressure dependence. The high-pressure ($p > 30$ hPa) value for K_{EQ} of Bröske and Zabel (2006) is similar to the *JPL 06-2* recommendation. The low-pressure result, considered to be more reliable by Bröske and Zabel (2006), leads to a value of K_{EQ} quite similar to the Plenge et al. (2005) value.

Ultimately, consistency between laboratory thermodynamic determinations of the heat of formation of ClOOCl and kinetic measurements of k_{1a} and the reverse of k_{1a} is desired. Determinations of K_{EQ} from kinetics studies are affected by uncertainties in k_{1a}. Bröske and Zabel (2006) note that the apparent pressure dependence of K_{EQ} points to inconsistencies between dissociation and recombination data, since K_{EQ} is independent of pressure on theoretical grounds. Consistency between thermodynamic and kinetic measurements has yet to be achieved, especially for temperatures relevant for the winter polar stratosphere.

Field Observations

Stimpfle et al. (2004) reported the first measurements of ClOOCl, acquired from an instrument aboard the NASA ER-2 aircraft in the Arctic stratosphere during the winter of 1999/2000. These observations, analyzed with simultaneous measurements of ClO from the same instrument, were used to test the understanding of k_{1a}, J_{1b}, and K_{EQ}. Assuming the *JPL 02-25* recommendation for k_{1a}, measurements made during daylight, over a wide range of solar zenith angles, indicate best agreement with a value for J_{1b} based on absorption cross sections from Burkholder et al. (1990) (Figure 4-15). The JPL Publication 00-3 (Sander et al., 2000; hereafter referred to as *JPL 00-3*) rate for k_{1a} is most consistent with a value of J_{1b} based on ClOOCl cross sections that lie between those given by *JPL 02-25* and Burkholder et al. (1990), while the Boakes et al. (2005) rate for k_{1a} implies faster photolysis of ClOOCl than given by any of the available cross section measurements. Figure 4-15 highlights the fact, emphasized by Stimpfle et al. (2004), that daytime measurements of ClO and ClOOCl constrain only the ratio k_{1a}/J_{1b}. The value of J_{1b} decreases by more than an order of magnitude as solar zenith angle (SZA) increases from 70° to 92° (Figure 4-15), so analysis of $[ClO]^2/[ClOOCl]$ provides a test of the partitioning of these species for a wide range of photolytic conditions (Stimpfle et al., 2004). This ratio is important because models adopting J_{1b} based on Burkholder as well as k_{1a} from *JPL 02-25* will calculate more rapid ozone loss than models using *JPL 02-25* kinetics, since photolysis of ClOOCl is the rate-limiting step for ozone loss by Cycle 1. Considering the ±25% (1σ) uncertainty in the observations used to define β (see caption of Figure 4-15), a model based solely on *JPL 02-25* kinetics is not consistent with the observations at the 1σ uncertainty level (Stimpfle et al., 2004).

Field observations of nighttime ClO and in some cases ClOOCl abundances by several groups suggest that the equilibrium constant K_{EQ} may be smaller than the *JPL 02-25* recommendation. Observations of ClO and ClOOCl by Stimpfle et al. (2004), obtained during nighttime when thermal equilibrium (e.g., equation (3)) can be assumed, indicate better overall agreement with values of K_{EQ} from the laboratory study of Cox and Hayman

(1988) compared with values from either *JPL 02-25* or Nickolaisen et al. (1994). Nighttime observations of ClO and ClOOCl abundances in the Arctic stratosphere during the winter of 2002/2003 reported by von Hobe et al. (2005) were used to determine an empirical value for K_{EQ} that implies faster thermal decomposition for ClOOCl than the *JPL 02-25* value, and somewhat faster decomposition than the Cox and Hayman (1988) and Plenge et al. (2005) values. Berthet et al. (2005) analyzed nighttime observations of ClO in the Arctic vortex during the winter of 2002/2003, obtained from a microwave radiometer onboard the Odin satellite. They concluded that K_{EQ} lies between the laboratory determination of Cox and Hayman (1988) and the empirical value of von Hobe et al. (2005) and that their data are not consistent with the *JPL 02-25* value for K_{EQ}. Finally, an analysis of daytime and nighttime field measurements together with thermodynamic calculations and unimolecular rate theory reveals that overall best consistency between theory and observation is obtained using the Plenge et al. (2005) value for K_{EQ}, the Nickolaisen et al. (1994) value for k_{1a}, and σ_{ClOOCl} that lies between *JPL 02-25* and the value given by Burkholder et al. (1990) (von Hobe et al., 2006). The uncertainty in the *JPL 02-25* recommendation for K_{EQ} encompasses all of the field observations as well as the recent laboratory determination based on measurement of the ClOOCl bond dissociation energy, so none of the recent results are outside of the range of prior expectation.

All of these recent results are in basic agreement with earlier analyses of nighttime atmospheric measurements of ClO (Avallone and Toohey, 2001, and references therein). Vogel et al. (2006) examined chemistry related to ClO-radical complexes, and concluded that this chemistry, while still highly uncertain, might be important for regulating the ratio of ClO and ClOOCl at night, which might complicate atmospheric, empirical determinations of K_{EQ}. However, the effect of uncertainty in K_{EQ} on ozone loss is small compared with other uncertainties, such as the abundance of BrO and

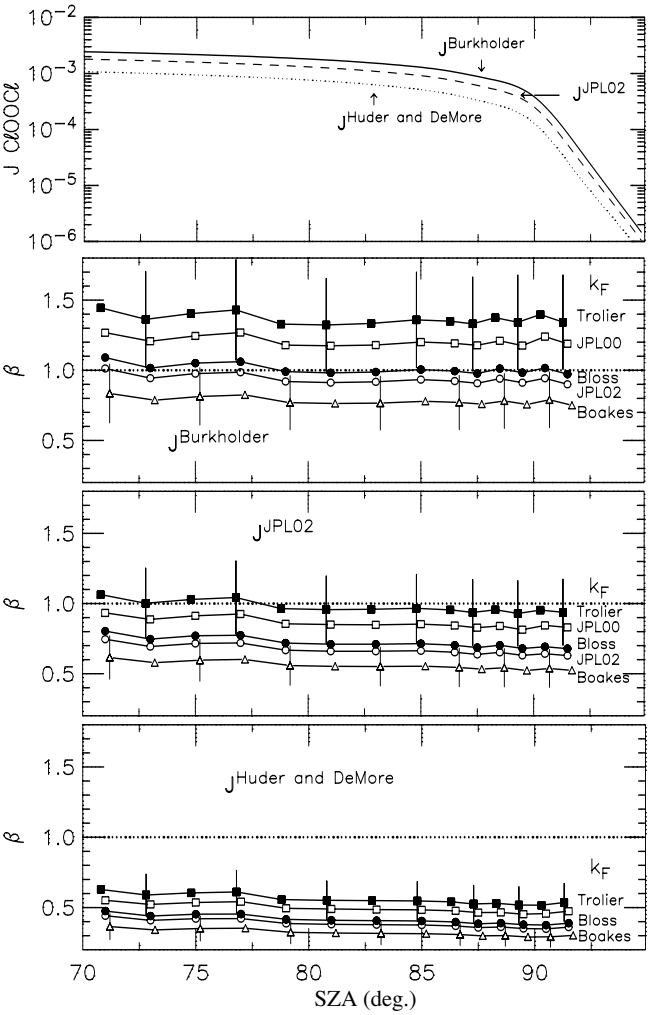

Figure 4-15. Daytime analysis of all SAGE III Ozone Loss and Validation Experiment (SOLVE) flights, β versus solar zenith angle (SZA), where $\beta = ([ClOOCl] / [ClO]^2)_{OBSERVED} / ([ClOOCl] / [ClO]^2)_{MODEL}$. Data selected for SZA < 92° and M < 3.0 x 10^{18} molec cm^{-3}. Average values of β are shown for 2°-wide SZA bins for 70° < SZA < 86°, and for 1°-wide bins for SZA > 86°. The top panel shows calculated values of J_{1b} versus SZA at 60 hPa for a model albedo of 0.24, using values of the ClOOCl cross section from Burkholder et al. (1990), *JPL 02-25*, and Huder and DeMore (1995), as indicated. Observed albedos are used for the calculations of β. The bottom three panels show results for using three values of the absorption cross section of ClOOCl: Huder and DeMore (1995), *JPL 02-25*, and Burkholder et al. (1990). Within each panel, results are shown for model simulations using five values of the rate constant of ClO + ClO + M: Trolier et al. (1990), *JPL 00-3*, Bloss et al. (2001), *JPL 02-25*, and Boakes et al. (2005). Error bars depict the ±25% uncertainty (1σ) in β attributable to the uncertainties in the observations of ClO and ClOOCl; error bars are shown only for simulations using the Trolier et al. (1990) and Boakes et al. (2005) rate constants. Points associated with these two model runs have been displaced slightly with respect to the actual mean SZA, for clarity of the error bars. After Stimpfle et al. (2004).

the photolysis rate of ClOOCl. Perhaps the most important reason to reduce uncertainties in K_{EQ} is that accurate knowledge of this parameter will enable better determination of ClO_x (ClO + 2 ×ClOOCl) from nighttime observations of ClO.

4.2.1.2 BROMINE

Measurements of BrO profiles in the Arctic vortex have been obtained for a number of winters using a balloonborne spectrometer (e.g., Pfeilsticker et al., 2000; Fitzenberger, 2000; Pundt et al., 2002; Dorf et al., 2006). Model studies that deduce BrO_x (BrO + BrCl) or Br_y from these BrO profiles estimate a total bromine loading of 20 to 24 parts per trillion by volume (pptv) (Canty et al., 2005; Dorf et al., 2006; Frieler et al., 2006), significantly larger than the abundance of bromine that can be delivered to the stratosphere by methyl bromide (CH_3Br) + halons alone (see Chapter 2). Most chemical transport models (CTMs), GCMs, and CCMs used to assess polar ozone loss use estimates of Br_y based only on supply of bromine from CH_3Br + halons. A value of bromine radicals (BrO_x) inferred from BrO in the Arctic vortex on 18 February 2000 is 40 to 60% higher (e.g., 6 to 9 pptv larger) than values of BrO_x (BrO + BrCl) used in typical simulations of the Modèle Isentropique de transport Mésoéchelle de l'Ozone Stratosphérique par Advection avec CHIMie (MIMOSA-CHIM) 3-D CTM and the Atmospheric and Environmental Research, Inc. (AER) two-dimensional (2-D) model (Figure 4-16), resulting in a larger relative contribution from bromine to polar ozone loss (Frieler et al., 2006). The BrO_x profile shown in Figure 4-16 provides additional and independent support to the results to the analyses shown in Chapter 2 because the chemistry used to infer BrO_x from BrO at high latitude (involving only bromine chloride (BrCl) and BrO) is distinct from the chemistry used to infer Br_y from BrO at midlatitudes (involving mainly BrO and bromine nitrate ($BrONO_2$), and hypobromous acid (HOBr) and hydrogen bromide (HBr) to a lesser degree).

Retrievals of BrO profiles from Scanning Imaging Absorption Spectrometer for Atmospheric Chartography (SCIAMACHY) limb scattered radiances, which provide near-global coverage and hence include the polar vortices, have been conducted by two research groups. Sinnhuber et al. (2005b) report a modest contribution, 3 ± 3 pptv, to Br_y from VSL compounds, whereas Sioris et al. (2006) deduce a much larger contribution, 8.4 ± 2 pptv. As discussed in Chapter 2, these discordant findings are driven by differences in the retrievals of BrO. Schofield et al. (2006) report ground-based observations of BrO over Arrival Heights, Antarctica (77.8°S), that are consistent

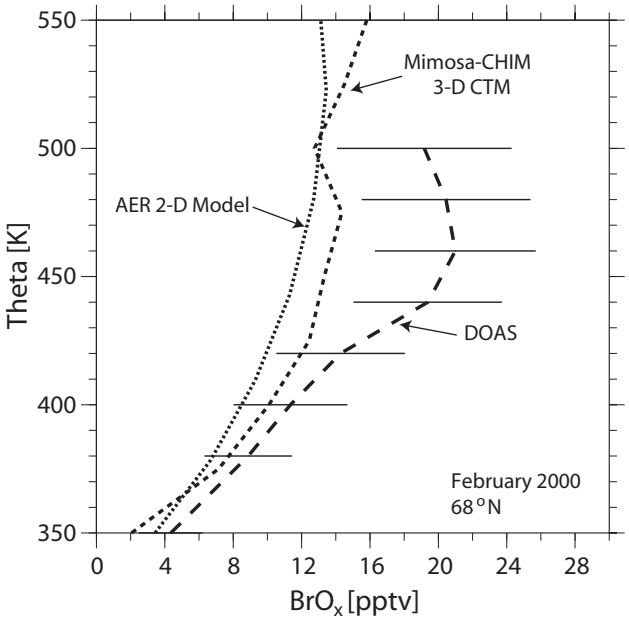

Figure 4-16. Profile of BrO_x (= BrO + BrCl) inferred from a DOAS measurement of BrO over Kiruna, Sweden (68°N), on 18 February 2000 (Canty et al., 2005; Fitzenberger, 2000) compared with a profile of BrO_x found for this region by the AER two-dimensional model assuming supply of stratospheric bromine from only CH_3Br and halons (Salawitch et al., 2005). Also shown is an estimate of Br_y from the MIMOSA-CHIM three-dimensional chemical transport model, assuming again stratospheric supply of Br_y only by CH_3Br + halons. Adapted from Frieler et al. (2006).

with Br_y of ~21.2 pptv at 20 km, suggesting again a significant role for the presence of more bromine in the polar regions than can be supplied solely by CH_3Br and halons. Giovanelli et al. (2005) obtained aircraft measurements of BrO over Antarctica that range from 4 to 10.3 pptv. Chapter 2 provides an extensive discussion on the quantification of the role of VSL compounds on the stratospheric bromine budget.

The reaction of BrO + ClO has three product channels:

$$\begin{aligned} BrO + ClO &\rightarrow ClOO + Br \quad (34\%) \quad (4a)\\ &\rightarrow BrCl + O_2 \quad (7\%) \quad (4b)\\ &\rightarrow OClO + Br \quad (59\%) \quad (4c) \end{aligned}$$

The percentage yields for the three branches at 195 K using *JPL 02-25* kinetics are noted. Channels 4a and 4b lead to

ozone loss (following thermal decomposition of ClOO or photolysis of BrCl), which is generically represented by process 2a in the depiction of Cycle 2. Channel 4c, the most efficient branch, results in a null cycle, since the O-O bond is not reformed upon loss of OClO.

The only direct determination of the yield of BrCl from BrO + ClO, a laboratory study conducted at room temperature (Poulet et al., 1990), resulted in a yield of ~12%, larger than the *JPL 02-25* room temperature recommendation of 9 ± 2%. Considerable uncertainty exists in the branching ratios at temperatures characteristic of the polar vortices, owing mainly to the lack of direct laboratory determinations at low temperature. Nighttime abundances of OClO are particularly sensitive to the branching ratios of BrO + ClO, since the twilight formation of BrCl as a nighttime reservoir of bromine affects the efficiency of OClO production. An analysis of nighttime OClO measurements, obtained by lunar and stellar occultation, suggests a higher yield for BrCl and a smaller yield for OClO from the BrO + ClO reaction at low temperature than is given by *JPL 02-25* (Canty et al., 2005). This result could imply a ~10% increase in the rate of ozone loss by the BrO + ClO cycle (Canty et al., 2005). While numerous uncertainties complicate the interpretation of nighttime OClO, the study of Canty et al. (2005) underscores the need for better definition of the branching ratios of the BrO + ClO reaction.

The precise level of BrO and Br_y in the polar vortices remains an area of active research. Many measurements are emerging from satellite, balloon, and in situ aircraft instruments. Quantification of the contribution of VSL bromocarbons to the Br_y budget of the polar vortices and of the branching ratios of the BrO + ClO reaction at low temperature are needed to improve future quantification of the polar ozone loss rates and to better quantify the relative contribution of bromine to polar ozone loss.

4.2.1.3 Ozone Loss Rates

This section focuses on studies that examine the consistency of modeled and measured chemical loss rates of polar ozone. The discussion is organized around two key concepts: (1) that models, using rate constants from *JPL 02-25* and estimates of bromine based on supply of bromine from only CH_3Br + halons, tend to underestimate measured chemical ozone loss rates, particularly during cold Arctic Januaries (e.g., Rex et al., 2003 and references therein); and (2) that the overall amount of chemical loss of column ozone, for specific Arctic winters, exhibits a tight correlation with the volume of air in the vortex that has been exposed to PSCs throughout winter (Rex et al., 2004; Tilmes et al., 2004).

Ozone Loss Rates: Measurement Overview

The estimates of ozone loss rates in Rex et al. (2003) are based on the Match technique applied to a series of ozonesonde measurements. This study showed that measured chemical loss rates of Arctic ozone exceed the maximum possible calculated rates, assuming complete chlorine activation and *JPL 00-3* kinetics, for four cold Januaries (1992, 1995, 1996, and 2000). A number of other studies, some of which have been discussed in previous assessments, also have documented similar discrepancies between measured and calculated chemical ozone loss rates during cold Arctic Januaries (e.g., Hansen et al., 1997; Becker et al., 1998). The estimates of ozone loss rates in Rex et al. (2004), which examine processes over longer time scales than Rex et al. (2003), are based on the "vortex-averaged descent" technique applied to temporal averages of ozonesonde profiles inside the polar vortex. Rex et al. (2004) showed a tight, near-linear relation between chemical loss of column ozone (ΔO_3) and the volume of air exposed to PSC conditions (V_{PSC}) in the Arctic vortex for data collected during 10 Arctic winters that span 12 years (Figure 4-13, previous section). A preliminary version of this relation was presented in the previous Assessment. The relation between ΔO_3 and V_{PSC} was poorly simulated by the 3-D CTM simulations of SLIMCAT shown in Rex et al. (2004). These SLIMCAT simulations exhibit a slope that is considerably less steep than the observations (Figure 4-13), implying the model might be underestimating the sensitivity of future polar ozone depletion to climate change. However, as shown below, updated runs of SLIMCAT result in an improved simulation of the relation between ΔO_3 and V_{PSC}.

Tilmes et al. (2004) conducted an independent analysis of the relation between ΔO_3 and V_{PSC} that was based on chemical loss rates deduced from analyses of Halogen Occultation Experiment (HALOE) data. Their study supports the linear relationship between ΔO_3 and V_{PSC} reported by Rex et al. (2004). They also showed that, if V_{PSC} is averaged over the same time period as ΔO_3, then solar illumination of the cold vortex is a factor that impacts ozone loss rates.

Ozone Loss Rates: Theory and Observation

A number of studies using various models have shown considerable improvement in our understanding of polar ozone loss rates since the previous Assessment. Feng et al. (2005b) reported 3-D CTM calculations using the SLIMCAT model of Arctic ozone for the winters of 1999/2000, 2002/2003, and 2003/2004. In their model, they assumed an extra 100 pptv of chlorine and an extra 6 pptv of bromine reaches the stratosphere, due to short-

lived halocarbons (these values are consistent with estimates given in Chapter 2). They used *JPL 02-25* kinetics, except the value for σ_{ClOOCl} was based on Burkholder et al. (1990), extrapolated to 450 nm as described by Stimpfle et al. (2004). They used a simple nitric acid trihydrate (NAT)-based denitrification scheme, described by Davies et al. (2002). Overall, the model calculations provided a realistic representation of chemical ozone loss for the three winters. Some discrepancies between observed and calculated ozone are noted during times of vortex disturbance, but overall these simulations provide a quantitative advance in the ability to accurately simulate chemical ozone loss rates using the SLIMCAT model. Grooß et al. (2005b) reported improvements in the agreement between modeled and measured ozone loss rates upon use of a more realistic denitrification scheme within the CLaMS Lagrangian trajectory model for the Arctic winter of 2002/2003. A study using the MIMOSA-CHIM CTM found that denitrification contributed about 23% and 17% more ozone depletion for the Arctic winters of 1999-2000 and 2002-2003, respectively, compared with model calculations that did not include denitrification (Tripathi et al., 2006). They also found best agreement between measured and modeled chemical loss of column ozone for Arctic winters of 1999/2000 and 2002/2003 for a simulation that used the Burkholder et al. (1990) cross section, allowed for supply of bromine from CH_3Br and halons as well as short-lived species methylene bromide (CH_2Br_2) and bromochloromethane (CH_2BrCl), and an adjustment to cooling rates that improved agreement with measured N_2O (i.e., that led to more realistic vortex descent).

Chipperfield et al. (2005) examined the relation between ΔO_3 and V_{PSC} using runs of the SLIMCAT CTM updated relative to results shown in Rex et al. (2004). These runs used the Burkholder et al. (1990) extrapolated value for σ_{ClOOCl}, an extra 100 pptv of inorganic chlorine (Cl_y) and an extra 6 pptv of Br_y due to VSL halocarbons (Chapter 2), and a treatment of denitrification by large nitric acid trihydrate (NAT) particles (Davies et al., 2002) that results in denitrification for the cold winters that was largely absent from earlier ice-based denitrification schemes. The new denitrification scheme increased modeled ozone depletion by ~30% for cold winters, such as 1999/2000 (Davies et al., 2002; Chipperfield et al., 2005). Also, the new SLIMCAT runs were at higher spatial resolution ($2.8° \times 2.8°$) than the older simulations ($7.5° \times 7.5°$) shown in Rex et al. (2004) and used a new radiation scheme; these improvements lead to stronger descent and a more isolated vortex. The new SLIMCAT runs simulate quite well the empirical relation between ΔO_3 and V_{PSC} (Figure 4-13). Improvements relative to the SLIMCAT results shown in Rex et al. (2004) are due to all three chemical factors as well as the improved model representation of vortex descent and isolation.

Douglass et al. (2006) simulated ΔO_3 versus V_{PSC} using a CTM driven by winds from a 50-year integration of the Goddard Earth Observing System (GEOS-4) GCM. Their calculations were conducted at a resolution of 2.5° (longitude) by 2.0° (latitude). They concluded that use of winds from a GCM tends to result in a more realistic simulation of vortex isolation than found using assimilated winds. Douglass et al. (2006) were able to simulate well the empirical relation between ΔO_3 and V_{PSC} for standard photochemistry (e.g., *JPL 02-25*) and for Br_y assuming no contribution from VSL halocarbons. They also reported that use of the Burkholder et al. (1990) value for σ_{ClOOCl} and extra bromine from VSL compounds resulted in excess ozone loss compared with observations. Hence, it is presently unclear whether changes in ClO_x photochemistry and representation of Br_y from VSL compounds are needed to achieve accurate representation of the ΔO_3 versus V_{PSC} relation within CTMs. Finally, Tripathi et al. (2006) examined the sensitivity of ozone loss to CTM resolution, and concluded that their model required a resolution of $1.0° \times 1.0°$ to properly represent ozone loss at the edge of the vortex at low solar illumination (i.e., during January in the Arctic).

Hoppel et al. (2005a) compared measured ozone loss rates in the Antarctic vortex, found using the Match approach applied to POAM III satellite data, with Lagrangian box model estimates of calculated ozone loss rates. They reported that agreement between modeled and measured ozone loss rates is improved if the model employs larger values of σ_{ClOOCl} (e.g., Burkholder et al., 1990) and a total bromine loading of 24 pptv, reflecting an ~8 pptv contribution from VSL bromocarbons. This amount of bromine from VSL species is near the upper limit of estimates based on satellite and aircraft data (Section 2.5, Chapter 2). Tripathi et al. (2006) concluded that a CTM simulation using *JPL 02-25* kinetics and bromine from CH_3Br, halons, CH_2Br_2, and CH_2BrCl tended to underestimate observed Antarctic ozone loss rates for several winters. Slightly better agreement was obtained using Burkholder et al. (1990) cross sections.

Frieler et al. (2006) examined measured and modeled ozone loss rates for the Arctic and Antarctic vortices, with the measured loss rates based on Match estimates applied to ozonesonde data, and the modeled loss rates based on Lagrangian box model calculations. Their reference simulation used *JPL 02-25* kinetics and a value for BrO_x based on supply of Br_y from only CH_3Br + halons. Using the maximum amount of ClO_x available, the reference simulation underestimates observed ozone loss rates for several Arctic winters, particularly during cold Januaries, such as in 2000 (Figure 4-17, top panel), consistent

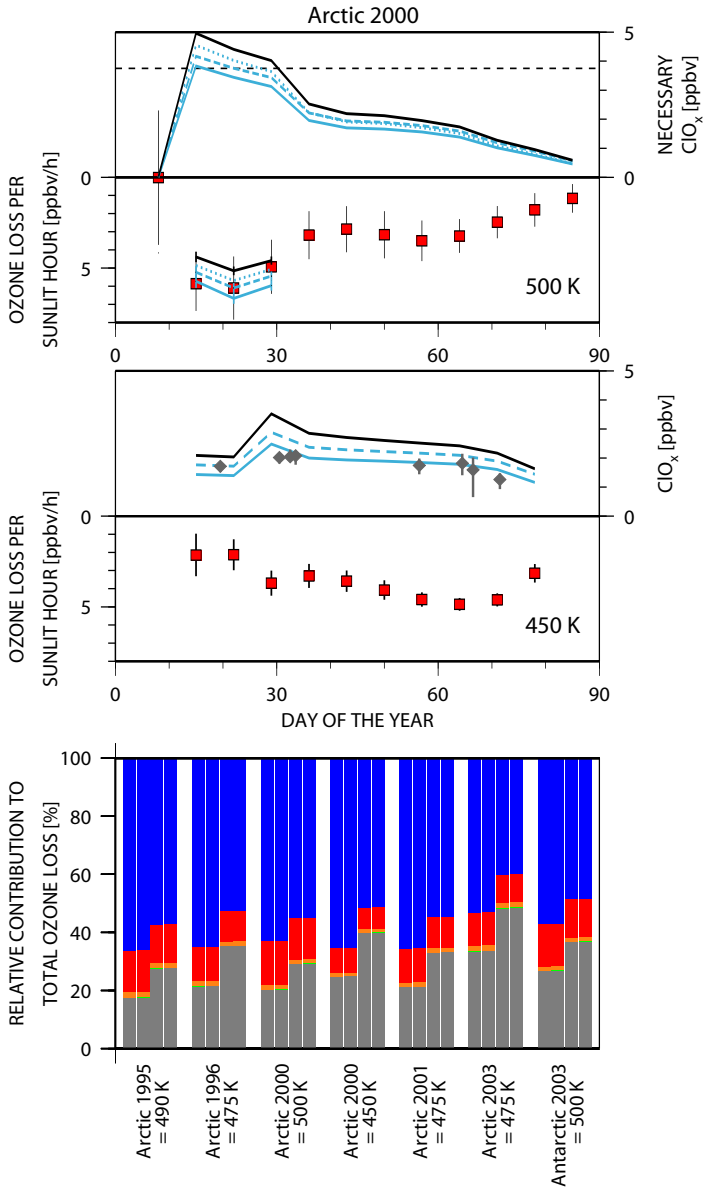

Figure 4-17. Top two panels: All results are for the Arctic winter 1999/2000. Gray diamonds represent the mean value of ClO_x measured at 450 ± 10 K potential temperature for 8 ER-2 flights that remained entirely inside the vortex; vertical bars represent the range between maximum and minimum ClO_x (Stimpfle et al., 2004). The lines represent the amount of ClO_x necessary to account for the measured ozone loss rate and the modeled ozone loss assuming ClO_x = 3.7 ppbv ("maximum possible ozone loss"), for the following four model runs:

- Run 1 (black): *JPL 02-25* kinetics and modeled BrO_x from CH_3Br and halons
- Run 2 (blue dashed): Burkholder et al. (1990) σ_{ClOOCl} and modeled BrO_x from CH_3Br + halons
- Run 3 (blue dotted): *JPL 02-25* kinetics and measured BrO_x
- Run 4 (blue solid): Burkholder et al. (1990) σ_{ClOOCl} and measured BrO_x

Red boxes show the observed chemical ozone loss rate per sunlit hour from Match (error bars denote 1σ uncertainty), used to constrain model estimates of necessary ClO_x. Bottom panel: Relative importance of ozone loss due to the BrO + ClO cycle (gray), the HOCl cycle (orange), the ClO + O cycle (red), and the ClO + ClO cycle (blue), for various Arctic winters (as indicated). Each grouping shows model results, in order, for the four model runs described above (e.g., run 4 has highest contribution of BrO + ClO to ozone loss). Adapted from Frieler et al. (2006).

with previous results (e.g., Rex et al., 2003). They show that the discrepancy between measured and maximum possible ozone loss rates in January (i.e., rates based on an assumption of complete chlorine activation) is largely resolved in a second model run that assumed a profile for BrO_x based on differential optical absorption spectroscopy (DOAS) balloon BrO that is considerably higher than BrO_x found assuming supply of Br_y from only CH_3Br + halons (Figure 4-16), and a value for J_{1b} based on the Burkholder et al. (1990) value for σ_{ClOOCl} (extrapolated to 450 nm). The largest effects on ozone removal rates were the faster value of J_{1b} (~20% effect) and the higher value of BrO_x (~15% effect). The relative contribution of Cycle 2 (BrO + ClO) to overall chemical loss for various winters increases from 17 to 33% for the reference run to 27 to 48% for the model run that agrees best with overall measured ozone loss rates (Figure 4-17, bottom panel).

Most important, Frieler et al. (2006) were able to examine ClO_x (Stimpfle et al., 2004), BrO_x (Fitzenberger, 2000; Canty et al., 2005), and measured and modeled ozone loss rates for the Arctic winter of 1999/2000. They showed good overall consistency between all of these quantities for the second model run (Figure 4-17, middle panel), suggesting a good quantitative explanation of the chemical loss rates of Arctic ozone for this winter at 450 K, the highest level where sufficient in situ measurements of ClO_x species are available. This finding relies on the validity of the larger value of J_{1b} and higher levels of stratospheric bromine. These aspects of polar chemistry are still subject to considerable uncertainty, due to differences in various laboratory measurements of σ_{ClOOCl} (Section 4.2.1.1) and uncertainty in the atmospheric abundance of BrO (Chapter 2). Also, quantitative consistency between observation of polar ozone loss rates and measured ClO_x and BrO has yet to be demonstrated at other altitudes and for other years.

In summary, numerous recent studies have shown that models are better able to capture the observed degree of chemical loss of polar ozone for a wide range of meteorological conditions that occurred during the past decade. This is an important advancement since the previous Assessment. The improvements of simulated ozone depletion are driven in part by the use of global models that are able to better capture the isolation of the polar vortices, due to improved horizontal resolution and/or winds that minimize excessive horizontal mixing across vortex boundaries. Previously noted discrepancies between measured and modeled ozone loss rates are largely resolved, within Lagrangian trajectory box models, assuming a faster rate of ClOOCl photolysis, higher levels of BrO that may be consistent with a significant source from VSL bromocarbons, and improved representation of denitrification that appears to be consistent with available observations (see Section 4.2.2). While the faster rate of ClOOCl photolysis appears to be consistent with atmospheric observations of ClO and ClOOCl, it is important to stress that daytime observations of these species constrain only the ratio k_{1a} / J_{1b}, and that considerable uncertainty exists in present laboratory determinations of k_{1a} and the cross sections used to calculate J_{1b}. Nighttime observations of ClO provide an important test of the consistency of our understanding of polar ozone photochemistry. However, field observations reveal inconsistencies with many laboratory studies. Also, we have yet to achieve consistency between thermodynamic and kinetic laboratory studies of ClO/ClOOCl photochemistry, in part due to the challenges associated with laboratory work at temperatures near 200 K. Finally, quantification of BrO and Br_y levels in the polar vortices, and the role of VSL bromocarbons, presents an additional source of uncertainty that is an active area of research.

4.2.2 PSC Processes

Polar stratospheric clouds (PSCs) influence ozone loss through two main processes: (1) chlorine activation on PSC particles leading to ozone losses and (2) sedimentation of PSCs causing denitrification and exacerbating ozone loss. Our understanding of denitrification in particular continues to evolve, mainly in response to research into the characteristics and formation of solid-phase nitric acid hydrate particles. WMO (2003) described the unexpectedly low (~10^{-4} cm^{-3}) concentrations of large nitric acid particles that were first observed during the 1999/2000 Arctic winter with the introduction of improved instrumentation (Fahey et al., 2001). Several studies have now concluded that such particles are widespread, both from in situ observations during the 2002/2003 Arctic winter (Larsen et al., 2004; Voigt et al., 2005) and from updated analyses of remote measurements (Poole et al., 2003; Adriani et al., 2004). Using multiple simultaneous PSC measurements, Larsen et al. (2004) have demonstrated that a low concentration of nitric acid trihydrate (NAT) particles can be masked when the coexisting liquid particles become optically dominant. Therefore, a background population of solid particles may be more pervasive than is apparent in remote sensing observations, requiring the introduction of new PSC formation mechanisms.

Synoptic-scale ice formation below the frost point (T_{ice}), which was considered to be a primary mechanism for solid nitric acid formation, is much too infre-

quent to account for the widespread formation of solid nitric acid particles in the Arctic. In contrast, mesoscale temperatures below T_{ice} may provide a NAT formation mechanism, through nucleation of nitric acid hydrates on mountain wave-induced ice clouds. High concentrations of mesoscale solid nitric acid particles have been unambiguously identified in multiple studies (Carslaw et al., 1999; Wirth et al., 1999; Hu et al., 2002; Fueglistaler et al., 2003; Luo et al., 2003). Modeling studies have demonstrated that sedimentation from the base of a NAT cloud with high particle concentrations (the "mother cloud") allows selective growth of a few NAT particles in the underlying supersaturated, cloud-free air (Fueglistaler et al., 2002a; Dhaniyala et al., 2002). Over several days, low concentrations (10^{-2}-10^{-5} cm^{-3}) of large NAT particles are generated over a wide vertical and horizontal extent. This mechanism can successfully explain observations of low NAT particle concentrations from clouds assumed to initially contain much higher solid particle concentrations (Fueglistaler et al., 2002b). Mann et al. (2005) have shown that including this mechanism in a 3-D model can produce large NAT particles in up to 60% of the NAT supersaturated region in the Arctic. Most studies have focused on the Arctic, but some Antarctic NAT PSC observations have also been attributed to mesoscale nucleation (Höpfner et al., 2006).

Other Arctic PSC observations, however, cannot be explained by mesoscale cloud formation (Pagan et al., 2004; Larsen et al., 2004; Voigt et al., 2005). Pagan et al. (2004) examined the role of mountain wave ice clouds in generating solid-phase nitric acid PSCs that were observed on three dates. Using satellite observations and model results to identify any regions with ice cloud formation, Pagan et al. (2004) concluded that none of the observed PSCs could have originated in an ice cloud. In situ measurements of large nitric acid particles at low concentrations made by Voigt et al. (2005) in the Arctic also cannot be attributed to ice formation, at either the synoptic scale or mesoscale. The observed particles formed within one day of the temperature dropping below the NAT temperature, T_{NAT}, with temperatures at most 3.1 K below T_{NAT} (implying NAT supersaturation ratios less than ten). The narrow range of environmental conditions strictly constrains the formation mechanism and the NAT freezing rate. Voigt et al. (2005) show that heterogeneous freezing of NAT, specifically triggered by meteoritic particles, could explain the observations. Homogeneous freezing of NAT is unlikely, because laboratory data show that such freezing is very slow under the observed conditions (Knopf et al., 2002). Alternative interpretations of the homogeneous freezing rates have been proposed (Tabazadeh, 2003). However, in a study of several proposed homogeneous freezing rates, Drdla and Browell (2004) concluded that none yielded model results consistent with observations of denitrification and PSC onset for the 1999/2000 Arctic winter. Heterogeneous freezing currently appears to be the most likely mechanism for producing nitric acid hydrate particles at synoptic scales in the Arctic. However, the specifics remain poorly defined, such as the nuclei involved, the factors that control the freezing rate, and the extent to which heterogeneous freezing also occurs in the Antarctic.

Based on these PSC formation mechanisms, new denitrification schemes for CTMs have been developed. Previous denitrification schemes that required synoptic scale temperatures below T_{ice} frequently failed to get any Arctic denitrification; the new schemes produce much more widespread denitrification. Revised denitrification has contributed to improvements in modeling ozone loss (see Section 4.2.1.3). Synoptic-scale particle formation has been approximated by applying a slow, uniform NAT particle-formation rate whenever NAT is supersaturated. Using this approach and an assumed rate of 8×10^{-10} $cm^{-3}s^{-1}$, Davies et al. (2005) have simulated several Arctic winters with the SLIMCAT CTM. Generally good agreement was found between model denitrification and observations (both satellite and in situ), but interannual variability in denitrification was not fully captured. The CLaMS has introduced a similar denitrification scheme (Grooß et al., 2005b); for the Arctic winter studied by Grooß et al. (2005b), a prescribed rate of 2×10^{-9} $cm^{-3}s^{-1}$ best reproduced observed denitrification. A single, constant particle formation rate appears insufficient to simulate interannual variability, but refinements will require a more detailed understanding of PSC formation mechanisms and their rates.

Alternatively, denitrification may be caused by mesoscale NAT PSCs. This mechanism has been studied with the SLIMCAT CTM (Mann et al., 2005) by introducing mountain wave-induced ice clouds that generate NAT "mother clouds." They concluded that approximately 80% of the denitrification observed in the 1999/2000 Arctic winter could have been caused by sedimentation of particles out of mountain wave-induced NAT mother clouds. Further quantification of this mechanism is limited by the requirement for accurate mountain wave information spanning the polar vortex. Therefore, the relative importance of synoptic scale and mesoscale processes for denitrification remains uncertain.

In summary, the mechanisms responsible for NAT PSC formation and thus denitrification have been refined

over the last four years, with increasing evidence that key processes occur above the ice frost point. However, specifics of PSC formation remain uncertain, forcing model denitrification to rely upon empirical freezing rates that are unable to fully capture interannual variability. Recent findings are primarily based on Arctic observations. Whether these PSC formation processes and denitrification mechanisms are equally applicable in the Antarctic remains to be evaluated.

4.3 RECENT POLAR OZONE CHANGES

4.3.1 2002 Antarctic Ozone Hole

In September 2002, a SH major stratospheric warming split the polar vortex and ozone hole for the first time in the observational record. Major warmings cause dramatic stratospheric circulation changes. Warmings are caused by planetary waves propagating up from the troposphere. These waves decelerate the polar night jet, increase polar temperatures, and distort and/or split the vortex. Warmings are classified as major if the 10 hPa zonal-mean temperatures increase poleward of 60° and 10 hPa zonal-mean winds turn easterly (Julian, 1967; Labitzke, 1968). Major warmings are distinguished from final warmings, where final warmings mark the transition from the cold vortex in winter to the warm anticyclone in summer.

The September 2002 major warming was puzzling because it was previously thought they only happened in the NH, where the tropospheric forced planetary wave activity is much stronger (see WMO, 1986, Section 6.1.7). The Arctic polar vortex is regularly disturbed by waves, with major warmings occurring every two to three years. The difference in planetary wave activity between the hemispheres is due to various factors: less orographic forcing and weaker longitudinal land-sea contrast in the SH, and the presence of the cold elevated Antarctic continent at the pole. As a consequence, Antarctic winter stratospheric temperatures are much colder than the Arctic and exhibit much less variability (see midwinter period in Figure 4-1). Furthermore, temperature records from 1940 do not show evidence of any major Antarctic warmings (Roscoe et al., 2005; Naujokat and Roscoe, 2005).

This unprecedented event induced a dramatic reduction of the ozone hole area to less than 5 million km^2 as compared with more than 20 million km^2 in the previous years (Stolarski et al., 2005). Its occurrence triggered numerous investigations using meteorological analyses, observations of chemical species from various satellite and ground-based instruments, and model simulations.

4.3.1.1 OBSERVATIONS

Chemistry

The major warming had a dramatic impact on total ozone (Stolarski et al., 2005). On 23 September, the ozone hole elongated and split in two pieces (Figure 4-18). One piece drifted over South America and dissipated, while the other drifted back over the pole as a significantly weakened ozone hole. The 2002 total ozone daily minimum value did not reach values lower than 150 DU, as compared with around 100 DU in the preceding decade. Higher total ozone values were observed in the polar region from mid-September to mid-October. Ozone hole metrics (Figures 4-7 and 4-8) all show remarkable deviations from averages over the last decade.

Ozone profiles showed that the vortex was not vertically aligned during the major warming. Solar Backscatter Ultraviolet (SBUV) measurements show an increase of ozone in the 70°-80°S region of about 200

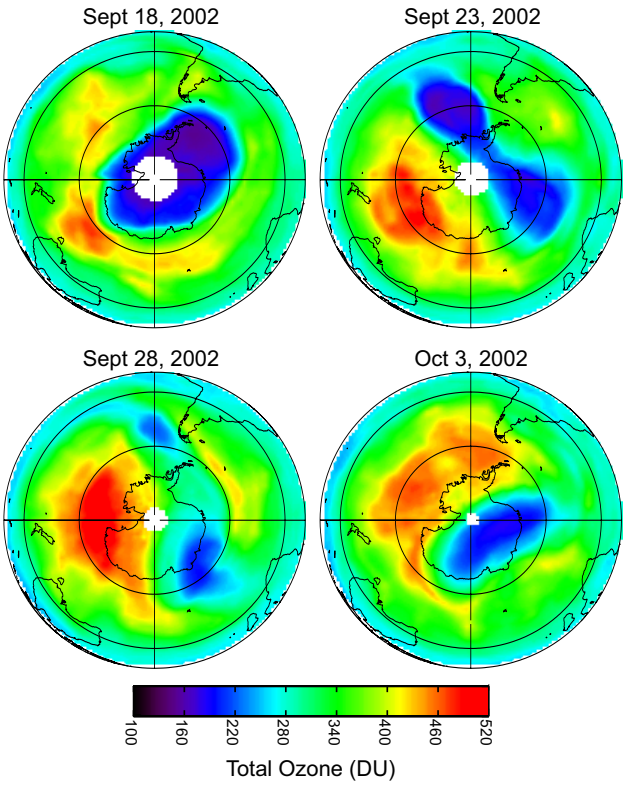

Figure 4-18. TOMS total ozone maps for four days during September and October 2002. The white space around the South Pole is polar night, where no measurements are made. Adapted from Stolarski et al. (2005).

DU due to the influx of low latitude air (Kondragunta et al., 2005). Upper levels of the vortex were displaced from the pole so that the ozone-depleted lower stratosphere region was overlaid by ozone-rich extra-vortex air (Allen et al., 2003; Randall et al., 2005a; Yela et al., 2005). POAM measurements showed that below 22 km, the chemical ozone loss was similar to previous years up to the major warming (Hoppel et al., 2003).

Measurements of minor chemical species provide further insights into the 2002 ozone hole. Most measurements showed that prior to the warming, the vortex was denitrified, with near-complete chlorine activation and extensive PSC areas up to 24 km (Ricaud et al., 2005; von Savigny et al., 2005). The large temperature increase during the warming induced rapid PSC disappearance and deactivation of chlorine radicals. Faster decay of the OClO slant column was measured by satellite and ground observations in September as compared with the same period in 1996-2001 (Richter et al., 2005; Frieß et al., 2005). The re-establishment in October of a weak vortex in the lowermost polar stratosphere was confirmed by satellite observations that showed low ozone mixing ratios below 20 km (Ricaud et al., 2005; von Savigny et al., 2005). As the middle stratosphere remained strongly perturbed, rapid NO_2 recovery above 25 km was observed, inducing larger than usual total NO_2 columns in the polar regions in October (Frieß et al., 2005; Richter et al., 2005; Yela et al., 2005).

Dynamics

Meteorological conditions in 2002 showed that the early winter was already unusually disturbed (Hio and Yoden, 2005; Newman and Nash, 2005; Allen et al., 2003). Figure 4-19 (second panel) displays the vertical distribution of the 2002 zonal-mean temperature departure from the 1979-2001 mean in the 55°-75°S latitude band. From June, temperatures steadily increased with respect to the climatological average until the September major warming. Temperature increases are associated with decreases of the zonal-mean wind intensity at 60°S and 10hPa (Figure 4-19, panels 1 and 3). In August, the zonal wind dropped below the 1979-2001 range of values and turned easterly during the warming. The temperature increase in the polar vortex collar is directly controlled by the planetary waves propagating upward from the troposphere to the stratosphere. The black line in the bottom panel of Figure 4-19 is the time series of midlatitude eddy heat flux in 2002 at 100 hPa for waves 1-3 (heat flux is proportional to the vertically propagating wave activity). The 2002 times series is compared with the climatological average over the 1979-2001 period (gray shading). There are several significant wave events from May to October. After each wave event, the stratosphere warmed by a few degrees until the major warming in late September. During this event, the eddy heat flux reached twice the largest value in the 1979-2001 period.

The synoptic development of the vortex split in September 2002 is described in several studies (e.g., Charlton et al., 2005; Krüger et al., 2005). The vortex began to split on 24 September. By 26 September, it had split completely at 10 hPa into two vortices of similar intensity with a tongue of anticyclonic circulation stretching across the pole and a region of high temperature between each vortex and the anticyclone. By 8 October, a single weakened vortex was re-established over the pole. The vortex split extended up to 1 hPa. In the lower stratosphere, the vortex did not split but formed two distinct cyclonic systems. During the major warming, polar temperatures south of 60° increased by about 25 K at 10 hPa and local temperature at several Antarctic stations showed an increase of up to 50 K at 30 and 10 hPa. The 60°S mean zonal wind reversed from ~60 m/s westerly to ~15 m/s easterly at 10 hPa until 30 September, when it switched back to westerlies. Much weaker westerly winds were re-established in October as one of the cyclonic remnants of the polar vortex moved back toward the pole. The final warming of the vortex occurred in late October, much earlier than in previous years.

4.3.1.2 Modeling of the Warming

The 2002 warming was simulated by mechanistic models for reproducing the event's dynamics, and by CTMs for a detailed evaluation of the vortex chemical evolution. The UK stratosphere-mesosphere model (USMM) reproduced the warming's dynamical features (Manney et al., 2005a). This simulation was initialized on 14 September 2002 and forced at 100 hPa by analyzed geopotential heights. The model produced a good simulation of the vortex recovery phase, suggesting that the warming's evolution was largely determined by the initial conditions and the prescribed 100 hPa geopotential heights. The modeled transport during the warming showed enhanced diabatic descent in the vortex below ~700 K and strong poleward transport and mixing in mid- to high-latitude regions. The strong vortex vertical tilt during the warming was well reproduced, showing low-latitude air surrounding and overlying the vortices after the split in the middle stratosphere. Sensitivity tests indicate a strong dependence on the boundary forcing, especially the amplitude and upward propagation of planetary wave-2.

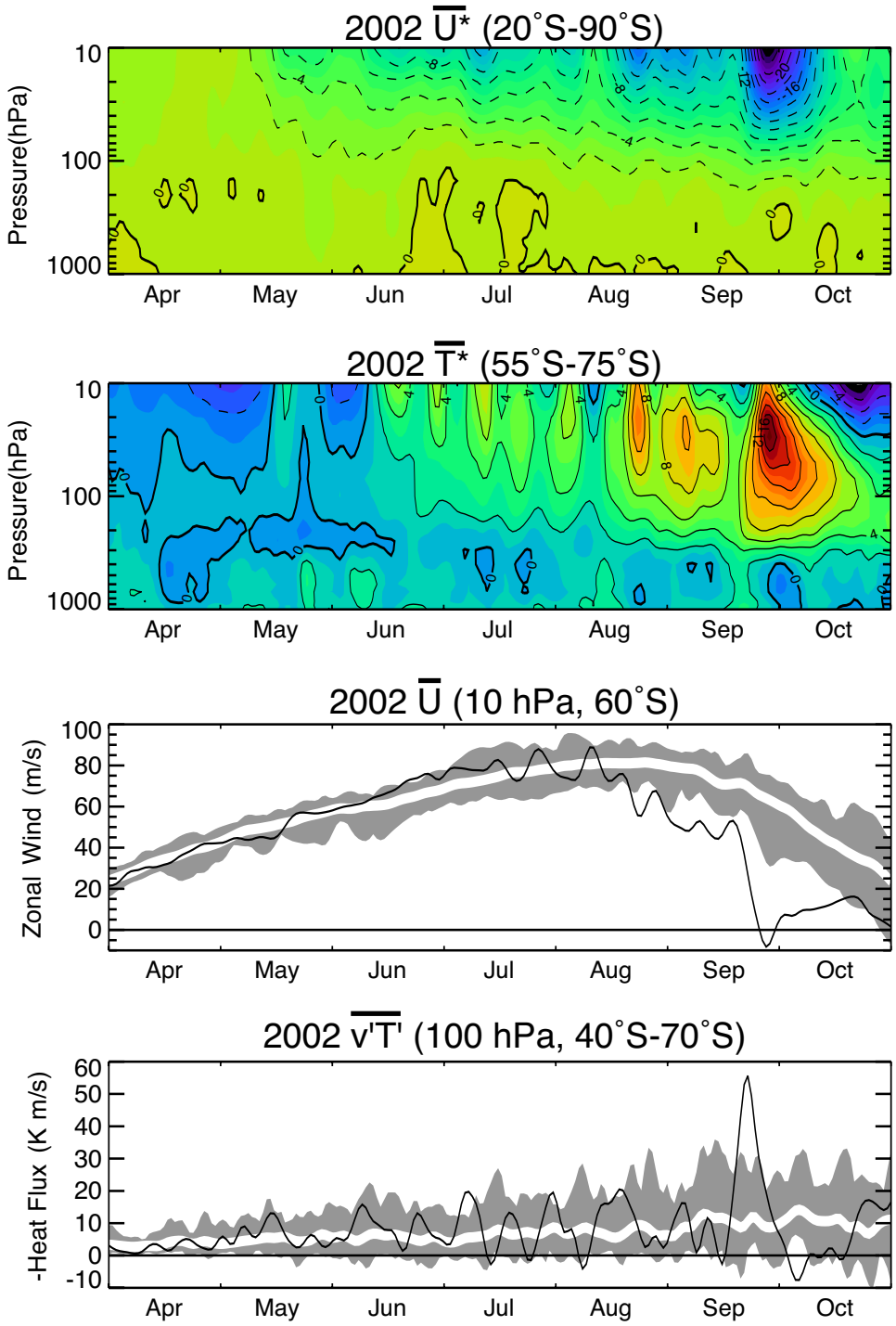

Figure 4-19. From top to bottom: (1) Daily zonal-mean zonal wind departures from the 1979-2001 mean for 1 April to 31 October 2002, averaged for 20°S to 90°S. Contour intervals are 2 m s^{-1} with dashed negative contours. (2) Daily zonal-mean temperature departures, averaged for 55°S to 75°S. Contour intervals are 2 K with dashed negative contours. (3) Daily zonal-mean zonal wind at 10 hPa and 60°S. Units are in m s^{-1}. (4) Daily zonal-mean eddy heat flux at 100 hPa, averaged for 40°S to 70°S. Units are in K m s^{-1}. In the two bottom panels, the black line shows 2002 values, which have been smoothed with a 1–2–1 filter applied three times. The white line displays the 23-year average (1979-2001), smoothed with a 15-day boxcar. The gray shading indicates the range of values (also 1–2–1 filtered) observed between 1979 and 2001. Adapted from Newman and Nash (2005) and Allen et al. (2003).

Several CTMs simulated the chemical polar ozone loss during the 2002 winter and spring. Using ECMWF or United Kingdom Meteorological Office (UKMO) analyses, the simulations successfully reproduced the main features of the 2002 Antarctic ozone hole (e.g., Ricaud et al., 2005; Konopka et al., 2005; Grooß et al., 2005a; Sinnhuber et al., 2003). Feng et al. (2005a) compared simulations of the 2002 Antarctic ozone hole with calculations for 2000. While large ozone losses were observed in 2002, the warmer than average 2002 vortex temperatures led to smaller amounts of ClO_x that induced smaller chemical ozone loss (Richter et al., 2005; Frieß et al., 2005). The accumulated chemical loss in the polar lower stratosphere was about 20 DU less than in 2000. Significant contributions to the larger September 2002 ozone column were caused by enhanced descent at the vortex edge and increased horizontal transport associated with the distorted vortex. Grooß et al. (2005a) showed that the rapid chlorine deactivation after the major warming depended on the ozone mixing ratio. Very low ozone mixing ratios favored formation of HCl, while larger ozone mixing ratios and less denitrification led to formation of $ClONO_2$. At higher altitudes (above 700 K), the midlatitude air masses transported to the polar region during the major warming experienced very large ozone depletion rates caused by NO_x catalytic cycles typical of polar summer chemistry. Several model simulations showed enhanced ozone loss in the midlatitudes due to the dilution of ozone-poor vortex air during the major warming (Grooß et al., 2005a; Feng et al., 2005a; Marchand et al., 2005). The polar vortex remnant that survived the major warming was strongly isolated from the extra vortex air until late November and did not experience any significant dilution with the midlatitude air (Konopka et al., 2005).

4.3.1.3 Theoretical Understanding

Several studies examined the conditions that led to the major warming in 2002 in order to explain this unprecedented event. Scaife et al. (2005) and Newman and Nash (2005) both argued that the stratosphere had been preconditioned throughout the preceding months by stratospheric vacillations in the zonal-mean winds. Scaife et al. (2005) further argued that the large September tropospheric wave pulse that caused the warming was also dependent on this preconditioning. Numerical simulations of the stratospheric flow show distinct stratospheric regimes that are either steady or vacillating. Vacillations are found for high levels of planetary wave forcing emanating from the troposphere (Scaife and James, 2000). The SH stratosphere flow is generally in quasi-steady state or in vacillating regimes for a short period of time. The 2002 winter was in a vacillating regime beginning in June. This vacillation induced a systematic weakening of the polar-night jet that ultimately allowed a strong pulse of planetary wave to propagate into the stratosphere.

Gray et al. (2005) examined the influence of the QBO on the major warming. Contrary to expectations, the warming event occurred during the QBO west phase in the lower stratosphere. NH major warmings are likelier in the QBO easterly phase when a zero wind line confines planetary wave propagation to higher latitudes, closer to the polar vortex. However, meteorological analyses indicated the presence of anomalously strong easterly equatorial winds above 10 hPa from January to September 2002. The influence of these anomalous winds was investigated in idealized model experiments where equatorial winds were relaxed to observations obtained in several years. It was shown that the 2002 equatorial winds hurried the simulated warming event. Harnik et al. (2005) also suggested that the low latitude, middle stratosphere easterly wind was a main factor in the warming. They showed that the zonal wind at 30°S and 10 hPa turned easterly in May 2002, due to a large burst of upward wave activity into the stratosphere. The primary effect of this event was the deceleration of the low-latitude winds in the upper stratosphere. The zero wind line was shifted significantly farther poleward than normal and the resulting enhanced poleward wave focusing is likely to have contributed to the erosion of the vortex.

Moreover the vortex preconditioning was connected with the persistence of large wave-2 amplitudes through the winter. The warming itself occurred when a large wave-1 disturbance combined with a traveling wave-2. Such a simultaneous combination was not observed during the period 1979-2001. Through a detailed study of the wave activity in both the troposphere and stratosphere in the winter 2002, Newman and Nash (2005) confirmed that the major warming could be explained by two main factors: (1) stronger than usual tropospheric wave forcing that propagated upward into the stratosphere and (2) a propagation state in the stratosphere that favored upward propagation of waves. They showed that for April-September, the heat flux at 200 hPa for wave 1-3 between 40°S and 70°S was 50% larger than climatology. The stronger wave-1 in the lower stratosphere was found to be statistically related to wave-1 in the lower troposphere, itself highly correlated with wave-1 in the tropics. The 2002 winter average wave-1 amplitudes in both the midlatitude lower troposphere and tropical upper troposphere were the largest observed over the 1979-2002 record.

During the 2002 winter, larger-than-normal planetary-scale wave events occurred regularly in the

midlatitude troposphere. The zonal-mean flow at the tropopause and in the tropical upper stratosphere was conducive to wave propagation, and these waves in the troposphere were efficiently refracted upward into the stratosphere. Each wave event warmed the polar lower stratosphere and weakened the jet stream. By mid-September the cumulative effect of wave activity had efficiently preconditioned the stratosphere. The major warming was preceded by an extraordinary strong pulse of eddy heat flux in the upper troposphere/lower stratosphere, much stronger than what is typically observed in the SH and even in a NH major warming (Harnik et al., 2005; Manney et al., 2005a).

4.3.2 Is Polar Ozone Getting Worse?

Observed total ozone columns in the polar regions have been larger in recent winters than in the 1990s, as emphasized in Section 4.1.2. The stabilization of ozone-depleting substances (ODSs) in the stratosphere has raised the question of its impact on observed ozone levels in the polar regions. This topic is discussed throughout the Assessment; see Chapter 1 for past and present ODS levels, Section 6.5.3 of Chapter 6 for attribution of recent changes in polar ozone as they pertain to changes in halogen loadings, Section 6.6.4 of Chapter 6 for projected future changes in polar ozone, and Chapter 8 for future ODS levels. The effect of anthropogenic elevated halogen levels in the stratosphere on polar ozone is different in both hemispheres due to differences in meteorological conditions. The Antarctic winter stratosphere is characterized by cold and stable meteorological conditions. The large chlorine activation induced by the very low temperatures in the vortex core leads to a nearly complete ozone destruction in the lower stratosphere by the end of September, which indicates that the Antarctic ozone depletion is saturated. The effects of ODS leveling off and saturation are difficult to discriminate. In contrast, Arctic chemical ozone loss is not saturated, due to much warmer conditions in the winter stratosphere. Arctic year-to-year variation is primarily controlled by the year-to-year variability in stratospheric temperatures. These temperature variations are much larger in the NH than in the SH. The large NH variability makes it difficult to establish long-term trends in Arctic ozone.

4.3.2.1 Arctic

Recent winters (since 1997/1998) have been characterized by higher than average temperatures than in the 1990s, although 1999/2000 and 2004/2005 stand out as being particularly cold, with record ozone chemical depletion (see Section 4.1.2). Major stratospheric warmings were more frequent prior to 1990, while the 1990s were remarkable by the absence of such events (except during the winter 1998/1999). Studies of Arctic chemical ozone loss over this range of years and meteorological conditions have shown that a near-linear relationship can be found between the vortex average chemical ozone loss and V_{PSC}, the stratospheric volume of potential PSC as shown in Figure 4-13 (Rex et al., 2004, 2006). Arctic ozone losses since 2000 are in line with the relationship based on data collected prior to 2000, with very low (as in 2001/2002) and very large (as in 2004/2005) chemical ozone loss that is clearly due to differences in V_{PSC} for these years. No specific change in the behavior of Arctic ozone loss can be detected from these observations, which is consistent with present understanding given the similar halogen loadings over the time period for which this relationship can be defined from observations.

4.3.2.2 Antarctic

Several studies have analyzed the evolution of the ozone hole since its appearance in the early 1980s. Newman et al. (2004) investigated the ozone hole area (OHA), while Bodeker et al. (2005) investigated OHA, annual minimum, and ozone mass deficit (OMD) (see Section 4.1.2 and Figure 4-8). The OHA and minimum ozone showed modest increases in severity in the 1990s, while OMD increased greatly in severity in the 1990s. The trend of monthly averaged OHA was analyzed by Alvarez-Madrigal and Pérez-Peraza (2005) in the period 1982-2003. After continuous growth since the eighties, the trend in October and November over 6-year subsets became negative since 2002. However, this trend did not account for temperature effects, or for dynamical effects during the breakup phase of the ozone hole.

Other studies investigated the relationship between the evolution of the Antarctic ozone hole and stratospheric chlorine and bromine levels over the last two decades. Newman et al. (2004) have shown that OHA is mainly controlled by catalytic ozone loss with stratospheric chlorine and bromine, and secondarily by the year-to-year variations in temperature in the collar region, near the edge of the polar vortex. Newman et al. (2004) fit the OHA to equivalent effective stratospheric chlorine (EESC, see Chapter 8, Box 8.1) with a 6-year time lag, and showed that OHA is currently decreasing at a very slow rate of 0.4% per year in response to halogen decreases. Huck et al. (2005) also fit the annual mean OMD to EESC with a 3-year time lag, the eddy heat flux anomalies at 20 hPa and 60°S, and South Pole 100 hPa temperature anomalies. In both studies, EESC and temperature explain almost all

of the variability of ozone-hole diagnostics. The residuals of the OHA fit to EESC and temperature have year-to-year variations of a few millions km^2 (compared with a current area of 23-24 millions km^2). This variance masks the area response to the small halogen decreases over Antarctica since 2000.

An increase of ozone due to ODS decreases can also be looked for in regions where the chemical loss is still the main factor affecting ozone variations but without saturation, as in the upper edge (above 20 km) or in the collar region (60°S-70°S) of the Antarctic ozone hole. Using measurements from ozonesondes and the satellite-borne POAM instrument, Hoppel et al. (2005b) showed that the ozone mixing ratio near the top of the ozone hole at 20-22 km in early October was higher in the period 2001-2004 than in the previous years of POAM measurements (1994-1996; 1998-2000). However, this increase was accompanied by higher temperatures and reduced PSC occurrence frequency, which indicates that the ozone changes were linked to temperature variability associated with changes in dynamical processes rather than a decline in ODSs. The relationship between ozone mixing ratios and temperature in recent years also was noted by Solomon et al. (2005) from the analysis of four decades of ozonesondes over Antarctica. Yang et al. (2005) studied the evolution of ozone in the extra-vortex collar region (60°S-70°S), but this study is not completely representative of ozone hole conditions.

The latest studies on polar ozone thus show no further increase of the severity of the polar ozone depletion both in the Arctic and the Antarctic stratosphere. The Antarctic ozone hole shows a clear leveling off since the beginning of the century. The leveling off is primarily due to saturation of losses because of ODSs. Both 2002 and 2004 were weak ozone holes, giving the appearance of a downward trend. However, these weak holes directly resulted primarily from active SH dynamical forcing. Interannual variability of the SH is currently masking the expected ozone hole improvement as ODSs decrease. Arctic losses also appear to be decreasing, but the very large interannual variability of the Arctic masks the improvement as ODSs decrease.

4.4 THE INFLUENCE OF PRECIPITATING CHARGED PARTICLES ON POLAR OZONE

Precipitating charged particles influence ozone and other constituents. Processes on the Sun and in Earth's magnetosphere, the interaction of the solar wind with Earth's magnetosphere, and the interplanetary magnetic field ultimately drive the flux of charged particles into the atmosphere and have led to observed and predicted stratospheric and mesospheric constituent changes in the past few years. Some of these natural charged-particle-driven variations have been measured to cause significant increases in odd nitrogen and odd hydrogen constituents, with corresponding significant ozone decreases. These effects are transient as ozone recovers to quiescent levels within days (middle to upper mesosphere) to several years (middle and lower stratosphere) after these natural impacts. Since the previous Ozone Assessment, a wealth of new satellite measurements have become available that have helped to better quantify the charged particle atmospheric influences.

The charged particle effects that influence the atmosphere can roughly be grouped into three types of perturbations: (1) solar particle events, which are primarily protons entering the polar regions and thereby often are referred to as solar proton events (SPEs); (2) energetic electrons precipitating in the auroral zone and lower latitudes; and (3) galactic cosmic rays. Galactic cosmic rays (GCRs) continually create odd nitrogen and odd hydrogen constituents in the lower stratosphere and upper troposphere but play a small role in polar ozone variations.

SPEs and energetic precipitating electrons influence polar ozone levels. The most recent solar cycle period (solar cycle 23) was very active, with both SPEs and periods of enhanced fluxes of energetic electrons. In particular, six of the nine largest SPEs in the past 40 years occurred in the most recent solar cycle. The precipitating particles associated with these solar-driven events produced ionizations, excitations, dissociations, and dissociative ionizations of the background constituents in both the polar cap (reaching to 60° geomagnetic latitude or lower during strong geomagnetic storms) and lower latitudes, including the auroral oval region. The solar protons primarily deposited their energy in the mesosphere and stratosphere, whereas the energetic electrons primarily deposited their energy in the thermosphere and upper mesosphere.

HO_x (odd hydrogen, atomic hydrogen (H), hydroxyl radical (OH), hydroperoxyl radical (HO_2)) constituents are created by a series of ion chemistry reactions (e.g., Solomon et al., 1981) as a result of the charged particle precipitation. The solar particles and associated secondary electrons (produced in ionization events) also create atomic nitrogen through dissociation-producing collisions with molecular nitrogen (N_2). Atomic nitrogen then leads to the production of other odd nitrogen constituents, NO_y (total reactive nitrogen; usually includes atomic nitrogen (N), nitric oxide (NO), NO_2, nitrogen trioxide (NO_3), dinitrogen radical (N_2O_5), nitric acid (HNO_3), peroxynitric acid (HNO_4), $BrONO_2$, $ClONO_2$) through chemical reactions.

The HO_x increases cause short-lived ozone decreases in the polar mesosphere and upper stratosphere due to the short lifetimes of the HO_x constituents. This HO_x-caused ozone effect was first observed in Weeks et al. (1972) and explained in Swider and Keneshea (1973). The NO_y increases lead to both short- and long-lived polar stratospheric ozone changes because of the long lifetime of the NO_y family in this region. This NO_y-caused ozone impact was first suggested by Crutzen et al. (1975) and observed in Heath et al. (1977). Since these early works, a number of papers have been published that document these solar-caused polar changes (recently reviewed in Jackman and McPeters, 2004). Although HO_x-driven short-lived decreases are useful for understanding the mesosphere and upper stratosphere, the NO_y enhancements cause the more important charged-particle-induced polar ozone decreases.

4.4.1 Odd Nitrogen (NO_y) Enhancements

Substantial increases in odd nitrogen (NO_y) constituents in the mesosphere and upper stratosphere as a direct result of SPEs have been measured by several satellite instruments during solar cycle 23. Very large fluxes of solar protons in July 2000 produced huge increases (>50 parts per billion by volume (ppbv) in the mesosphere) in Arctic NO_x ($NO + NO_2$) (Jackman et al., 2001). The large SPEs in late October and early November 2003 also caused very large proton fluxes that created substantial amounts of NO_x (Jackman et al., 2005a; López-Puertas et al., 2005a; Seppälä et al., 2004). Other NO_y constituents also were elevated as a result of huge SPEs that occurred in October/November 2003, including HNO_3(Orsolini et al., 2005; López-Puertas et al., 2005b) and N_2O_5 and $ClONO_2$ (López-Puertas et al., 2005b).

Solar protons also caused long-term NO_y enhancements. For example, Randall et al. (2001) showed that Antarctic middle stratospheric NO_x in September 2000 was enhanced as a result of the transport of huge NO_x enhancements from the lower mesosphere and upper stratosphere, which were originally produced by the solar protons during the July 2000 SPE. Large enhancements of polar stratospheric NO_2 through November and into early December of 2003 probably were caused by the solar protons from the October/November 2003 SPEs (Seppälä et al., 2004; López-Puertas et al., 2005a).

High Arctic NO_x was observed in January to July 2004 by several satellite instruments (Natarajan et al., 2004; Randall et al., 2005b; Rinsland et al., 2005; López-Puertas et al., 2005a, 2006). Figure 4-20 (top, adapted from Randall et al., 2005b) shows NO_2 at 40 km for years 1994-1996 and 1998-2004. Very significant NO_2 enhance-

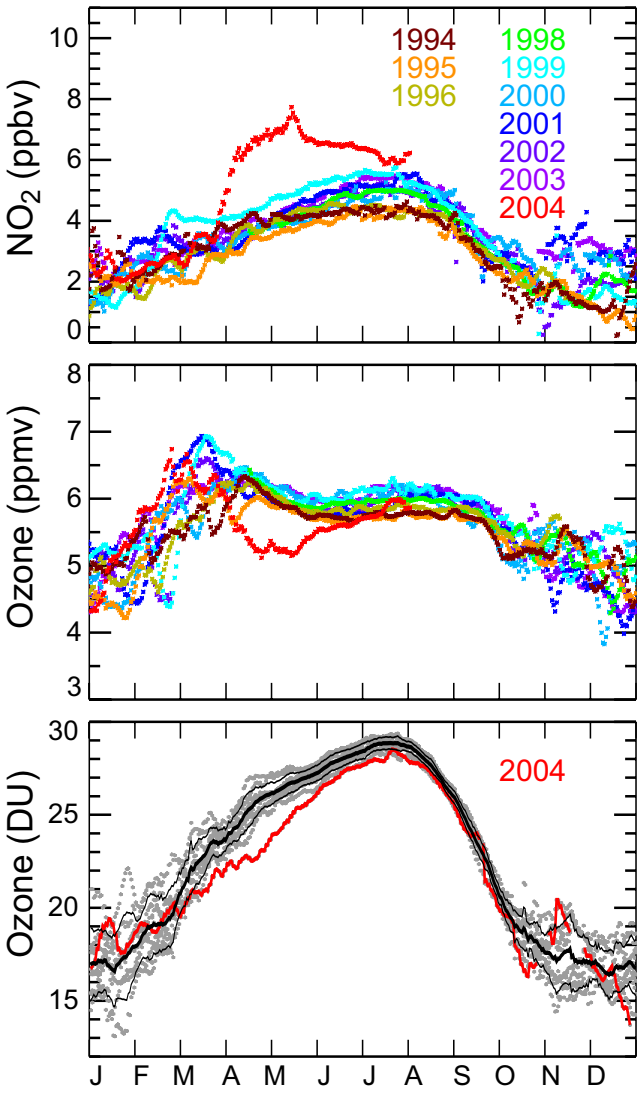

Figure 4-20. Seven-day running means of POAM II (1994-1996) and POAM III (1998-2004) NO_2 (top) and ozone (middle) mixing ratios in the NH at 40 km. The NO_2 enhancements and ozone reductions in the spring of 2004 resulted from transport to the stratosphere of NO_x produced by energetic particles precipitating in the mesosphere and thermosphere during the winter. The bottom panel shows 7-day running means of POAM partial column ozone over the vertical region from 35 to 50 km. Black lines represent the average (thick) ± 1σ standard deviation (thin) for column measurements from 1994 to 1996 and 1998 to 2004 (gray dots), excluding 2004. The red curve shows results for 2004 in all three panels. POAM II measurements have been corrected for instrument biases as determined by comparisons with independent satellite measurements. Adapted from Randall et al. (2005b).

ments are observed from March through July in 2004. It is unclear when these enhanced Northern Hemisphere NO_x levels were generated, although it is likely that energetic particle precipitation was the cause. The energetic electron fluxes associated with the geomagnetic storms of October/November 2003 were large and probably generated significant mesospheric and thermospheric NO_x (Natarajan et al., 2004), which could have been transported to lower levels. Other active geomagnetic periods in late November and December 2003 and even January 2004 could have been the main sources of the NO_x observed in the stratosphere and mesosphere (Randall et al., 2005b; López-Puertas et al., 2005a, 2006).

Funke et al. (2006) found high levels of Antarctic upper stratospheric NO_x during May to August 2003. This NO_x enhancement was attributed to precipitating electrons in the lower thermosphere and subsequent descent during polar night.

4.4.2 Ozone Decreases

Substantial mesospheric and upper stratospheric ozone decreases during and shortly after the July 2000, October/November 2003, and January 2005 SPEs were measured by several satellite instruments (see Jackman et al., 2001, 2005a, b; Seppälä et al., 2004, 2006; Verronen et al., 2005; Degenstein et al., 2005; López-Puertas et al., 2005a; Rohen et al., 2005). The transported NO_y enhancements from SPEs also resulted in observed ozone decreases. Randall et al. (2001) used POAM III observations to show middle stratospheric ozone decreases in September 2000 up to 45% (at 33 km) as a result of the solar proton precipitation in July 2000.

The long-lasting polar upper stratospheric ozone depletion was measured to be >30% for late November through December 2003 (Seppälä et al., 2004) and conjectured to be from the SPEs of October/November 2003. The polar upper stratospheric ozone depletion of more than 60% measured in the spring of 2004 (Natarajan et al., 2004; Randall et al., 2005b; López-Puertas et al., 2005a) is likely connected with the huge enhancements of geomagnetic storm-generated NO_x in November/December 2003 and January 2004 (see Section 4.4.1). Figure 4-20 (middle and bottom, adapted from Randall et al., 2005b) shows the measured variations in ozone at 40 km (middle plot) and partial column ozone between 35 and 50 km (bottom plot). Total ozone decreases were measured to be ~0.5-1% (~1.5-3 DU, compared with unperturbed levels of ~300 DU) in the spring and early summer of 2004 and are correlated with the NO_2 enhancements.

Models have been used to predict the impact of the solar protons in solar cycle 23. Krivolutsky et al. (2005) predicted significant short-term ozone changes as a result of SPEs in July and November 2000, November 2001, and October/November 2003 with the use of a one-dimensional (1-D) photochemical model. Jackman et al. (2005b) simulated the influences of all the solar proton fluxes between 2000 and 2003 with a two-dimensional (2-D) CTM and predicted polar total ozone decreases of ~0.5-3% (~2-10 DU). These computed depletions resulted from the large solar proton fluxes in 2000, 2001, and 2003. The ozone decreases last beyond the SPEs and gradually diminish over several years as the NO_y (mainly in the form of nitric acid (HNO_3)) is transported to the troposphere and rained out from the atmosphere through wet deposition or sedimentation.

The electron impacts associated with geomagnetic storms are more difficult to simulate, since the magnitude of the precipitating electrons is hard to measure. However, Rozanov et al. (2005) and Langematz et al. (2005) simulated the impact of energetic electron precipitation with 3-D CCMs and suggest that the solar cycle variation of the electron flux could cause polar middle stratospheric ozone changes of 20% or more. Sinnhuber et al. (2005a) analyzed polar ozonesonde measurements with the use of a 3-D CTM, which includes measured temperatures and wind fields. They find that the residual ozone (modeled minus measured) at 800 K correlates very well with Geostationary Operational Environmental Satellite (GOES)-measured electron fluxes greater than 2 MeV, which are not in phase with 10.7-cm solar radio flux. Precipitating electrons may be somewhat important in determining long-term stratospheric ozone variability in both the SH and in the NH during years when there is a strong polar vortex accompanied by significant downward transport from the mesosphere to the stratosphere (e.g., early 2004 in the NH) (Manney et al., 2005a; Semeniuk et al., 2005).

REFERENCES

Adriani, A., P. Massoli, G. Di Donfrancesco, F. Cairo, M.L. Moriconi, and M. Snels, Climatology of polar stratospheric clouds based on lidar observations from 1993 to 2001 over McMurdo Station, Antarctica, *J. Geophys. Res.*, *109*, D24211, doi: 10.1029/2004 JD004800, 2004.

Allen, D.R., R.M. Bevilacqua, G.E. Nedoluha, C.E. Randall, and G.L. Manney, Unusual stratospheric transport and mixing during the 2002 Antarctic winter, *Geophys. Res. Lett., 30* (12), 1599, doi: 10.1029/2003GL017117, 2003.

Alvarez-Madrigal, M., and J. Pérez-Peraza, Analysis of the evolution of the Antarctic ozone hole size, *J.*

Geophys. Res., 110, D02107, doi: 10.1029/2004 JD004944, 2005.

Anderson, J.G., W.H. Brune, S.A. Lloyd, D.W. Toohey, S.P. Sander, W.L. Starr, M. Loewenstein, and J.R. Podolske, Kinetics of O_3 destruction by ClO and BrO within the Antarctic vortex: An analysis based on in situ ER-2 data, *J. Geophys. Res.*, *94* (D9), 11480-11520, 1989.

Anderson, J.G., D.W. Toohey, and W.H. Brune, Free radicals within the Antarctic vortex: The role of CFCs in Antarctic ozone loss, *Science*, *251* (4989), 39-46, 1991.

Avallone, L.M., and D.W. Toohey, Tests of halogen photochemistry using in situ measurements of ClO and BrO in the lower polar stratosphere, *J. Geophys. Res., 106* (D10), 10411-10422, 2001.

Becker, G., R. Müller, D.S. McKenna, M. Rex, and K.S. Carslaw, Ozone loss rates in the Arctic stratosphere in the winter 1991/92: Model calculations compared with Match results, *Geophys. Res. Lett.*, *25* (23), 4325-4328, 1998.

Bengtsson, L., S. Hagemann, and K.I. Hodges, Can climate trends be calculated from reanalysis data?, *J. Geophys. Res., 109*, D11111, doi: 10.1029/2004 JD004536, 2004.

Berthet, G., P. Ricaud, F. Lefèvre, E. Le Flochmoën, J. Urban, B. Barret, N. Lautié, E. Dupuy, J. De La Noë, and D. Murtagh, Nighttime chlorine monoxide observations by the Odin satellite and implications for the ClO/Cl_2O_2 equilibrium, *Geophys. Res. Lett., 32*, L11812, doi: 10.1029/2005GL022649, 2005.

Bloss, W.J., S.L. Nickolaisen, R.J. Salawitch, R.R. Friedl, and S.P. Sander, Kinetics of the ClO self reaction and 210 nm absorption cross section of the ClO dimer, *J. Phys. Chem. A, 105*, 11226-11239, 2001.

Boakes, G., W.H. Hindy Mok, and D.M. Rowley, Kinetic studies of the ClO + ClO association reaction as a function of temperature and pressure, *Phys. Chem. Chem. Phys., 7* (24), 4102-4113, 2005.

Bodeker, G.E., H. Shiona, and H. Eskes, Indicators of Antarctic ozone depletion, *Atmos. Chem. Phys*., *5*, 2603-2615, 2005.

Bröske, R. and F. Zabel, Thermal decomposition of ClOOCl, *J. Phys. Chem. A*, *110* (9), 3280-3288, 2006.

Brune, W.H., J.G. Anderson, and K.R. Chan, In situ observations of BrO over Antarctica: ER-2 aircraft results from 54°S to 72°S latitude, *J. Geophys. Res.*, *94* (D14), 16639-16647, 1989a.

Brune, W.H., J.G. Anderson, and K.R. Chan, In situ observations of ClO in the Antarctic: ER-2 aircraft results from 54°S to 72°S latitude, *J. Geophys. Res.*, *94* (D14), 16649-16663, 1989b.

Burkholder, J.B., J.J. Orlando, and C.J. Howard, Ultraviolet absorption cross sections of chlorine oxide (Cl_2O_2) between 210 and 410 nm, *J. Phys. Chem., 94* (2), 687-695, 1990.

Canty, T., E.D. Rivière, R.J. Salawitch, G. Berthet, J.-B. Renard, K. Pfeilsticker, M. Dorf, A. Butz, H. Bösch, R.M. Stimpfle, D.M. Wilmouth, E.C. Richard, D.W. Fahey, P.J. Popp, M.R. Schoeberl, L.R. Lait, and T.P. Bui, Nighttime OClO in the winter Arctic vortex, *J. Geophys. Res., 110*, D01301, doi: 10.1029/2004JD005035, 2005.

Carslaw, K.S., T. Peter, J.T. Bacmeister, and S.D. Eckermann, Widespread solid particle formation by mountain waves in the Arctic stratosphere, *J. Geophys. Res., 104* (D1), 1827-1836, 1999.

Charlton, A.J., A. O'Neill, W.A. Lahoz, and P. Berrisford, The splitting of the stratospheric polar vortex in the Southern Hemisphere, September 2002: Dynamical evolution, *J. Atmos. Sci., 62* (3), 590-602, 2005.

Chipperfield, M.P., New version of the TOMCAT/ SLIMCAT off-line chemical transport model: Intercomparison of stratospheric tracer experiments, *Quart. J. Roy. Meteorol. Soc.*, *132* (617), 1179-1203, 2006.

Chipperfield, M.P., W. Feng, and M. Rex, Arctic ozone loss and climate sensitivity: Updated three-dimensional model study, *Geophys. Res. Lett., 32*, L11813, doi: 10.1029/2005GL022674, 2005.

Christensen, T., B.M. Knudsen, M. Streibel, S.B. Andersen, A. Benesova, G. Braathen, H. Claude, J. Davies, H. De Backer, H. Dier, V. Dorokhov, M. Gerding, M. Gil, B. Henchoz, H. Kelder, R. Kivi, E. Kyrö, Z. Litynska, D. Moore, G. Peters, P. Skrivankova, R. Stübi, T. Turunen, G. Vaughan, P. Viatte, A.F. Vik, P. von der Gathen, and I. Zaitcev, Vortex-averaged Arctic ozone depletion in the winter 2002/2003, *Atmos. Chem. Phys., 5*, 131-138, 2005.

Christiansen, B., Evidence for nonlinear climate change: Two stratospheric regimes and a regime shift, *J. Clim., 16* (22), 3681-3690, 2003.

Corti, S., F. Molteni, and T.N. Palmer, Signature of recent climate change in frequencies of natural atmospheric circulation regimes, *Nature, 398* (6730), 799-802, 1999.

Cox, R.A., and G.D. Hayman, The stability and photochemistry of dimers of the ClO radical and implications for Antarctic ozone depletion, *Nature, 332* (6167), 796-800, 1988.

Crutzen, P.J., and F. Arnold, Nitric-acid cloud formation in the cold Antarctic stratosphere: A major cause

for the springtime 'ozone hole', *Nature, 324*, 651-655, 1986.

Crutzen, P.J., I.S.A. Isaksen, and G.C. Reid, Solar proton events: Stratospheric sources of nitric oxide, *Science, 189* (4201), 457-459, 1975.

Davies, S., M.P. Chipperfield, K.S. Carslaw, B.M. Sinnhuber, J.G. Anderson, R.M. Stimpfle, D.M. Wilmouth, D.W. Fahey, P.J. Popp, E.C. Richard, P. von der Gathen, H. Jost, and C.R. Webster, Modeling the effect of denitrification on Arctic ozone depletion during winter 1999/2000, *J. Geophys. Res., 108* (D5), 8322, doi: 10.1029/2001 JD000445, 2002.

Davies, S., G.W. Mann, K.S. Carslaw, M.P. Chipperfield, J.A. Kettleborough, M.L. Santee, H. Oelhaf, G. Wetzel, Y. Sasano, and T. Sugita, 3-D microphysical model studies of Arctic denitrification: Comparison with observations, *Atmos. Chem. Phys., 5*, 347-393, 2005.

Degenstein, D.A., N.D. Lloyd, A.E. Bourassa, R.L. Gattinger, and E.J. Llewellyn, Observations of mesospheric ozone depletion during the October 28, 2003 solar proton event by OSIRIS, *Geophys. Res. Lett., 32*, L03S11, doi: 10.1029/2004 GL021521, 2005.

de Zafra, R.L., M. Jaramillo, A. Parrish, P. Solomon, B. Connor, and J. Barrett, High concentrations of chlorine monoxide at low altitudes in the Antarctic spring stratosphere: Diurnal variation, *Nature*, *328* (6129), 408-411, 1987.

Dhaniyala, S., K.A. McKinney, and P.O. Wennberg, Lee-wave clouds and denitrification of the polar stratosphere, *Geophys. Res. Lett.*, *29* (9), 1322, doi: 10.1029/2001GL013900, 2002.

Dorf, M., H. Bösch, A. Butz, C. Camy-Peyret, M.P. Chipperfield, A. Engel, F. Goutail, K. Grunow, F. Hendrick, S. Hrechanyy, B. Naujokat, J.-P. Pommereau, M. Van Roozendael, C. Sioris, F. Stroh, F. Weidner, and K. Pfeilsticker, Balloon-borne stratospheric BrO measurements: Comparison with ENVISAT/SCIAMACHY BrO limb profiles, *Atmos. Chem. Phys.*, *6*, 2483-2501, 2006.

Douglass, A.R., R.S. Stolarski, S.E. Strahan, and B.C. Polansky, Sensitivity of Arctic ozone loss to polar stratospheric cloud volume and chlorine and bromine loading in a chemistry and transport model, *Geophys. Res. Lett.*, *33*, L17809, doi: 10.1029/ 2006GL026492, 2006.

Drdla, K., and E.V. Browell, Microphysical modeling of the 1999-2000 Arctic winter: 3. Impact of homogeneous freezing on polar stratospheric clouds, *J. Geophys. Res.*, *109*, D10201, doi: 10.1029/2003 JD004352, 2004.

Dufour, G., R. Nassar, C.D. Boone, R. Skelton, K.A. Walker, P.F. Bernath, C.P. Rinsland, K. Semeniuk, J.J. Jin, J.C. McConnell, and G.L. Manney, Partitioning between the inorganic chlorine reservoirs, HCl and $ClONO_2$, during the Arctic winter 2005 derived from ACE-FTS, *Atmos. Chem. Phys.*, *6*, 2355-2366, 2006.

Fahey, D.W., R.S. Gao, K.S. Carslaw, J. Kettleborough, P.J. Popp, M.J. Northway, J.C. Holecek, S.C. Ciciora, R.J. McLaughlin, T.L. Thompson, R.H. Winkler, D.G. Baumgardner, B. Gandrud, P.O. Wennberg, S. Dhaniyala, K. McKinney, Th. Peter, R.J. Salawitch, T.P. Bui, J.W. Elkins, C.R. Webster, E.L. Atlas, H. Jost, J.C. Wilson, R.L. Herman, A. Kleinböhl, and M. von König, The detection of large HNO_3-containing particles in the winter Arctic stratosphere, *Science, 291* (5506), 1026-1031, 2001.

Farman, J.C., B.G. Gardiner, and J.D. Shanklin, Large losses of total ozone in Antarctica reveal seasonal ClO_x/NO_x interaction, *Nature*, *315*, 207-210, 1985.

Farmer, C.B., G.C. Toon, P.W. Schaper, J.-F. Blavier, and L.L. Lowes, Stratospheric trace gases in the spring 1986 Antarctic atmosphere, *Nature*, *329* (6135), 126-130, doi: 10.1038/329126a0, 1987.

Feng, W., M.P. Chipperfield, H.K. Roscoe, J.J. Remedios, A.M. Waterfall, G.P. Stiller, N. Glatthor, M. Höpfner, and D.-Y. Wang, Three-dimensional model study of the Antarctic ozone hole in 2002 and comparison with 2000, *J. Atmos. Sci., 62* (3), 822-837, 2005a.

Feng, W., M.P. Chipperfield, S. Davies, B. Sen, G. Toon, J.-F. Blavier, C.R. Webster, C.M. Volk, A. Ulanovsky, F. Ravegnani, P. von der Gathen, H. Jost, E.C. Richard, and H. Claude, Three-dimensional model study of the Arctic ozone loss in 2002/2003 and comparison with 1999/2000 and 2003/2004, *Atmos. Chem. Phys., 5*, 139-152, 2005b.

Fitzenberger, R., Investigation of the stratospheric inorganic bromine budget for 1996-2000: Balloon-borne measurements and model comparison, Ph.D. thesis, University of Heidelberg, Germany, 2000.

Free, M., S.J. Seidel, J.K. Angell, J. Lanzante, I. Durre, and T.C. Peterson, Radiosonde Atmospheric Temperature Products for Assessing Climate (RATPAC): A new data set of large-area anomaly time series, *J. Geophys. Res.*, *110*, D22101, doi: 10.1029/2005JD006169, 2005.

Frieler, K., M. Rex, R.J. Salawitch, T. Canty, M. Streibel, R.M. Stimpfle, K. Pfeilsticker, M. Dorf, D.K. Weisenstein, S. Godin-Beekmann, and P. von der Gathen, Toward a better quantitative understanding

of polar stratospheric ozone loss, *Geophys. Res. Lett.*, *33*, L10812, doi: 10.1029/2005GL025466, 2006.

Frieß, U., K. Kreher, P.V. Johnston, and U. Platt, Ground-based DOAS measurements of stratospheric trace gases at two Antarctic stations during the 2002 ozone hole period, *J. Atmos. Sci., 62* (3), 765-777, 2005.

Fueglistaler, S., B.P. Luo, C. Voigt, K.S. Carslaw, and Th. Peter, NAT-rock formation by mother clouds: A microphysical model study, *Atmos. Chem. Phys., 2*, 93-98, 2002a.

Fueglistaler, S., B.P. Luo, S. Buss, H. Wernli, C. Voigt, M. Müller, R. Neuber, C.A. Hostetler, L.R. Poole, H. Flentje, D.W. Fahey, M.J. Northway, and Th. Peter, Large NAT particle formation by mother clouds: Analysis of SOLVE/THESEO-2000 observations, *Geophys. Res. Lett., 29* (12), 1610, doi: 10.1029/2001GL014548, 2002b.

Fueglistaler, S., S. Buss, B.P. Luo, H. Wernli, H. Flentje, C.A. Hostetler, L.R. Poole, K.S. Carslaw, and Th. Peter, Detailed modeling of mountain wave PSCs, *Atmos. Chem. Phys., 3*, 697-712, 2003.

Funke, B., M. López-Puertas, S. Gil-López, T. von Clarmann, G.P. Stiller, H. Fischer, and S. Kellmann, Downward transport of upper atmospheric NO_x into the polar stratosphere and lower mesosphere during Antarctic 2003 and Arctic 2002/2003 winters, *J. Geophys. Res.*, *110*, D24308, doi: 10.1029/2005JD006463, 2005.

Fusco, A.C., and M.L. Salby, Interannual variations of total ozone and their relationship to variations of planetary wave activity, *J. Clim., 12* (6), 1619-1629, 1999.

Giovanelli, G., D. Bortoli, A. Petritoli, E. Castelli, I. Kostadinov, F. Ravegnani, G. Redaelli, C.M. Volk, U. Cortesi, G. Bianchini, and B. Carli, Stratospheric minor gas distribution over the Antarctic Peninsula during the APE-GAIA campaign, *Int. J. Remote Sens.*, *26* (16), 3343-3360, 2005.

Godin, S., V. Bergeret, S. Bekki, C. David, and G. Mégie, Study of the interannual ozone loss and the permeability of the Antarctic polar vortex from aerosol and ozone lidar measurements in Dumont d'Urville (66.4°S, 140°E), *J. Geophys. Res., 106* (D1), 1311-1330, 2001.

Golden, D.M., Reaction ClO + ClO → Products: Modeling and parameterization for use in atmospheric models, *Int. J. Chem. Kinet.*, *35* (5), 206-211, 2003.

Goutail, F., J.-P. Pommereau, F. Lefèvre, M. Van Roozendael, S.B. Andersen B.-A. Kåstad Høiskar, V. Dorokhov, E. Kyrö, M.P. Chipperfield, and W. Feng, Early unusual ozone loss during the Arctic winter 2002/2003 compared to other winters, *Atmos. Chem. Phys., 5*, 665-677, 2005.

Gray, L., W. Norton, C. Pascoe, and A. Charlton, A possible influence of equatorial winds on the September 2002 Southern Hemisphere sudden warming event, *J. Atmos. Sci., 62* (3), 651-667, 2005.

Grooß, J.-U., and R. Müller, The impact of mid-latitude intrusions into the polar vortex on ozone loss estimates, *Atmos. Chem. Phys., 3*, 395-402, 2003.

Grooß, J.-U., P. Konopka, and R. Müller, Ozone chemistry during the 2002 Antarctic vortex split, *J. Atmos. Sci., 62* (3), 860-870, 2005a.

Grooß, J.-U., G. Günther, R. Müller, P. Konopka, S. Bausch, H. Schlager, C. Voigt, C.M. Volk, and G.C. Toon, Simulation of denitrification and ozone loss for the Arctic winter 2002/2003, *Atmos. Chem. Phys., 5*, 1437-1448, 2005b.

Hansen, G., T. Svenøe, M.P. Chipperfield, A. Dahlback, and U.-P. Hoppe, Evidence of substantial ozone depletion in winter 1995/96 over northern Norway, *Geophys. Res. Lett.*, *24* (7), 799-802, 1997.

Harnik, N., R.K. Scott, and J. Perlwitz, Wave reflection and focusing prior to the major stratospheric warming of September 2002, *J. Atmos. Sci., 62* (3), 640-650, 2005.

Harris, N.R.P., M. Rex, F. Goutail, B.M. Knudsen, G.L. Manney, R. Müller, and P. von der Gathen, Comparison of empirically derived ozone losses in the Arctic vortex, *J. Geophys. Res., 107* (D20), 8264, doi: 10.1029/2001JD000482, 2002.

Heath, D.F., A.J. Krueger, and P.J. Crutzen, Solar proton event: Influence on stratospheric ozone, *Science, 197* (4306), 886-889, 1977.

Hio, Y., and S. Yoden, Interannual variations of the seasonal March in the Southern Hemisphere stratosphere for 1979-2002 and characterization of the unprecedented year 2002, *J. Atmos. Sci., 62* (3), 567-580, 2005.

Hofmann, D.J., and S.J. Oltmans, Anomalous Antarctic ozone during 1992: Evidence for Pinatubo volcanic aerosol effects, *J. Geophys. Res., 98* (D10), 18555-18562, 1993.

Höpfner, M., N. Larsen, R. Spang, B.P. Luo, J. Ma, S.H. Svendsen, S.D. Eckermann, B. Knudsen, P. Massoli, F. Cairo, G. Stiller, T.v. Clarmann, and H. Fischer, MIPAS detects Antarctic stratospheric belt of NAT PSCs caused by mountain waves, *Atmos. Chem. Phys., 6*, 1221-1230, 2006.

Hoppel, K., R. Bevilacqua, D. Allen, G. Nedoluha, and C. Randall, POAM III observations of the anomalous 2002 Antarctic ozone hole, *Geophys. Res. Lett., 30*

(7), 1394, doi: 10.1029/2003GL016899, 2003.

Hoppel, K., R. Bevilacqua, T. Canty, R. Salawitch, and M. Santee, A measurement/model comparison of ozone photochemical loss in the Antarctic ozone hole using Polar Ozone and Aerosol Measurement observations and the Match technique, *J. Geophys. Res., 110*, D19304, doi: 10.1029/2004JD005651, 2005a.

Hoppel, K., G. Nedoluha, M. Fromm, D. Allen, R. Bevilacqua, J. Alfred, B. Johnson, and G. König-Langlo, Reduced ozone loss at the upper edge of the Antarctic ozone hole during 2001-2004, *Geophys. Res. Lett., 32*, L20816, doi: 10.1029/2005GL023968, 2005b.

Hu, R.-M., K.S. Carslaw, C. Hostetler, L.R. Poole, B. Luo, T. Peter, S. Fueglistaler, T.J. McGee, and J.F. Burris, Microphysical properties of wave polar stratospheric clouds retrieved from lidar measurements during SOLVE/THESEO 2000, *J. Geophys. Res., 107* (D20), 8294, doi: 10.1029/2001JD001125, 2002.

Huck, P.E., A.J. McDonald, G.E. Bodeker, and H. Struthers, Interannual variability in Antarctic ozone depletion controlled by planetary waves and polar temperature, *Geophys. Res. Lett., 32*, L13819, doi: 10.1029/2005GL022943, 2005.

Huder, K.J., and W.B. DeMore, Absorption cross sections of the ClO dimer, *J. Phys. Chem., 99*, 3905-3908, 1995.

Huth, R., and P.O. Canziani, Classification of hemispheric monthly mean stratospheric potential vorticity fields, *Ann. Geophys., 21*, 805-817, 2003.

Jackman, C.H., and R.D. McPeters, The effect of solar proton events on ozone and other constituents, in *Solar Variability and its Effects on Climate*, edited by J.M. Pap, P.A. Fox, and C. Frohlich, *AGU Monograph 141*, 305-319, Washington, D.C., 2004.

Jackman, C.H., R.D. McPeters, G.J. Labow, E.L. Fleming, C.J. Praderas, and J.M. Russell, Northern Hemisphere atmospheric effects due to the July 2000 solar proton event, *Geophys. Res. Lett., 28* (15), 2883-2886, 2001.

Jackman, C.H., M.T. DeLand, G.J. Labow, E.L. Fleming, D.K. Weisenstein, M.K.W. Ko, M. Sinnhuber, and J.M. Russell, Neutral atmospheric influences of the solar proton events in October-November 2003, *J. Geophys. Res., 110*, A09S27, doi: 10.1029/2004JA010888, 2005a.

Jackman, C.H., M.T. DeLand, G.J. Labow, E.L. Fleming, D.K. Weisenstein, M.K.W. Ko, M. Sinnhuber, J. Anderson, and J.M. Russell, The influence of the several very large solar proton events in years 2000-2003 on the neutral middle atmosphere, *Adv. Space Res., 35*, 445-450, 2005b.

Jin, J.J., K. Semeniuk, G.L. Manney, A.I. Jonsson, S.R. Beagley, J.C. McConnell, G. Dufour, R. Nassar, C.D. Boone, K.A. Walker, P.F. Bernath, and C.P. Rinsland, Severe Arctic ozone loss in the winter 2004/2005: Observations from ACE-FTS, *Geophys. Res. Lett., 33*, L15801, doi: 10.1029/2006GL026752, 2006.

Jones, A.E., and J.D. Shanklin, Continued decline of total ozone over Halley, Antarctica since 1985, *Nature, 376*, 409-411, 1995.

Julian, P.R., Midwinter stratospheric warmings in the Southern Hemisphere: General remarks and a case study, *J. Appl. Meteorol., 6* (3), 557-563, 1967.

Knopf, D.A., T. Koop, B.P. Luo, U.G. Weers, and T. Peter, Homogeneous nucleation of NAD and NAT in liquid stratospheric aerosols: Insufficient to explain denitrification, *Atmos. Chem. Phys., 2*, 207-214, 2002.

Kondragunta, S., L.E. Flynn, A. Neuendorffer, A.J. Miller, C. Long, R. Nagatani, S. Zhou, T. Beck, E. Beach, R. McPeters, R. Stolarski, P.K. Bhartia, M.T. DeLand, and L.-K. Huang, Vertical structure of the anomalous 2002 Antarctic ozone hole, *J. Atmos. Sci., 62* (3), 801-811, 2005.

Konopka, P., J.-U. Grooß, K.W. Hoppel, H.-M. Steinhorst, and R. Müller, Mixing and chemical ozone loss during and after the Antarctic polar vortex major warming in September 2002, *J. Atmos. Sci., 62* (3), 848-859, 2005.

Krivolutsky, A., A. Kuminov, and T. Vyushkova, Ionization of the atmosphere caused by solar protons and its influence on ozonosphere of the Earth during 1994-2003, *J. Atmos. Sol.-Terr. Phys., 67* (1-2), 105-117, 2005.

Krüger, K., B. Naujokat, and K. Labitzke, The unusual midwinter warming in the Southern Hemisphere stratosphere 2002: A comparison to Northern Hemisphere phenomena, *J. Atmos. Sci., 62* (3), 603-613, 2005.

Labitzke, K., Midwinter warmings in the stratosphere and lower mesosphere and the behavior of ionospheric absorption, *Zeitschr. Geophys., 34*, 555-566, 1968.

Labitzke, K., and collaborators, *The Berlin Stratospheric Data Series* CD from Meteorological Institute, Freie Universität Berlin, Germany, 2002.

Labitzke, K., and M. Kunze, Stratospheric temperatures over the Arctic: Comparison of three data sets, *Meteorol. Z.*, *14* (1), 65-74, 2005.

Langematz, U., and M. Kunze, An update on dynamical changes in the Arctic and Antarctic stratospheric polar vortices, *Clim. Dyn.*, *27* (6), 647-660, doi:

10.1007/s00382-006-0156-2, 2006.

Langematz, U., J.L. Grenfell, K. Matthes, P. Mieth, M. Kunze, B. Steil, and C. Brühl, Chemical effects in 11-year solar cycle simulations with the Freie Universität Berlin Climate Middle Atmosphere Model with online chemistry (FUB-CMAM-CHEM), *Geophys. Res. Lett., 32*, L13803, doi: 10.1029/2005GL022686, 2005.

Lanzante, J.R., S.A. Klein, and D.J. Seidel, Temporal homogenization of monthly radiosonde temperature data. Part I: Methodology, *J. Clim*., *16* (2), 224-240, 2003.

Larsen, N., B.M. Knudsen, S.H. Svendsen, T. Deshler, J.M. Rosen, R. Kivi, C. Weisser, J. Schreiner, K. Mauerberger, F. Cairo, J. Ovarlez, H. Oelhaf, and R. Spang, Formation of solid particles in synoptic-scale Arctic PSCs in early winter 2002/2003, *Atmos. Chem. Phys., 4*, 2001-2013, 2004.

Lee, A.M., H.K. Roscoe, A.E. Jones, P.H. Haynes, E.F. Shuckburgh, M.W. Morrey, and H.C. Pumphrey, The impact of the mixing properties within the Antarctic stratospheric vortex on ozone loss in spring, *J. Geophys. Res., 106* (D3), 3203-3212, doi: 10.1029/2000JD900398, 2001.

Lehmann, R., P. von der Gathen, M. Rex, and M. Streibel, Statistical analysis of the precision of the Match method, *Atmos. Chem. Phys., 5*, 2713-2727, 2005.

López-Puertas, M., B. Funke, S. Gil-López, T. von Clarmann, G.P. Stiller, M. Höpfner, S. Kellman, H. Fischer, and C.H. Jackman, Observation of NO_x enhancement and ozone depletion in the Northern and Southern Hemispheres after the October-November 2003 solar proton events, *J. Geophys. Res., 110*, A09S43, doi: 10.1029/2005JA011050, 2005a.

López-Puertas, M., B. Funke, S. Gil-López, T. von Clarmann, G.P. Stiller, M. Höpfner, S. Kellman, G.M. Tsidu, H. Fischer, and C.H. Jackman, HNO_3, N_2O_5, and $ClONO_2$ enhancements after the October-November 2003 solar proton events, *J. Geophys. Res.*, *110*, A09S44, doi: 10.1029/2005 JA011051, 2005b.

López-Puertas, M., B. Funke, T.V. Clarmann, H. Fischer, and G.P. Stiller, The variability of stratospheric and mesospheric NO_y in the Arctic and Antarctic 2002-2004 polar winters, *Space Sci. Rev.*, in press, 2006.

Luo, B.P., C. Voigt, S. Fueglistaler, and T. Peter, Extreme NAT supersaturations in mountain wave ice PSCs: A clue to NAT formation, *J. Geophys. Res., 108* (D15), 4441, doi: 10.1029/2002JD003104, 2003.

Malanca, F.E., P.O. Canziani, and G.A. Argüello, Trends evolution of ozone between 1980 and 2000 at mid-latitudes over the Southern Hemisphere. Decadal differences in trends, *J. Geophys. Res., 110*, D05102, doi: 10.1029/2004JD004977, 2005.

Mann, G.W., K.S. Carslaw, M.P. Chipperfield, S. Davies, and S.D. Eckermann, Large nitric acid trihydrate particles and denitrification caused by mountain waves in the Arctic stratosphere, *J. Geophys. Res., 110*, D08202, doi: 10.1029/2004JD005271, 2005.

Manney, G.L., L. Froidevaux, M.L. Santee, N.J. Livesey, J.L. Sabutis, and J.W. Waters, Variability of ozone loss during Arctic winter (1991-2000) estimated from UARS Microwave Limb Sounder measurements, *J. Geophys. Res., 108* (D4), 4149, doi: 10.1029/2002JD002634, 2003a.

Manney, G.L., J.L. Sabutis, S. Pawson, M.L. Santee, B. Naujokat, R. Swinbank, M.E. Gelman, and W. Ebisuzaki, Lower stratospheric temperature differences between meteorological analyses in two cold Arctic winters and their impact on polar processing studies, *J. Geophys. Res.*, *108* (D5), 8328, doi: 10.1029/2001JD001149, 2003b.

Manney, G.L., J.L. Sabutis, D.R. Allen, W.A. Lahoz, A.A. Scaife, C.E. Randall, S. Pawson, B. Naujokat, and R. Swinbank, Simulations of dynamics and transport during the September 2002 Antarctic major warming, *J. Atmos. Sci., 62* (3), 690-707, 2005a.

Manney, G.L., M.L. Santee, N.J. Livesey, L. Froidevaux, W.G. Read, H.C. Pumphrey, J.W. Waters, and S. Pawson, EOS Microwave Limb Sounder observations of the Antarctic polar breakup in 2004, *Geophys. Res. Lett., 32*, L12811, doi: 10.1029/ 2005GL022823, 2005b.

Manney, G.L., K. Krüger, J.L. Sabutis, S.A. Sena, and S. Pawson, The remarkable 2003-2004 winter and other recent warm winters in the Arctic stratosphere since the late 1990s, *J. Geophys. Res., 110*, D04107, doi: 10.1029/2004JD005367, 2005c.

Manney, G.L., M.L. Santee, L. Froidevaux, K. Hoppel, N.J. Livesey, and J.W. Waters, EOS MLS observations of ozone loss in the 2004-2005 Arctic winter, *Geophys. Res. Lett*., *33*, L04802, doi: 10.1029/ 2005GL024494, 2006.

Marchand, M., S. Bekki, A. Pazmino, F. Lefèvre, S. Godin-Beekmann, and A. Hauchecorne, Model simulations of the impact of the 2002 Antarctic ozone hole on the midlatitudes, *J. Atmos. Sci.*, *62* (3), 871-884, 2005.

McElroy, M.B., R.J. Salawitch, S.C. Wofsy, and J.A. Logan, Reductions of Antarctic ozone due to synergistic interactions of chlorine and bromine, *Nature, 321*, 759-762, 1986.

Molina, L.T., and M.J. Molina, Production of Cl_2O_2 from the self-reaction of the ClO radical, *J. Phys. Chem., 91*, 433-436, 1987.

Moore, T.A., M. Okumura, J.W. Seale, and T.K. Minton, UV photolysis of ClOOCl, *J. Phys. Chem. A*, *103* (12), 1691-1695, 1999.

Morris, G.A., B.R. Bojkov, L.R. Lait, and M.R. Schoeberl, A review of the Match technique as applied to AASE-2/EASOE and SOLVE/THESEO 2000, *Atmos. Chem. Phys., 5*, 2571-2592, 2005.

Müller, R., S. Tilmes, J.-U. Grooß, D.S. McKenna, M. Müller, U. Schmidt, G.C. Toon, R.A. Stachnik, J.J. Margitan, J.W. Elkins, J. Arvelius, and J.M. Russell III, Chlorine activation and chemical ozone loss deduced from HALOE and balloon measurements in the Arctic during the winter of 1999-2000, *J. Geophys. Res., 108* (D5), 8302, doi: 10.1029/2001 JD001423, 2002.

Müller, R., S. Tilmes, P. Konopka, J.-U. Grooß, and H.-J. Jost, Impact of mixing and chemical change on ozone-tracer relations in the polar vortex, *Atmos. Chem. Phys., 5,* 3139-3151, 2005.

Nash, E.R., P.A. Newman, J.E. Rosenfield, and M.R. Schoeberl, An objective determination of the polar vortex using Ertel's potential vorticity, *J. Geophys. Res., 101* (D5), 9471-9478, 1996.

Natarajan, M., E.E. Remsberg, L.E. Deaver, and J.M. Russell III, Anomalously high levels of NO_x in the polar upper stratosphere during April, 2004: Photochemical consistency of HALOE observations, *Geophys. Res. Lett., 31*, L15113, doi: 10.1029/2004GL020566, 2004.

Naujokat, B., and H.K. Roscoe, Evidence against an Antarctic stratospheric vortex split during the periods of pre-IGY temperature measurements, *J. Atmos. Sci., 62* (3), 885-889, 2005.

Newman, P.A., and E.R. Nash, The unusual Southern Hemisphere stratosphere winter of 2002, *J. Atmos. Sci., 62* (3), 614-628, 2005.

Newman, P.A., E.R. Nash, and J.E. Rosenfield, What controls the temperature of the Arctic stratosphere during the spring?, *J. Geophys. Res., 106* (D17), 19999-20010, 2001.

Newman, P.A., S.R. Kawa, and E.R. Nash, On the size of the Antarctic ozone hole, *Geophys. Res. Lett., 31*, L21104, doi: 10.1029/2004GL020596, 2004.

Newman, P.A., E.R. Nash, S.R. Kawa, S.A. Montzka, and S.M. Schauffler, When will the Antarctic ozone hole recover?, *Geophys. Res. Lett.*, *33*, L12814, doi: 10.1029/2005GL025232, 2006.

Nickolaisen, S.L., R.R. Friedl, and S.P. Sander, Kinetics and mechanism of the ClO + ClO reaction – pressure and temperature dependences of the bimolecular and termolecular channels and thermal-decomposition of chlorine peroxide, *J. Phys. Chem., 98* (1), 155-169, 1994.

Nishizawa, S., and S. Yoden, Distribution functions of a spurious trend in a finite length data set with natural variability: Statistical considerations and a numerical experiment with a global circulation model, *J. Geophys. Res*., *110*, D12105, doi: 10.1029/ 2004JD005714, 2005.

Orsolini, Y.J., G.L. Manney, M.L. Santee, and C.E. Randall, An upper stratospheric layer of enhanced HNO_3 following exceptional solar storms, *Geophys. Res. Lett., 32*, L12S01, doi: 10.1029/ 2004GL021588, 2005.

Pagan, K.L., A. Tabazadeh, K. Drdla, M.E. Hervig, S.D. Eckermann, E.V. Browell, M.J. Legg, and P.G. Foschi, Observational evidence against mountain-wave generation of ice nuclei as a prerequisite for the formation of three solid nitric acid polar stratospheric clouds observed in the Arctic in early December 1999, *J. Geophys. Res., 109*, D04312, doi: 10.1029/2003JD003846, 2004.

Pawson, S., K. Labitzke, and S. Leder, Stepwise changes in stratospheric temperature, *Geophys. Res. Lett., 25* (12), 2157-2160, 1998.

Perlwitz, J., and H.-F. Graf, Troposphere-stratosphere dynamic coupling under strong and weak polar vortex conditions, *Geophys. Res. Lett., 28* (2), 271-274, 2001.

Perlwitz, J., and N. Harnik, Observational evidence of a stratospheric influence on the troposphere by planetary wave reflection, *J. Clim., 16* (18), 3011-3026, 2003.

Peterson, K.A., and J.S. Francisco, Does chlorine peroxide absorb below 250 nm?, *J. Chem. Phys.*, *121* (6), 2611-2616, 2004.

Pfeilsticker, K., W.T. Sturges, H. Bösch, C. Camy-Peyret, M.P. Chipperfield, A. Engel, R. Fitzenberger, M. Müller, S. Payan, and B.-M. Sinnhuber, Lower stratospheric organic and inorganic bromine budget for the arctic winter 1998/99, *Geophys. Res. Lett., 27* (20), 3305-3308, 2000.

Plenge, J., R. Flesch, S. Kühl, B. Vogel, R. Müller, F. Stroh, and E. Rühl, Ultraviolet photolysis of the ClO dimer, *J. Phys. Chem., A, 108* (22), 4859-4863, 2004.

Plenge, J., S. Kühl, B. Vogel, R. Müller, F. Stroh, M. von Hobe, R. Flesch, and E. Rühl, Bond strength of chlorine peroxide, *J. Phys. Chem. A*, *109* (30), 6730-6734, doi: 10.1021/jp044142h, 2005.

Poole, L.R., C.R. Trepte, V.L. Harvey, G.C. Toon, and R.L. Van Valkenburg, SAGE III observations of Arctic

polar stratospheric clouds – December 2002, *Geophys. Res. Lett., 30* (23), 2216, doi: 10.1029/2003GL018496, 2003.

Poulet, G., I.T. Lancar, G. Laverdet, and G. Le Bras, Kinetics and products of the BrO + ClO reaction, *J. Phys. Chem.*, *94* (1), 278-284, 1990.

Pundt, I., J.-P. Pommereau, M.P. Chipperfield, M. Van Roozendael, and F. Goutail, Climatology of the stratospheric BrO vertical distribution by balloon-borne UV-visible spectrometry, *J. Geophys. Res.*, *107* (24), 4806, doi: 10.1029/2002JD002230, 2002.

Raffalski, U., G. Hochschild, G. Kopp, and J. Urban, Evolution of stratospheric ozone during winter 2002/2003 as observed by a ground-based millimetre wave radiometer at Kiruna, Sweden, *Atmos. Chem. Phys., 5*, 1399-1407, 2005.

Ramaswamy, V., M.L. Chanin, J. Angell, J. Barnett, D. Gaffen, M. Gelman, P. Keckhut, Y. Koshelkov, K. Labitzke, J.J.R. Lin, A. O'Neill, J. Nash, W. Randel, R. Rood, K. Shine, M. Shiotani, and R. Swinbank, Stratospheric temperature trends: Observations and model simulations, *Rev. Geophys*., *39* (1), 71-122, 2001.

Ramaswamy, V., M.D. Schwarzkopf, W.J. Randel, B.D. Santer, B.J. Soden, and G.L. Stenchikov, Anthropogenic and natural influences in the evolution of lower stratospheric cooling, *Science, 311* (5764), 1138-1141, 2006.

Randall, C.E., D.E. Siskind, and R.M. Bevilacqua, Stratospheric NO_x enhancements in the Southern Hemisphere vortex in winter/spring of 2000, *Geophys. Res. Lett., 28* (12), 2385-2388, 2001.

Randall, C.E., G.L. Manney, D.R. Allen, R.M. Bevilacqua, J. Hornstein, C. Trepte, W. Lahoz, J. Ajtic, and G. Bodeker, Reconstruction and simulation of stratospheric ozone distributions during the 2002 Austral winter, *J. Atmos. Sci., 62* (3), 748-764, 2005a.

Randall, C.E., V.L. Harvey, G.L. Manney, Y. Orsolini, M. Codrescu, C. Sioris, S. Brohede, C.S. Haley, L.L. Gordley, J.M. Zawodny, and J.M. Russell III, Stratospheric effects of energetic particle precipitation in 2003-2004, *Geophys. Res. Lett., 32*, L05802, doi: 10.1029/2004GL022003, 2005b.

Randel, W.J., and F. Wu, Biases in stratospheric and tropospheric temperature trends derived from historical radiosonde data, *J. Clim.*, *19* (10), 2094-2104, 2006.

Randel, W.J., F. Wu, and R. Stolarski, Changes in column ozone correlated with EP flux, *J. Meteorol. Soc. Japan, 80* (4B), 849-862, 2002.

Renwick, J.A., Trends in the Southern Hemisphere polar vortex in NCEP and ECMWF reanalyses, *Geophys. Res. Lett., 31*, L07209, doi: 10.1029/2003GL019302, 2004.

Rex, M., P. von der Gathen, N.R.P. Harris, D. Lucic, B.M. Knudsen, G.O. Braathen, S.J. Reid, H. De Backer, H. Claude, R. Fabian, H. Fast, M. Gil, E. Kyrö, I.S. Mikkelsen, M. Rummukainen, H.G. Smit, J. Stähelin, C. Varotsos, and I. Zaitcev, In situ measurements of stratospheric ozone depletion rates in the Arctic winter of 1991/1992: A Lagrangian approach, *J. Geophys. Res., 103* (D5), 5843-5854, 1998.

Rex, M., R.J. Salawitch, N.R.P. Harris, P. von der Gathen, G.O. Braathen, A. Schulz, H. Deckelmann, M. Chipperfield, B.M. Sinnhuber, E. Reimer, R. Alfier, R. Bevilacqua, K. Hoppel, M. Fromm, J. Lumpe, H. Küllmann, A. Kleinböhl, H. Bremer, M. von König, K. Künzi, D. Toohey, H. Vömel, E. Richard, K. Aikin, H. Jost, J.B. Greenblatt, M. Loewenstein, J.R. Podolske, C.R. Webster, G.J. Flesch, D.C. Scott, R.L. Herman, J.W. Elkins, E.A. Ray, F.L. Moore, D.F. Hurst, P. Romashkin, G.C. Toon, B. Sen, J.J. Margitan, P. Wennberg, R. Neuber, M. Allart, B.R. Bojkov, H. Claude, J. Davies, W. Davies, H. De Backer, H. Dier, V. Dorokhov, H. Fast, Y. Kondo, E. Kyrö, Z. Litynska, I.S. Mikkelsen, M.J. Molyneux, E. Moran, T. Nagai, H. Nakane, C. Parrondo, F. Ravegnani, P. Skrivankova, P. Viatte, and V. Yushkov, Chemical depletion of Arctic ozone in winter 1999/2000, *J. Geophys. Res., 107* (D20), 8276, doi: 10.1029/2001JD000533, 2002.

Rex, M., R.J. Salawitch, M.L. Santee, J.W. Waters, K. Hoppel, and R. Bevilacqua, On the unexplained stratospheric ozone losses during cold Arctic Januaries, *Geophys. Res. Lett., 30* (1), 1008, doi: 10.1029/2002GL016008, 2003.

Rex, M., R.J. Salawitch, P. von der Gathen, N.R.P. Harris, M.P. Chipperfield, and B. Naujokat, Arctic ozone loss and climate change, *Geophys. Res. Lett., 31*, L04116, doi: 10.1029/2003GL018844, 2004.

Rex, M., R.J. Salawitch, H. Deckelmann, P. von der Gathen, N.R.P. Harris, M.P. Chipperfield, B. Naujokat, E. Reimer, M. Allaart, S.B. Andersen, R. Bevilacqua, G.O. Braathen, H. Claude, J. Davies, H. De Backer, H. Dier, V. Dorokhov, H. Fast, M. Gerding, S. Godin-Beekmann, K. Hoppel, B. Johnson, E. Kyrö, Z. Litynska, D. Moore, H. Nakane, M.C. Parrondo, A.D. Risley Jr., P. Skrivankova, R. Stübi, P. Viatte, V. Yushkov, and C. Zerefos, Arctic winter 2005: Implications for stratospheric ozone loss and climate change, *Geophys. Res. Lett*., *33*, L23808, doi: 10.1029/2006GL026731, 2006.

Ricaud, P., F. Lefèvre, G. Berthet, D. Murtagh, E.J.

Llewellyn, G. Mégie, E. Kyrölä, G.W. Leppelmeier, H. Auvinen, C. Boonne, S. Brohede, D.A. Degenstein, J. de La Noë, E. Dupuy, L. El Amraoui, P. Eriksson, W.F.J. Evans, U. Frisk, R.L. Gattinger, F. Girod, C.S. Haley, S. Hassinen, A. Hauchecorne, C. Jimenez, E. Kyrö, N. Lautié, E. Le Flochmoën, N.D. Lloyd, J.C. McConnell, I.C. McDade, L. Nordh, M. Olberg, A. Pazmio, S.V. Petelina, A. Sandqvist, A. Seppälä, C.E. Sioris, B.H. Solheim, J. Stegman, K. Strong, P. Taalas, J. Urban, C. von Savigny, F. von Scheele, and G. Witt, Polar vortex evolution during the 2002 Antarctic major warming as observed by the Odin satellite, *J. Geophys. Res., 110*, D05302, doi: 10.1029/2004JD005018, 2005.

Richter, A., F. Wittrock, M. Weber, S. Beirle, S. Kühl, U. Platt, T. Wagner, W. Wilms-Grabe, and J.P. Burrows, GOME observations of stratospheric trace gas distributions during the splitting vortex event in the Antarctic winter of 2002, Part I: Measurements, *J. Atmos. Sci., 62* (3), 778-785, 2005.

Rinsland, C.P., C. Boone, R. Nassar, K. Walker, P. Bernath, J.C. McConnell, and L. Chiou, Atmospheric Chemistry Experiment (ACE) Arctic stratospheric measurements of NO_x during February and March 2004: Impact of intense solar flares, *Geophys. Res. Lett., 32*, L16S05, doi: 10.1029/2005GL022425, 2005.

Rohen, G., C. von Savigny, M. Sinnhuber, E.J. Llewellyn, J.W. Kaiser, C.H. Jackman, M.-B. Kallenrode, J. Schröter, K.-U. Eichmann, H. Bovensmann, and J.P. Burrows, Ozone depletion during the solar proton events of October/November 2003 as seen by SCIAMACHY, *J. Geophys. Res., 110*, A09S39, doi: 10.1029/2004JA010984, 2005.

Roscoe, H.K., J.D. Shanklin, and S.R. Colwell, Has the Antarctic vortex split before 2002?, *J. Atmos. Sci., 62* (3), 581-588, 2005.

Rozanov, E., L. Callis, M. Schlesinger, F. Yang, N. Andronova, and V. Zubov, Atmospheric response to NO_y source due to energetic electron precipitation, *Geophys. Res. Lett., 32*, L14811, doi: 10.1029/2005GL023041, 2005.

Salawitch, R.J., D.K. Weisenstein, L.J. Kovalenko, C.E. Sioris, P.O. Wennberg, K. Chance, M.K.W. Ko, and C.A. McLinden, Sensitivity of ozone to bromine in the lower stratosphere, *Geophys. Res. Lett., 32*, L05811, doi: 10.1029/2004GL021504, 2005.

Sander, S.P., R.R. Friedl, W.B. DeMore, D.M. Golden, M.J. Kurylo, R.F. Hampson, R.E. Huie, G.K. Moortgat, A.R. Ravishankara, C.E. Kolb, and M.J. Molina, *Chemical Kinetics and Photochemical Data for Use in Stratospheric Modeling, Evaluation No. 13, JPL Publication 00-03*, Jet Propulsion Laboratory, Pasadena, Calif., 2000.

Sander, S.P., R.R. Friedl, D.M. Golden, M.J. Kurylo, R.E. Huie, V.L. Orkin, G.K. Moortgat, A.R. Ravishankara, C.E. Kolb, M.J. Molina, and B.J. Finlayson-Pitts, *Chemical Kinetics and Photochemical Data for Use in Atmospheric Studies, Evaluation No. 14, JPL Publication 02-25*, Jet Propulsion Laboratory, Pasadena, Calif., 2003.

Sander, S.P., R.R. Friedl, D.M. Golden, M.J. Kurylo, G.K. Moortgat, H. Keller-Rudek, P.H. Wine, A.R. Ravishankara, C.E. Kolb, M.J. Molina, B.J. Finlayson-Pitts, R.E. Huie, and V.L. Orkin, *Chemical Kinetics and Photochemical Data for Use in Atmospheric Studies, Evaluation Number 15, JPL Publication 06-02,* Jet Propulsion Laboratory, Pasadena, Calif., [Available: http://jpldataeval.jpl.nasa.gov/], 2006.

Sankey, D., and T.G. Shepherd, Correlations of long-lived chemical species in a middle atmosphere general circulation model, *J. Geophys. Res., 108* (D16), 4494, doi: 10.1029/2002JD002799, 2003.

Santee, M.L., G.L. Manney, N.J. Livesey, L. Froidevaux, I.A. MacKenzie, H.C. Pumphrey, W.G. Read, M.J. Schwartz, J.W. Waters, and R.S. Harwood, Polar processing and development of the 2004 Antarctic ozone hole: First results from MLS on Aura, *Geophys. Res. Lett., 32*, L12817, doi: 10.1029/2005GL022582, 2005.

Santer, B.D., T.M.L Wigley, A.J. Simmons, P.W. Kållberg, G.A. Kelly, S.M. Uppala, C. Ammann, J.S. Boyle, W. Brüggemann, C. Doutriaux, M. Fiorino, C. Mears, G.A. Meehl, R. Sausen, K.E. Taylor, W.M. Washington, M.F. Wehner, and F.J. Wentz, Identification of anthropogenic climate change using a second-generation reanalysis, *J. Geophys. Res.*, *109*, D21104, doi: 10.1029/2004JD005075, 2004.

Scaife, A.A., and I.N. James, Response of the stratosphere to interannual variability of tropospheric planetary waves, *Quart. J. Roy. Meteorol. Soc., 126* (562), 275-297, 2000.

Scaife, A.A., D.R. Jackson, R. Swinbank, N. Butchart, H.E. Thornton, M. Keil, and L. Henderson, Stratospheric vacillations and the major warming over Antarctica in 2002, *J. Atmos. Sci., 62* (3), 629-639, 2005.

Schnadt, C., M. Dameris, M. Ponater, R. Hein, V. Grewe, and B. Steil, Interaction of atmospheric chemistry and climate and its impact on stratospheric ozone, *Clim. Dyn., 18* (6), 501-517, 2002.

Schoeberl, M.R., S.R. Kawa, A.R. Douglass, T.J. McGee, E.V. Browell, J. Waters, N. Livesey, W. Read, L. Froidevaux, M.L. Santee, H.C. Pumphrey, L.R. Lait,

and L. Twigg, Chemical observations of a polar vortex intrusion, *J. Geophys. Res.*, *111*, D20306, doi: 10.1029/2006JD007134, 2006.

Schofield, R., P.V. Johnston, A. Thomas, K. Kreher, B.J. Connor, S. Wood, D. Shooter, M.P. Chipperfield, A. Richter, R. von Glasow, and C.D. Rodgers, Tropospheric and stratospheric BrO columns over Arrival Heights, Antarctica, 2002, *J. Geophys. Res.*, *111*, D22310, doi: 10.1029/2005JD007022, 2006.

Seidel, D.J., and J.R. Lanzante, An assessment of three alternatives to linear trends for characterizing global atmospheric temperature changes, *J. Geophys. Res., 109*, D14108, doi: 10.1029/2003 JD004414, 2004.

Seidel, D.J., J.K. Angell, M. Free, J. Christy, R. Spencer, S.A. Klein, J.R. Lanzante, C. Mears, M. Schabel, F. Wentz, D. Parker, P. Thorne, and A. Sterin, Uncertainty in signals of large-scale climate variations in radiosonde and satellite upper-air temperature data sets, *J. Clim*., *17* (11), 2225-2240, 2004.

Semeniuk, K., J.C. McConnell, and C.H. Jackman, Simulation of the October-November 2003 solar proton events in the CMAM GCM: Comparison with observations, *Geophys. Res. Lett., 32*, L15S02, doi: 10.1029/2004GL022392, 2005.

Seppälä, A., P.T. Verronen, E. Kyrölä, S. Hassinen, L. Backman, A. Hauchecorne, J.L. Bertaux, and D. Fussen, Solar proton events of October-November 2003: Ozone depletion in the Northern Hemisphere polar winter as seen by GOMOS/Envisat, *Geophys. Res. Lett., 31*, L19107, doi: 10.1029/2004 GL021042, 2004.

Seppälä, A., P.T. Verronen, V.F. Sofieva, J. Tamminen, E. Kyrölä, C.J. Rodger, and M.A. Clilverd, Destruction of the tertiary ozone maximum during a solar proton event, *Geophys. Res. Lett., 33*, L07804, doi: 10.1029/2005GL025571, 2006.

Shine, K.P., On the modeled thermal response of the Antarctic stratosphere to a depletion of ozone, *Geophys. Res. Lett.*, *13*, 1331-1334, 1986.

Singleton, C.S., C.E. Randall, M.P. Chipperfield, S. Davies, W. Feng, R.M. Bevilacqua, K.W. Hoppel, M.D. Fromm, G.L. Manney, and V.L. Harvey, 2002-2003 Arctic ozone loss deduced from POAM III satellite observations and the SLIMCAT chemical transport model, *Atmos. Chem. Phys., 5*, 597-609, 2005.

Singleton, C.S., C.E. Randall, V.L. Harvey, M.P. Chipperfield, W. Feng, L. Froidevaux, G.L. Manney, P.F. Bernath, K.A. Walker, C.D. Boone, and T. McElroy, Quantifying Arctic ozone loss during the 2004-2005 winter using satellite observations and a chemical transport model, *J. Geophys. Res.,* in press, 2006.

Sinnhuber, B.-M., M. Weber, A. Amankwah, and J.P. Burrows, Total ozone during the unusual Antarctic winter of 2002, *Geophys. Res. Lett., 30* (11), 1580, doi: 10.1029/2002GL016798, 2003.

Sinnhuber, B.-M., P. von der Gathen, M. Sinnhuber, M. Rex, G. König-Langlo, and S.J. Oltmans, Large decadal scale changes of polar ozone suggest solar influence, *Atmos. Chem. Phys. Discuss., 5,* 12103-12117, 2005a.

Sinnhuber, B.-M., A. Rozanov, N. Sheode, O.T. Afe, A. Richter, M. Sinnhuber, F. Wittrock, J.P. Burrows, G.P. Stiller, T. von Clarmann, and A. Linden, Global observations of stratospheric bromine monoxide from SCIAMACHY, *Geophys. Res. Lett.*, *32*, L20810, doi: 10.1029/2005GL023839, 2005b.

Sioris, C.E., L.J. Kovalenko, C.A. McLinden, R.J. Salawitch, M. Van Roozendael, F. Goutail, M. Dorf, K. Pfeilsticker, K. Chance, C. von Savigny, X. Liu, T.P. Kurosu, J.-P. Pommereau, H. Bösch, and J. Frerick, Latitudinal and vertical distribution of bromine monoxide in the lower stratosphere from Scanning Imaging Absorption Spectrometer for Atmospheric Chartography limb scattering measurements, *J. Geophys. Res.*, *111*, D14301, doi: 10.1029/2005JD006479, 2006.

Solomon, P.M., B. Connor, R.L. de Zafra, A. Parrish, J. Barrett, and M. Jaramillo, High concentrations of chlorine monoxide at low altitudes in the Antarctic spring stratosphere: Secular variation, *Nature*, *328* (6129), 411-413, 1987.

Solomon, S., D.W. Rusch, J.-C. Gérard, G.C. Reid, and P.J. Crutzen, The effect of particle precipitation events on the neutral and ion chemistry of the middle atmosphere, 2, Odd hydrogen, *Planet. Space Sci., 29* (8), 885-893, 1981.

Solomon, S., R.R. Garcia, F.S. Rowland, and D.J. Wuebbles, On the depletion of Antarctic ozone, *Nature, 321*, 755-758, 1986.

Solomon, S., G.H. Mount, R.W. Sanders, and A.L. Schmeltekopf, Visible spectroscopy at McMurdo Station, Antarctica, 2. Observations of OClO, *J. Geophys. Res.*, *92* (D7), 8329-8338, 1987.

Solomon, S., R.W. Portmann, T. Sasaki, D.J. Hofmann, and D.W.J. Thompson, Four decades of ozonesonde measurements over Antarctica, *J. Geophys. Res.*, *110*, D21311, doi: 10.1029/2005JD005917, 2005.

Stimpfle, R., D.M. Wilmouth, R.J. Salawitch, and J.G. Anderson, First measurements of ClOOCl in the stratosphere: The coupling of ClOOCl and ClO in the Arctic polar vortex, *J. Geophys. Res., 109*, D03301, doi: 10.1029/2003JD003811, 2004.

Stolarski, R.S., A.J. Kreuger, M.R. Schoeberl, R.D. McPeters, P.A. Newman, and J.C. Alpert, Nimbus-7 satellite measurements of the springtime Antarctic ozone decrease, *Nature*, *322* (6082), 808-811, 1986.

Stolarski, R.S., R.D. McPeters, and P.A. Newman, The ozone hole of 2002 as measured by TOMS, *J. Atmos. Sci., 62* (3), 716-720, 2005.

Streibel, M., M. Rex, P. von der Gathen, R. Lehmann, N.R.P. Harris, G.O. Braathen, E. Reimer, H. Deckelmann, M. Chipperfield, G. Millard, M. Allaart, S.B. Andersen, H. Claude, J. Davies, H. De Backer, H. Dier, V. Dorokov, H. Fast, M. Gerding, E. Kyrö, Z. Litynska, D. Moore, E. Moran, T. Nagai, H. Nakane, C. Parrondo, P. Skrivankova, R. Stübi, G. Vaughan, P. Viatte, and V. Yushkov, Chemical ozone loss in the Arctic winter 2002/2003 determined with Match, *Atmos. Chem. Phys.*, *6*, 2783-2792, 2006.

Swider, W., and T.J. Keneshea, Decrease of ozone and atomic oxygen in the lower mesosphere during a PCA event, *Planet. Space Sci., 21* (11), 1969-1973, 1973.

Tabazadeh, A., Commentary on "Homogeneous nucleation of NAD and NAT in liquid stratospheric aerosols: Insufficient to explain denitrification" by Knopf et al., *Atmos. Chem. Phys., 3*, 827-833, 2003.

Taguchi, M., and S. Yoden, Internal interannual variability of the troposphere-stratosphere coupled system in a simple global circulation model, Part II: Millennium integrations, *J. Atmos. Sci., 59* (21), 3037-3050, 2002.

Thorne, P.W., D.E. Parker, S.F.B. Tett, P.D. Jones, M. McCarthy, H. Coleman, and P. Brohan, Revisiting radiosonde upper air temperatures from 1958 to 2002, *J. Geophys. Res., 110*, D18105, doi: 10.1029/2004JD005753, 2005.

Tilmes, S., R. Müller, J.-U. Grooß, D.S. McKenna, J.M. Russell III, and Y. Sasano, Calculation of chemical ozone loss in the Arctic winter 1996-1997 using ozone-tracer correlations: Comparison of Improved Limb Atmospheric Spectrometer (ILAS) and Halogen Occultation Experiment (HALOE) results, *J. Geophys. Res., 108* (D2), 4045, doi: 10.1029/2002JD002213, 2003.

Tilmes, S., R. Müller, J.-U. Grooß, and J.M. Russell III, Ozone loss and chlorine activation in the Arctic winters 1991-2003 derived with the tracer-tracer correlations, *Atmos. Chem. Phys., 4* (8), 2181-2213, 2004.

Tilmes, S., R. Müller, J.-U. Grooß, H. Nakajima, and Y. Sasano, Development of tracer relations and chemical ozone loss during the setup phase of the polar vortex, *J. Geophys. Res.*, in press, 2006a.

Tilmes, S., R. Müller, J.-U. Grooß, R. Spang, T. Sugita, H. Nakajima, and Y. Sasano, Chemical ozone loss and related processes in the Antarctic winter 2003 based on improved limb atmospheric spectrometer (ILAS)-II observations, *J. Geophys. Res., 111*, D11S12, doi: 10.1029/2005JD006260, 2006b.

Toohey, D.W., L.M. Avallone, L.R. Lait, P.A. Newman, M.R. Schoeberl, D.W. Fahey, E.L. Woodbridge, and J.G. Anderson, The seasonal evolution of reactive chlorine in the Northern-Hemisphere stratosphere, *Science, 261* (5125), 1134-1136, 1993.

Toon, O.B., P. Hamill, R.P. Turco, and J. Pinto, Condensation of HNO_3 and HCl in the winter polar stratospheres, *Geophys. Res. Lett.*, *13* (12), 1284-1287, 1986.

Tripathi, O.P., S. Godin-Beekmann, F. Lefèvre, M. Marchand, A. Pazmiño, A. Hauchecorne, F. Goutail, H. Schlager, C.M. Volk, B. Johnson, G. König-Langlo, S. Balestri, F. Stroh, T.P. Bui, H.J. Jost, T. Deshler, and P. von der Gathen, High resolution simulation of recent Arctic and Antarctic stratospheric chemical ozone loss compared to observations, *J. Atmos. Chem., 55* (3), doi: 10.1007/s10874-006-9028-8, 2006.

Trolier, M., R.L. Mauldin III, and A.R. Ravishankara, Rate coefficient for the termolecular channel of the self-reaction of ClO, *J. Phys. Chem., 94*, 4896-4907, 1990.

Uchino, O., R.D. Bojkov, D.S. Balis, K. Akagi, M. Hayashi, and R. Kajihara, Essential characteristics of the Antarctic-spring ozone decline: Update to 1998, *Geophys. Res. Lett., 26* (10), 1377-1380, 1999.

Urban, J., N. Lautié, E. Le Flochmoën, D. Murtagh, P. Ricaud, J. De La Noë, E. Dupuy, A. Drouin, L. El Amraoui, P. Eriksson, U. Frisk, C. Jiménez, E. Kyrölä, E.J. Llewellyn, G. Mégie, L. Nordh, and M. Olberg, The northern hemisphere stratospheric vortex during the 2002-03 winter: Subsidence, chlorine activation, and ozone loss observed by the Odin Sub-Millimetre Radiometer, *Geophys. Res. Lett., 31*, L07103, doi: 10.1029/2003GL019089, 2004.

Verronen, P.T., A. Seppälä, M.A. Clilverd, C.J. Rodger, E. Kyrölä, C.-F. Enell, T. Ulich, and E. Turunen, Diurnal variation of ozone depletion during the October-November 2003 solar proton events, *J. Geophys. Res., 110*, A09S32, doi: 10.1029/2004JA010932, 2005.

Vogel, B., W. Feng, M. Streibel, and R. Müller, The potential impact of ClO_x radical complexes on polar stratospheric ozone loss processes, *Atmos. Chem. Phys.*, *6*, 3099-3114, 2006.

Voigt, C., H. Schlager, B.P. Luo, A.D. Dornbrack, A.

Roiger, P. Stock, J. Curtius, H. Vossing, S. Borrmann, S. Davies, P. Konopka, C. Schiller, G. Shur, and T. Peter, Nitric acid trihydrate (NAT) formation at low NAT supersaturation in polar stratospheric clouds (PSCs), *Atmos. Chem. Phys., 5*, 1371-1380, 2005.

von Hobe, M., J.-U. Grooß, R. Müller, S. Hrechanyy, U. Winkler, and F. Stroh, A re-evaluation of the ClO/Cl_2O_2 equilibrium constant based on stratospheric in-situ observations, *Atmos. Chem. Phys. Discuss., 4* (5), 5075-5102, 2004.

von Hobe, M., R.J. Salawitch, T. Canty, H. Keller-Rudek, G. Moortgat, J.-U. Grooß, R. Müller, and F. Stroh, Understanding the kinetics of the ClO dimer cycle, *Atmos. Chem. Phys. Discuss.*, *6*, 7905-7944, 2006.

von Savigny, C., A. Rozanov, H. Bovensmann, K.-U. Eichmann, S. Noël, V. Rozanov, B.-M. Sinnhuber, M. Weber, J.P. Burrows, and J.W. Kaiser, The ozone hole breakup in September 2002 as seen by SCIAMACHY on ENVISAT, *J. Atmos. Sci., 62* (3), 721-734, 2005.

Waters, J.W., L. Froidevaux, W.G. Read, G.L. Manney, L.S. Elson, D.A. Flower, R.F. Jarnot, and R.S. Harwood, Stratospheric ClO and ozone from the Microwave Limb Sounder on the Upper Atmosphere Research Satellite, *Nature, 362,* 597-602, 1993.

Weber, M., S. Dhomse, F. Wittrock, A. Richter, B.-M. Sinnhuber, and J.P. Burrows, Dynamical control of NH and SH winter/spring total ozone from GOME observations in 1995-2002, *Geophys. Res. Lett., 30* (11), 1583, doi: 10.1029/2002GL016799, 2003.

Weber, M., L.N. Lamsal, M. Coldewey-Egbers, K. Bramstedt, and J.P. Burrows, Pole-to-pole validation of GOME WFDOAS total ozone with ground-based data, *Atmos. Chem. Phys., 5*, 1341-1355, 2005.

Weeks, L.H., R.S. Cuikay, and J.R. Corbin, Ozone measurements in the mesosphere during the solar proton event of 2 November 1969, *J. Atmos. Sci., 29* (6), 1138-1142, 1972.

Wirth, M., A. Tsias, A. Dörnbrack, V. Weiß, K.S. Carslaw, M. Leutbecher, W. Renger, H. Volkert, and T. Peter, Model-guided Lagrangian observation and simulation of mountain polar stratospheric clouds, *J. Geophys. Res., 104* (D19), 23971-23982, 1999.

WMO (World Meteorological Organization), *Atmospheric Ozone: 1985, Global Ozone Research and Monitoring Project–Report No. 16*, Geneva, Switzerland, 1986.

WMO (World Meteorological Organization), *International Ozone Trends Panel: 1988, Global Ozone Research and Monitoring Project–Report No. 18*, Geneva, Switzerland, 1990a.

WMO (World Meteorological Organization), *Scientific Assessment of Stratospheric Ozone: 1989, Global Ozone Research and Monitoring Project–Report No. 20*, Geneva, Switzerland, 1990b.

WMO (World Meteorological Organization), *Scientific Assessment of Ozone Depletion: 1991, Global Ozone Research and Monitoring Project–Report No. 25*, Geneva, Switzerland, 1992.

WMO (World Meteorological Organization), *Scientific Assessment of Ozone Depletion: 1994, Global Ozone Research and Monitoring Project–Report No. 37*, Geneva, Switzerland, 1995.

WMO (World Meteorological Organization), *Scientific Assessment of Ozone Depletion: 1998, Global Ozone Research and Monitoring Project–Report No. 44*, Geneva, Switzerland, 1999.

WMO (World Meteorological Organization), *Scientific Assessment of Ozone Depletion: 2002, Global Ozone Research and Monitoring Project–Report No. 47*, Geneva, Switzerland, 2003.

Yang, E.-S., D.M. Cunnold, M.J. Newchurch, and R.J. Salawitch, Change in ozone trends at southern high latitudes, *Geophys. Res. Lett., 32*, L12812, doi: 10.1029/2004GL022296, 2005.

Yela, M., C. Parrondo, M. Gil, S. Rodríguez, J. Araujo, H. Ochoa, G. Deferrari, and S. Díaz, The September 2002 Antarctic vortex major warming as observed by visible spectroscopy and ozonesoundings, *Int. J. Remote Sens., 26* (16), 3361-3376, 2005.